Bridge River Project Water Use Plan

Carpenter Reservoir Productivity Model Validation and Refinement

Implementation Year 1

Reference: BRGMON-10

Study Period: 2015-2016

Chris Perrin, Roger Pieters, Jennifer Harding, Shauna Bennett and Greg Lawrence

May 30, 2016

CARPENTER RESERVOIR PRODUCTIVITY MODEL VALIDATION AND REFINEMENT
PROGRESS IN 2015-2016

Bridge – Seton Water Use Plan Study Number BRGMON#10

May 30, 2016

LIMNOTEK

CARPENTER RESERVOIR PRODUCTIVITY MODEL VALIDATION AND REFINEMENT

PROGRESS IN 2015-2016

Bridge – Seton Water Use Plan Study Number BRGMON10

Submitted to
BC Hydro
Burnaby, B.C.

Prepared by:
C.J. Perrin, MSc., RPBio., Roger Pieters, PhD., Jennifer Harding, PhD.,
Shauna. Bennett, MSc., RPBio, and Greg Lawrence, PhD.

May 30, 2016

Citation: Perrin, C. J, R. Pieters, J. N. Harding, S. Bennett, G. A. Lawrence. 2016. Carpenter Reservoir Productivity Model Validation and Refinement (BRGMON10): Progress in 2015-16. Report prepared for BC Hydro. 90p.

The study was managed by St'at'imc Eco-Resources Ltd.

Cover photo: Annika Putt operating the Sea-Bird CTD, June 17, 2015: C. Perrin photo

EXECUTIVE SUMMARY

This report provides information from the first of three years of monitoring, sample collection, laboratory work, and analysis that is required to answer four management questions addressing uncertainties about relationships between water management actions and biological production in Carpenter Reservoir. Statistical modeling and a hydrodynamic model called CE-QUAL-W2 both using empirical data were developed in 2015-16 and will be linked and further refined in subsequent years to answer the questions. Progress in 2015-16 is as follows.

Question 1: Is light the primary factor regulating productivity of littoral habitat in Carpenter Reservoir?

Littoral production was assessed using a novel yet basic study design that was meant to capture the variation in substrates in Carpenter Reservoir. Multiple arrays of polystyrene balls were deployed at various depths in the reservoir for this project as well as in Anderson and Seton Lakes. The polystyrene balls were meant to simulate stony substrate common amongst all three water bodies while sand pails were deployed in Carpenter Reservoir only, to simulate growth on smaller substrate unique to Carpenter. Based on one year of data from 2015, light is an important driver of littoral periphyton production on stony substrates as is water temperature and dissolve inorganic nitrogen concentration. However, light did not describe as much variation in periphyton growing on sand. Temperature, turbidity and dissolved inorganic nitrogen were better predictors of periphyton growing on sand but additional data collected in 2016 and further analysis will be required to increase the predictive power of the model and better assess the community assemblage in these samples.

The periphyton community was quite different among the polystyrene and sand samples. The former was primarily occupied by attached chlorophytes and some diatoms while organisms in the sand samples were primarily chryso-cryptophytes. These organisms are flagellated and likely do not originate from the sand samples but rather were associated with the sand – water interface and captured from the water column during sampler retrieval. There was also 2-20x more biomass collected from the polystyrene balls than from the sand samples. The variation in community composition and size are likely responsible for the slight variation response to environmental variables tested in the regression models.

Next steps include adding data collected from the 2016 sampling period to the regression models and integrating the CE-QUAL-W2 model results once they are complete. A final version of the periphyton regression model will be presented in 2018 in the final report.

Question 2: Is light the primary factor regulating productivity of pelagic habitat in Carpenter Reservoir?

Pelagic production was measured as phytoplankton and zooplankton production and biomass. For this report we have focused on zooplankton biomass, which was measured monthly from May to October in Carpenter Reservoir and May to September in Anderson and Seton Lakes along with environmental variables deemed important for zooplankton biomass. We found that zooplankton biomass increased with water residence time and temperature but declined with the smaller size class of phytoplankton and turbidity. Light may influence zooplankton production indirectly by influencing phytoplankton production, the food source for zooplankton. This interaction will be determined once all associated data are collected in 2016.

Of the four variables found to be important determinants of zooplankton production, water residence time is one measure that can be altered through water use plans by increasing or decreasing the outflow in Carpenter Reservoir. We found that despite zooplankton biomass increasing with water residence time by approximately 70 mg dry weight/m^2 over a doubling in water residence time, the effect of water temperature was much more pronounced. A 77% increase in zooplankton biomass was correlated with a 2.8 °C increase in water temperature. This correlation may be due to the seasonal patterns in species phenology, which will be further explored in subsequent analyses.

Monthly sampling of phytoplankton and zooplankton will continue this year along with pertinent environmental variables in Carpenter, Anderson and Seton. The data collected this year will be analyzed and integrated into the regression models to improve their predictive power and fit, with a final version of the model prepared in 2018 once the CE-QUAL-W2 modelling is complete.

Question 3: Is light penetration in Carpenter Reservoir impacted by changes in reservoir operations?

Simulation modeling supported with empirical data is being used to answer questions 3 and 4. The simulation model is CE-QUAL-W2, which is a hydrodynamic and water quality model for rivers, lakes, reservoirs and estuaries. CE-QUAL-W2 laterally averages calculations (across channel) with segments along the length of the water body, and bins from the surface to the bottom.

An interface was developed in MATLAB for reading and writing data to and from CE-QUAL-W2. The simulation model was set up to simulate conditions measured in 2015 and will be adjusted once the 2016 data are available. With this model, we will be able to distinguish between the relative importance of management actions compared to natural processes in determining the change in light, temperature, nutrient concentrations and water residence time that drive production in the littoral and pelagic habitats in Carpenter Reservoir.

Question 4: Can suspended sediment transport into Seton be altered by changes in Carpenter Reservoir operation?

To answer this question, we will need to integrate information from the regression analyses for biological production and data from the CE-QUAL-W2 model, which will occur in 2017 and be ready for the final report in 2018.

A summary of the status of BRGMON10 study findings is listed in the following table:

Study objectives	Management questions	Status
Determine if light or other environmental variables affect periphyton production on sand or stony substrate in Carpenter Reservoir.	Is light the primary factor regulating productivity of littoral habitat in Carpenter Reservoir?	The study is on track to answering the management question with additional data in 2016-2017 using the current approach/study design
Determine if light or other environmental variables affect phytoplankton and zooplankton production in pelagic habitat in Carpenter Reservoir.	Is light the primary factor regulating productivity of pelagic habitat in Carpenter Reservoir?	The study is on track to answering the management question with additional data in 2016-2017 using the current approach/study design
Determine whether water management in Carpenter Reservoir affects light penetration or other environmental variables.	Is light penetration in Carpenter Reservoir impacted by changes in reservoir operations?	The study is on track to answering the management question with additional data in 2016-2017 using the current approach/study design
Determine if changes to reservoir operation affect the inflow of suspended sediment into Seton Lake.	Can suspended sediment transport into Seton be altered by changes in Carpenter Reservoir operation?	The study is on track to answering the management question with additional data in 2016-2017 using the current approach/study design

ACKNOWLEDGEMENTS

This project was performed under contract to BC Hydro as part of the Bridge River Water Use Plan Studies. The authors thank many people who contributed to the project as follows. Bonnie Adolf (Project Coordinator), Gilda Davis (contract manager), and Jude Manahan (bookkeeper) with St'at'imc Eco-Resources Ltd. (SER) are thanked for contract administration. Dave Marmorek (ESSA Technologies Ltd.) is thanked for discussions about study design in early phases of the project.

We thank the 2015 field crew including Annika Putt, Marc Laynes, Tyler Creasey, Allison Hebert, and Allison James for energy and enthusiasm to complete long and often complicated days in the field. Allison Hebert worked with Shannon Harris to complete lab work and calculations for the primary production measurements. The field crew was assisted by L.J Wilson and Caroline Melville who were safety check-in people on most field days.

Chemical analyses of stream and lake water samples and periphyton biomass were completed at ALS Environmental under the management of Courtney Duncan. Chemical analysis of passive samplers and ion exchange columns was completed by Dr. Julian Aherne and Jaime Morrison of Trent University. Danusia Dolecki performed the zooplankton enumerations and biomass measurements and Lech Dolecki completed the algal cell identifications, enumerations, and bio-volume measurements.

Odin Scholz (Split Rock Environmental Ltd.) and Brad Oleman (BC Ministry of Forests Lands and Natural Resource Operations) are thanked for support on access to meteorological data from the 5-Mile Forest Service weather station. We are grateful to Dr. David Levy, Fisheries Advisor to SER for numerous discussions regarding study scope and integration with other SER projects. Joes Goes is thanked for organizing access for our crew to use the boat ramp at the east end of Anderson Lake. Mike Chung is thanked for assisting with data entry from field and lab sheets.

Several people from BC Hydro are thanked for attention to contract management with SER and for the provision of hydrology data from BC Hydro Power Records. They included Teri Neighbour, Dr. Ahmed Gelchu, Darin Nishi, and Jeff Walker. Jim Coles (Area Manager, BC Hydro), Rick Enegren (Dam Safety Engineer, B.C. Hydro), and Mark Thorsteinson (Dam Safety Engineer, B.C. Hydro) are thanked for approving our installation of meteorological instruments and samplers on the Terzaghi Dam and for approving our installation of samplers on the trash boom in Carpenter Reservoir.

GIS analysis and mapping in support of the CE-QUAL modeling was completed by Nicole Fink (GIS Specialist, BC Hydro) and Faizal Yusuf (Hydrotechnical Engineer, BC Hydro). Meaghan Leslie-Gottschligg produced the site location map. Special thanks goes to Dorian Turner of BC Hydro for arranging a location on grounds of the BRG1 generating station for us to install a solar radiation sensor and for organizing building space on the same property for our field crew to set up and operate a field lab. We would also like to thank Adjoa Quanioo and Alex Huang, UBC co-op students, who helped with the CE-QUAL-W2 modelling as well as Thea Rodgers and Melanie Mewhort who helped with instrument servicing and data analysis and whose salaries were subsidized by the UBC Work Learn program.

TABLE OF CONTENTS

Page

LIST OF FIGURES

LIST OF TABLES

Page

1 INTRODUCTION

The Bridge-Seton Water Use Plan Consultative Committee (CC) developed aquatic ecosystem objectives for the Bridge River watershed that included efforts to maximize the abundance and diversity of fish populations while establishing flow controls for hydroelectric power generation, among other interests (Bridge River WUP CC, 2003). The Bridge River watershed provides habitat for resident fish species, which are valued from commercial, recreational, and cultural perspectives. Tradeoffs occurred in the water use planning, resulting in decisions to set water elevations in reservoirs of the Bridge River watershed (Downton, Carpenter, Seton), manage spills from the reservoirs, and define flows in rivers (Middle and Lower Bridge River, Seton River). The complete package of flow controls is collectively known as N2-2P. While N2-2P was accepted, the Bridge River WUP CC (2003) was constrained in making decisions by lack of information about the effects of change in flows on fish populations and biological production that support those populations. Despite this uncertainty, N2-2P was implemented on March 30, 2011 (Water Act Order 2011, Bridge River Power Development Water Use Plan, 17 March, 2011) with a commitment to fund monitoring studies to fill data gaps and better inform people tasked with water management decisions in future years, including the St'át'imc people and St'át'imc Eco-Resources Ltd. (SER).

Uncertainty among members of the Consultative Committee included unknown effects of low water temperature and turbidity produced by flow from upper reaches of the Bridge River on biological production in Carpenter Reservoir and the effect of the diversion of that cool and turbid water on sockeye salmon and Gwenis in Seton Lake. A small diversion of water from the Bridge River to Seton Lake started in 1934. The diversion increased in 1954 to power four turbines at Shalalth (located on the north shore of Seton Lake, Figure 1) and it was fully developed by 1960 with the installation of four more turbines. Effects of this diversion on fish populations were first investigated by the International Pacific Salmon Fisheries Commission (Geen and Andrew 1961) and later by Fisheries and Oceans Canada (Shortreed et al. 2001). Those studies suggested the diversion of cold and turbid water from the glacial Bridge River and Carpenter Reservoir, reduced water temperature, increased light attenuation, and decreased primary productivity in Seton Lake. These observations imply the existence of a "footprint" impact on fish production in Seton Lake due to the diversion that is being further investigated in water use plan monitoring study number BRGMON6.

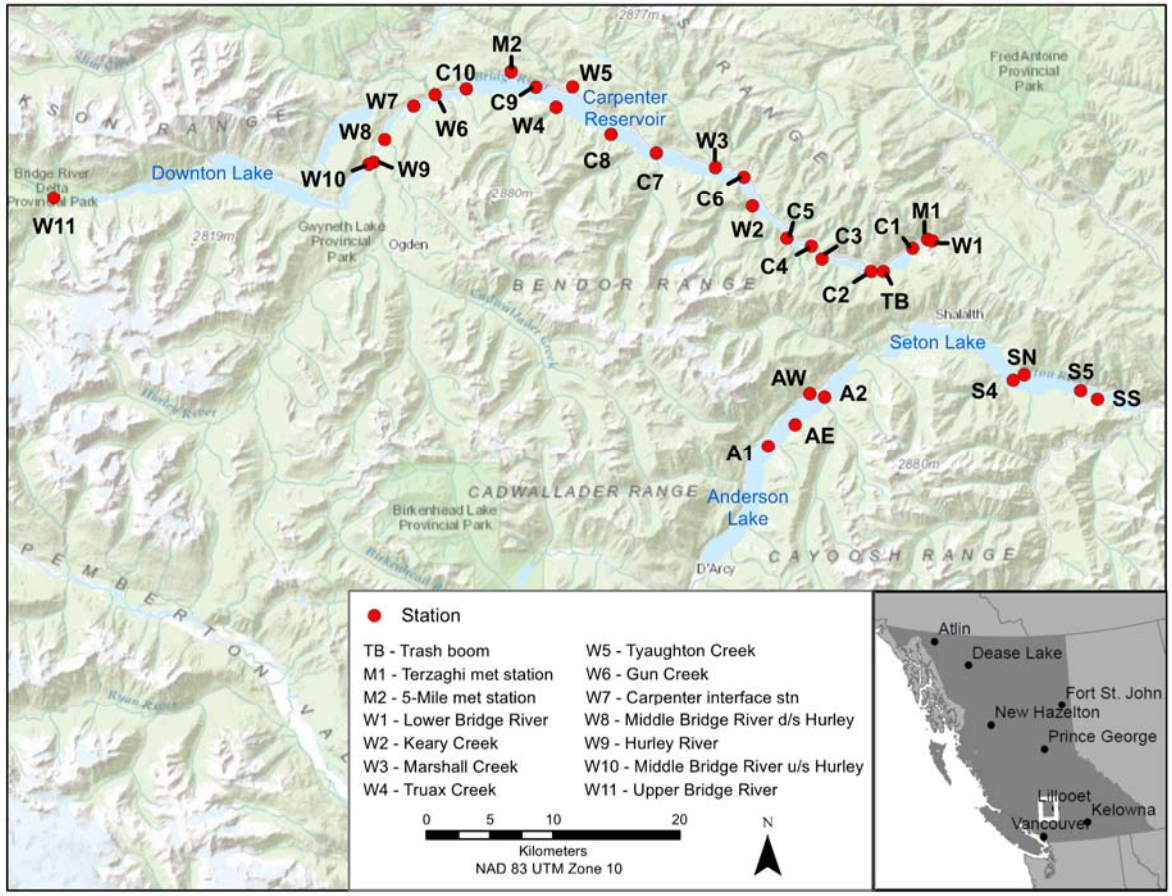

Figure 1. Sampling stations and landmarks in Carpenter Reservoir, Anderson Lake and Seton Lake. Markers on Seton and Anderson Lakes (lower right) are part of BRGMON6.

Light was a focus of the Carpenter Reservoir Reservoir Productivity Model (CLRPM) created by the Consultative Committee because of an assumption that light solely limited biological production. There is no question that light or more correctly photosynthetically active radiation (PAR) limits photosynthesis that drives biological production in lakes and reservoirs (Wetzel 2001). A general rule is that photosynthesis is active where PAR occurs at intensities of more than 1% of irradiance at the water surface (Wetzel 2001). In addition to the basic physics of light attenuation in clear water, PAR attenuation is affected by particles in water. In Carpenter Reservoir, those particles most notably include inorganic fines that are carried in suspension from upstream erosion by glaciers and snow fields in the headwaters of the Bridge River and potentially within the drawdown zone of Downton and Carpenter Reservoirs. The particles add to attenuation of PAR in the reservoirs, resulting in a smaller depth of photosynthetic production and shallower euphotic zone than would occur if turbidity was not present. Hence, the assumption about light limitation of biological production in CLRPM was really a statement about turbidity affecting the amount of habitat in Carpenter Reservoir where photosynthesis can occur.

Within a water column where the amount of PAR is sufficient to support photosynthesis, production of algae can be limited by nutrient supply (Biggs 2000, Bothwell 1989, Guildford and Hecky 2000, Wetzel 2001), turbidity (Liess et al. 2015) and temperature (Bothwell 1988, Goldman and Carpenter 1974) within available habitat, which is determined by water residence time, area of habitat, and volume of habitat that is influenced by reservoir filling and drawdown.

The CC found that uncertainties about the relative importance of the several habitat attributes that potentially drive biological production in pelagic and littoral habitats of Carpenter Reservoir and the influence of reservoir operations versus natural hydrology on those processes could not be resolved with existing information. Studies were recommended to fill data gaps and determine what water management actions, if any, could be used to mitigate effects of reservoir operations on biological production in pelagic and littoral habitat.

Four management questions resulted from analysis by the CC. They are listed as follows:

1) Is light the primary factor regulating productivity of littoral habitat in Carpenter Reservoir?
2) Is light the primary factor regulating productivity of pelagic habitat in Carpenter Reservoir?
3) Is light penetration in Carpenter Reservoir impacted by changes in reservoir operations?
4) Can suspended sediment transport into Seton be altered by changes in Carpenter Reservoir operation?

This report summarizes information from the first year of data collection and analyses from Carpenter Reservoir as well as supporting information from Anderson and Seton Lakes. Using periphyton in littoral habitats and zooplankton in the pelagic as examples, this report will highlight the methods and analyses used thus far and make recommendations for subsequent field sampling and analyses required to answer the above management questions.

2 STUDY DESIGN AND METHODS

2.1 Study site description

2.1.1 Geographic characteristics

Carpenter Reservoir is situated within the original Bridge River floodplain between the Bendor Range of the Coast Mountains to the south and the Shulaps Range, Pearson Ridge, and Marshall Ridge of the Chilcotin Ranges to the north. The reservoir was formed with construction of the Mission Dam on the Bridge River in 1960. In 1965 it was renamed the Terzaghi Dam. The dam is located 40 km upstream of the confluence of the Bridge River and the Fraser River near Lillooet. The width of the original flood plain and the present reservoir at the top water surface elevation is up to 1.5 km. Substrata within the draw down zone consists of a thin sediment veneer overlying glacial silts and sand with localized gravel and cobble remnants. At drawdown the river typically erodes a profile of approximately 1 m below floodplain elevation, re-suspending substratum materials in the process. Deposits of organic debris including small branches and forest litter that is transported from upstream are evident in most locations where cut banks have been formed.

Access to the reservoir is via a well-maintained gravel road on the north side. It connects the community of Gold Bridge with Lillooet. The road is maintained year round. Boat access to the reservoir is available at ramps located at Tyaughton Creek, a BC Hydro recreation site at Big Horn Creek, at Marshall Creek, and at the Terzaghi Dam. Ice cover develops over the reservoir in winter months thus preventing boat access at that time.

The Terzaghi Dam is located at a narrows between bedrock outcrops at the eastern extent of the original Bridge River floodplain. The dam was constructed over an original diversion dam that was built in 1948 (BC Hydro 1995). The dam is an earthfill structure, 60 m high with a crest length of 366 m. A spillway with two gates and a free overflow section is located in rock on the right abutment. A low level outlet tunnel is located below the spillway.

The dam is used to store water for power generation. Water is diverted through two tunnels located 3 and 4 km respectively upstream of the dam. The intake tunnels

pass through Mission Mountain to the south and through penstocks to powerhouses called BRG1 and BRG2 located at Shalalth.

2.1.2 Catchment and Reservoir Areas

The Carpenter Reservoir is 50 km long and has an average width of 1 km at full pool with a longitudinal axis lying east west. It extends westward from the Terzaghi Dam along the Bridge River floodplain. In 2015, the maximum reservoir surface elevation was 648.84 m on October 29 (BC Hydro Power Supply Operations). This elevation was 18.06 m higher than the elevation at complete drawdown that occurred on 21 March 2015 (BC Hydro Power Supply Operations). The reservoir surface area at full pool is 46.2 x 10^6 m^2 but it declines to approximately half this area at full drawdown. The dewatered area at drawdown occurs along 25 km of the Bridge River floodplain in the western half of the reservoir. From the reservoir shorelines, ridges to the north rise to 2,445 m and peaks to the south are at elevations of more than 3,000 m.

Main catchments that drain into the reservoir include the upper Bridge River (via Downton Reservoir), the Hurley River, Gun Creek, Tyaughton Creek, Marshall Creek and numerous other streams (Table 1). The Upper Bridge River upstream of the Hurley River confluence represents 26.7% of total catchment area for the reservoir. The Tyaughton Creek and Hurley River drainage is 20.5% and 18.2% respectively of the total catchment area. Other local drainage represents 34.6% of the catchment area.

Table 1. Catchment areas that drain into Carpenter Reservoir.

Drainage Name	Area (ha)	Percent of total area
Upper Bridge River	99,069	26.7
Hurley River	67,640	18.2
Tyaughton Creek	75,973	20.5
Marshall Creek	9,352	2.5
Gun Creek	58,988	15.9
Other local drainage	60,007	16.2
TOTAL (to Terzaghi Dam and tunnel intakes)	371,029	100

Most inflow is from the Upper Bridge River system that drains the Coast Mountains. Although Tyaughton Creek has a relatively large catchment area, it is all within the relatively dry Chilcotin Mountains and water yield is low compared to that from the upper Bridge and the Hurley Rivers. Water from the west and south originates as glacial meltwater at alpine elevations of the Coast Mountains (1,800 to 3,000 m). Parent materials in much of the headwater areas are granitic and volcanic and they have the potential to contribute phosphorus from rock weathering to drainage streams. The Bridge River is a 6th order system at the Carpenter Reservoir.

2.1.3 Reservoir Morphometry

Daily surface elevation and live storage volume were downloaded directly from BC Hydro, System Control Centre (Power Supply Operations). The storage data were from a regression model produced by BC Hydro that determines live storage volume as a function of water surface elevation. Volumes for the model were determined from interpretation of air photos taken at a low water surface elevation. Water surface area determined at several elevations on the air photo using planimetry multiplied by depth interval between elevations provided volumes for those selected elevations. For a given elevation, the sum of strata volumes below that elevation provided live storage volume. The calculated model is run daily to determine live storage volume from measurements of water surface elevation in the dam forebay at midnight.

The intake gates to the Seton Lake tunnels limit the lowest water surface elevation at 600.61m and 599.54 m (to bottom of gate). In 2015 the reservoir ranged from 630.77 m on March 21 to a maximum of 648.84 m on October 29 (BC Hydro Power Supply Operations). The original riverbed elevation immediately downstream of Terzaghi dam is approximately 609 m (Topographic map 92 J/16, 1992). Thus, the tunnels are located at approximately as low as the original riverbed and virtually the entire storage volume is available as live storage. Typical water depths in the region of the tunnels at full pool are 30-50m.

A summary of morphometric features of the reservoir is shown in Table 2.

Table 2. Morphometric and bathymetric measures for Carpenter Reservoir.

Measure	Value at Maximum Water Elevation in 2015 (648.84 m)
Reservoir Length (km)	50
Average Reservoir Width (km)	1
Reservoir Area (ha)	46.2×10^6 m^2
Maximum water depth (m)	55
Live storage volume (m^3)	91.13×10^7 m^3
Dead storage volume	0
Total storage (m^3)	91.13×10^7 m^3

2.2 Study design and overview

Biological production will be defined as algal production because photosynthetic algae are the only part of the food web that uses PAR as an energy source for production of organic matter that supports the food web in littoral and pelagic habitats and PAR is the main variable of interest among the management questions. For question 1, algal production is measured as periphytic algal accrual in units of μg chl-a·cm^{-2} (Perrin et al. 1987, Bothwell 1988) where chl-a is chlorophyll-a, a primary plant pigment that is commonly used as a measure of biomass in algae (Wetzel 2001, Behrenfeld et al. 2005). Chlorophyll-a can be approximately converted to carbon (e.g. Riemann et al. 1989, Cloern et al. 1995, Li et al. 2010, Behrenfeld et al. 2005) to yield

units of mg $C \cdot m^{-2} \cdot d^{-1}$. For question 2, algal production will be production of phytoplankton measured as the amount of ^{14}C incorporated into algal biomass in a 1 m^2 column of water, per unit time and expressed in units of mg $C \cdot m^{-2} \cdot d^{-1}$ (Steemann Nielsen 1952, Wetzel 2001). Phytoplankton biomass measured as chl-a concentration will also be measured because it is needed in calculations of algal production from the ^{14}C data. These measurements of algal production in each of littoral and pelagic habitats are standard procedures. They show the amount of carbon fixed per unit area per unit time, allowing direct comparison of amounts of algal production between pelagic and littoral habitats.

Fish populations that are of ultimate interest by the consultative committee ingest invertebrates or other fish as food sources. Invertebrates ingested by fish include zooplankton, benthic invertebrates that use bottom sediment as habitat and emerge through the water column during transition from larval and pupal stages to adults, benthic invertebrates that drift into the reservoir from tributary streams, and terrestrial insects that land on the water surface and fail to escape the surface tension. To facilitate bridging the gap between algal production and fish, zooplankton biomass was measured and modeled. Zooplankton are an important food source for Gwenish in the reservoir that in turn can be prey for the piscivorous bull trout (Griffiths 1999). In addition, zooplankton are sensitive to the hydrology of Carpenter Reservoir (Perrin and MacDonald, 1999). Hence, zooplankton are a good indicator of interactions between water management actions, natural hydrology, and food web processes supporting fish populations making them ideal for providing insight into links between primary production and fish.

2.3 Questions 1 & 2: Is light the primary factor regulating productivity of littoral habitat in Carpenter Reservoir and is light the primary factor regulating productivity of pelagic habitat in Carpenter Reservoir?

2.3.1 Periphyton production in the littoral habitat

Algal production in littoral habitat was measured as periphyton (algae growing on substrates) accrual on installed substrates (Bothwell, 1989, Perrin et al. 1987) using a novel and simple substrate sampling system. There are two common types of substrata in Carpenter Reservoir: stony materials that occur on steeper benches and sand flats that occupy most of the original river valley and dominate the drawdown zone. We used a customized sampler for each type of substrata. To represent stony sites, we deployed a sampler that consisted of six arrays of two replicate 2.5-cm diameter polystyrene balls attached at equidistant positions on a vertical mooring line over a depth that was 1.5 times the depth of the euphotic zone using horizontal line clips. To represent sand sites, six pairs of pails containing sand were suspended at different depths from vertical lines with the depth again being 1.5 times the depth of the euphotic zone. Sand for the pails was collected in early April 2015 from depths >10 cm among exposed sand flats within

the Carpenter drawdown zone. A sufficient amount of sand was stock piled for use in samplers for the duration of April through October. That sand was exposed for most of the previous winter. Collection of sand from below the sand surface was required to avoid presence of algal biomass in the samplers at the start of an incubation.

The samplers were deployed during three time series in 2015: Series 1 (spring) was April 16 to June 18, Series 2 (summer) was June 18 to August 12, and Series 3 (fall) was August 12 to October 20. A sampling time series involved installation of the samplers on the first day and removal on the last day, a period of approximately 2 months. On the transition day between sampling series (June 18 and August 12), samples from the preceding series were collected and new substrata for the following series were installed.

The polystyrene and sand samplers were installed on moorings in each of the three reservoirs/lakes. Duplicate samplers of each type were installed at the trash boom in Carpenter Reservoir (Figure 1). In each of Seton Lake and Anderson Lake a polystyrene sampler was installed on each of opposite shores (A1 and A2 in Anderson Lake and S4 and S5 in Seton Lake) in close proximity to stations used for measurements of algal production that is part of BRGMON6. Sand samplers were not installed in Seton or Anderson Lakes because they do not have sand substrata in littoral zones. In Seton and Anderson Lakes where there is little change in water surface elevation, the mooring line was secured between an anchor and submerged float. Depth of the samplers were recorded based on their distance from the anchor and depths recorded by a depth logger that was attached to the anchor. In Carpenter Reservoir where there was a continuous increase in water depth in spring through fall, mooring lines were secured to the trash boom that crosses the reservoir (Figure 1). This approach ensured that the sampler arrays maintained constant depth during incubation in Carpenter Reservoir.

Each polystyrene sampler was deployed with clean polystyrene balls. One polystyrene ball (surface area = 19.63 cm^2) from each of the duplicate samplers from each depth was retrieved after the approximate 60 day incubation period (mean $\pm$ standard error; 62.75 days $\pm$ 0.54). Each ball with adhered biomass was placed into a labelled plastic vial and packed on dry ice for shipment to the lab. Each ball was analyzed for biomass measured as chlorophyll-a concentration (corrected by sample surface area). Chlorophyll-a was extracted in 5 ml of 90% acetone and stored in the dark for 20 to 24 hours at –20 ^oC. The polystyrene dissolved in the acetone leaving only the chlorophyll extract in solution. Fluorescence of the acetone extract was measured before and after the addition of three drops of 10% HCl in a Turner Designs™ Model 10-AU fluorometer that was calibrated with a solution of commercially available chlorophyll-a. Calculations to determine chlorophyll-a concentration were made using equations reported by Parsons et al. (1984). Three blank balls that were not deployed at sampling sites were processed the same way to measure starting biomass. In each case,

biomass on the blank replicates were below the detection limit of the fluorometer and assumed to be zero.

Each sand sampler was a pail with a surface area of 551.5cm^2 filled to 2/3 of total volume with new sand. After approximately 60 days of incubation (62.14 days $\pm$ 0.98) a sample (8-15.9 cm^2) was removed from each of the duplicate pails with a separate plastic vial. As with the polystyrene balls, the vials were capped, packed on dry ice for shipment to the lab and analyzed for chlorophyll-a concentration (corrected by sample surface area) using the same methods as for the polystyrene samples.

An additional sample was collected from each of the polystyrene and sand samplers closest to the surface for analysis of species composition.

In the laboratory each sand sample was shaken vigorously for 1 minute, emptied into a graduated cylinder and the volume of the sample solution was recorded. Then the sample was diluted according to the amount of sediment in the sample to avoid covering the algal cells by the sediment. The different volumes of aliquots were pre-settled in settling chambers to determine proper concentration of subsamples used for counting.

Processing of the polystyrene ball periphyton samples first required the modification of an existing sample jar lid for adaptation to a “Waterpik Flossing System”. This system was used for accurately clearing the porous polystyrene surface of algae and debris using high-pressure water injection. The modification of the sample jar lid required the drilling of two small holes. One hole (approximately 3mm in size) was needed for a snug fit of rubberized Waterpik system injection nozzle. The other smaller hole on the opposite end of the lid was made to allow for air to escape as the sample jar would fill up with water without allowing the splash of sample contents to escape.

After a modified sample jar was prepared, a sample with an original and unmodified lid was shaken vigorously for 30 seconds and had its contents emptied into a graduated cylinder. The volume of the liquid contents was then recorded. Next, the polystyrene ball was taken out using forceps and mounted onto a skewer and placed back in the jar. The skewer prevented the polystyrene ball from spinning and moving around during Waterpik pressure wash. The jar was then closed using the modified pressure wash lid.

The Waterpik flossing system was set to its maximum setting of 12 PSI spray and the nozzle was then inserted through the larger hole in the lid. While observing the direction of spray, the nozzle was adjusted accordingly to pressure wash the entire hemisphere of the polystyrene ball. After one hemisphere had been thoroughly power washed, the lid was opened and the position of the skewer mounted polystyrene ball was inverted. The pressure washing procedure was the repeated to wash the other hemisphere of the polystyrene ball.

Once the polystyrene ball had been thoroughly washed, the lid was removed and the polystyrene ball was then held by the skewer within the sample jar. Lastly, the ball was gently scrubbed using an electric toothbrush to remove any remaining visible debris off and rinsed into sample jar using the gentle spray of filtered water from a squeeze bottle.

Algal cell counts and measurement of biovolume by species was conducted the same way for each of the sand and polystyrene samples once sample was prepared in the settling chambers. Chamber contents were settled for 24 hours. Cell counts and biovolume measurements were completed at 500x magnification under an Olympus CK20 Inverted Microscope. Only cells containing cytoplasm were enumerated. A minimum of 100 cells of the most abundant species and a minimum of 300 cells in total were counted per sample. Biovolume, by species, was determined by multiplying cell counts by the volume of representative geometric shapes or combination of shapes that most closely approximated cell shape.

2.3.2 Phytoplankton production in the pelagic habitat

Monthly chlorophyll-a concentration was measured at 6 depths through the euphotic zone from May through October on Carpenter Reservoir. Similar methods were employed on Seton and Anderson Lake from May to September as part of BRGMON6 following the methods described in section 2.2.2 of the proposal. Each sample was parallel filtered through 0.2 and 0.75 μm polycarbonate Nucleopore™ filters.

The algal production measurements were done *in situ* as the amount of ^{14}C incorporated into particulate organic carbon. Discrete water samples collected with a Van Dorn water bottle from the six depths over the profile of the euphotic zone were transferred directly into two light and one dark 300 ml acid-cleaned BOD glass bottles assigned as a group of bottles to each depth.; hence there were six sets of two light and one dark bottle. Each BOD bottle were rinsed three times with the sample before filling. The water samples were maintained under low light conditions during all manipulations until the start of the incubation that were started within 1 h of the water collections. Water in the BOD bottles were inoculated with 0.185 MBq (5 μCi) of $NaH^{14}CO_3$ New England Nuclear (NEC-086H). The cluster of BOD bottles for each depth were attached to an acrylic plate and suspended at each of the six depths from which the water samples are taken. These samples were then incubated *in situ* for 4-5 h between the hours of 1000 and 1500 to allow the carbon uptake to proceed. Following retrieval of the incubation array, the BOD bottles were transported to facilities at BC Hydro in Shalalth in a cool dark box.

The incubations were terminated by parallel filtration of 100 ml of sample onto 0.2 and 0.75 μm polycarbonate Nucleopore™ filters, the same pore sizes used for primary production measurements on Seton and Anderson Lakes. Each folded wet filter

and retained biomass were placed in a 7 ml scintillation vial and stored in the dark until processing at the University of British Columbia.

In the fumehood, 100 µL of 0.5 N HCl was added to each vial to eliminate the unincorporated inorganic $NaH^{14}CO_3$. The scintillation vials were then left uncapped in the fumehood for approximately 48 h until dry. After 5 ml of Scintisafe® scintillation fluor was added to each vial, and stored in the dark for >24 hours, the samples were counted using a Beckman® Model #LS 6500 liquid scintillation counter. Each vial was counted for 10 minutes in an external standard mode to correct for quenching. The specific activity of the stock was determined by adding 100 µL ^{14}C-bicarbonate solution to scintillation vials containing 100 µL of ethanoalamine and 5 ml Scintisafe® scintillation cocktail. Calculation of rates of carbon incorporation followed methods reported by Parsons et al. (1984). Primary productivity values were vertically integrated according to procedures of Ichimura et al. (1980) for calculation of annual rates of primary production and each value from a discrete depth were considered to be independent observations for the regression modeling. Daily rates of primary production were calculated by multiplying the hourly primary productivity by the incubation time and by the ratio of the solar irradiance during the incubation to the solar irradiance of the incubation day where solar irradiance was measured using a Li-Cor irradiance meter. Corrections for solar irradiance over periods of time were determined from ambient irradiance logged using a sensor and data logger installed at a meteorological station at the Terzaghi Dam for the during sampling (May – October). The difference between the ^{14}C incorporation in the light bottles (includes photosynthetic and non-photosynthetic uptake) and the ^{14}C incorporation in the dark bottle (includes only non-photosynthetic ^{14}C uptake) indicated carbon uptake by photosynthesis.

The algal production measurements required measurement of chlorophyll-a concentration at the same depths where the BOD bottles were incubated. Samples for these chlorophyll-a measurements were collected at C1 and at two other pelagic stations called C2 and C3 that are west of the Terzaghi Dam (Figure 1). C2 was dewatered in the spring, resulting in measurements only at C1 and C3 at that time. Data from all stations will show longitudinal patterns of algal biomass, which will assist with interpretation of the algal production data collected at C1.

Chlorophyll-a concentration was determined by *in vitro* fluorometry (Yentsch and Menzel, 1963) in aliquots from each of the six water samples that were used for primary production analysis. The aliquots were parallel filtered through 0.2 and 0.75 µm polycarbonate Nucleopore™ filters as was done for the aliquots used for primary production analysis using a vacuum pressure differential of <100 mm of Hg. Care was taken to limit light exposure of the chlorophyll samples during field handling of water samples and laboratory analysis. The water filtrations were completed on the day of sample collection at the Shalalth field lab. The filters with phytoplankton biomass were stored in the dark at –20°C prior to analysis at the University of British Columbia. Chlorophyll-a was extracted in 5 ml of 90% acetone and stored in the dark for 20 to 24

hours at –20°C. Fluorescence of the acetone extract was measured before and after the addition of three drops of 10% HCl in a Turner Designs™ Model 10-AU fluorometer that was calibrated with a solution of commercially available chlorophyll-a. Chlorophyll-a concentration was determined using equations reported by Parsons et al. (1984).

At the same stations where chlorophyll-a concentration was measured, aliquots from a depth integrated water sample were collected for phytoplankton cell enumeration by species. These data were used to describe the assemblage of algae that is contributing to the pelagic algal production. The depth integrated water sample was prepared by mixing equal aliquots of water from at least three depths in the euphotic zone. An aliquot was dispensed to a glass amber jar, preserved with acid-Lugol's solution, and stored in a cool and dark location until the algal cells were counted. Prior to the enumeration, the samples were gently shaken for 60 seconds and allowed to settle in 25 mL chambers for a minimum of 8 hrs (Utermohl 1958). Counts of algal cells, by taxa, were done using an inverted phase-contrast plankton microscope. Cells of large micro-plankton (20-200 µm) were counted at 250X magnification. All cells within one 10-15 mm random transect were counted at 1560X magnification. In total, 250-300 cells were counted in each sample. The biovolume of each taxa were determined as the cell count multiplied by the volume of a simple geometric shape corresponding most closely with the size and shape of the algal taxon. Canter-Lund and Lund (1995) and Prescott (1978) were used as taxonomic references.

2.3.3 Zooplankton production in the pelagic habitat

Zooplankton biomass was measured monthly from May to October from duplicate vertical hauls of a 153 µm mesh Wisconsin net having a 30 cm intake opening. The depth of haul was 30m or the complete water column where and when water depths were <30m (28.69 m $\pm$ 0.51). The net was raised at a speed of approximately 0.5 $m \cdot s^{-1}$. The zooplankton was washed into the cod-end of the net and anaesthetized to prevent egg shedding in a wash of Club Soda before being added to a 10% sugared formalin solution. Each zooplankton sample was split using a Folsom plankton splitter to a subsample volume containing post-naupliar stages of >100 of the most abundant taxa of crustaceans. For each sub-sample, the species were enumerated at 5-100x magnification under a GSZ-Zeiss stereo microscope. The number of attached eggs were counted. Sub-sample counts were then extrapolated to the total sample. Biomass of zooplankton were determined from length-to-weight regressions reported by McCauley (1984) using lengths measured with a digitizing system. Up to 25 random length measurements per taxon were taken per sample, and the final biomass was expressed as µg dry weight per sample. The amount of zooplankton biomass per sample was converted to volumetric zooplankton biomass (µg dry weight$\cdot L^{-1}$) using the known volume of water that was filtered by the Wisconsin net. This value was corrected to the

amount of biomass in a 1 m^2 column of water over the depth of water at the sampling site to yield areal biomass units of mg dry weight·m^{-2}.

Zooplankton production was measured at each of the two sampling stations on each lake. Secondary production, in this case by zooplankton (in units of mass·m^{-2}·yr^{-1}), is an indicator of food available to fish, and is the most commonly used indicator of ecological function, water quality, energy flow, disturbance, and recovery in freshwater ecosystems (Benke and Huryn 2010). Secondary production integrates several aspects of ecological performance including density, biomass, growth rate, reproduction, survivorship, and developmental time. Zooplankton production in Seton and Anderson Lakes was determined by re-organizing the equation:

$$\frac{P}{B} = y$$

Equation 1

where P is annual zooplankton production (mass·m^{-2}·yr^{-1}), B is mean annual dry weight biomass (mass·m^{-2}) of the population of interest, and y is a rate in units of yr^{-1} (Benke and Huryn 2006). Given that biomass can be measured and y, known as a production/biomass or P/B ratio, can be found in the literature for many taxa, the product of B and y gives P.

Production of zooplankton was determined from Equation 1, but P/B was calculated from a temperature dependent model reported by Shuter and Ing (1997) and shown to work well by Clarke and Bennett (2007):

$$[P{:}\,B]_{daily} = 10^{(\alpha_{taxon} + \beta T_{daily})}$$

Equation 2

where $[P{:}\,B]_{daily}$ is daily $P{:}\,B$, $\propto_{taxon}$ is -1.725 for cladocerans, -1.766 for cyclopoid copepods, and -2.458 for calanoid copepods, β is 0.044 for cladocerans, 0.040 for cyclopoid copepods, and 0.050 for calanoid copepods, and T is average water temperature (ºC) measured over the depth that zooplankton were collected on each sampling day. Zooplankton biomass and $[P{:}\,B]_{daily}$ was linearly interpolated between the six sample dates distributed between May and October, and the product of $[P{:}\,B]_{daily}$ and zooplankton biomass was summed over the sampling period May through October to estimate annual zooplankton production. In this approach, zooplankton production in the active growing season of May through October was considered to include most production for the calendar year and was called annual zooplankton production.

2.3.4 Environmental variables

Environmental variables (predictor variables for statistical (regression) modeling) were measured monthly, corresponding with the time of primary production measurements in pelagic habitat at C1 and over the time series of periphyton sampler incubation in littoral habitat also at C1. The same data from each station on Seton and Anderson Lakes where biological production was measured as part of BRGMON6 were also used as part of the regression analyses.

We prioritized five abiotic variables that have been shown to affect periphyton production in littoral habitats and one biotic and six abiotic variables known to affect zooplankton production in pelagic habitats. Hypotheses for each variable included in the periphyton and zooplankton analyses are detailed in Table 3 and Table 4, respectively.

Table 3. Hypotheses for predictor variables included in the polystyrene ball and sand pail periphyton analyses.

Variable	Metric/Unit	Hypothesis	Prediction	Level	Reference
PAR	Accumulated PAR over incubation time (μMol/m^2)	PAR is a limiting factor for the growth and production of photosynthetic algae	Positive	By Depth	(Lamberti and Steinman, 1997)
Temperature	(°C)	Affects metabolic activity and consequently periphyton growth	Positive	By Depth	(Allan and Castillo, 2007c; Bothwell, 1988; Lamberti and Steinman, 1997)
Phosphorus	Soluble reactive phosphorus (mg/L)	Periphyton growth can be limited by phosphorus	Positive to a threshold	Station	(Perrin, Bothwell, and Slaney, 1987; Rosemond, Mulholland, and Elwood, 1993)
Nitrogen	Dissolved inorganic nitrogen (mg/L)	Periphyton growth can be limited by nitrogen	Positive to a threshold	Station	(Perrin and Richardson, 1997; Rosemond, Mulholland and Elwood, 1993)
Turbidity	(NTU)	Increases light scatter and subsequently decreases light availability for algal production	Negative	By Depth	(Leland, 1995)

Table 4. Hypotheses for predictor variables included in the zooplankton analyses.

Variable	Metric/Unit	Hypothesis	Prediction	Level	Reference
Phytoplankton production	0.20 μm Chlorophyll-a (μg/L) 0.75 μm Chlorophyll-a (μg/L)	Food source for zooplankton	Negative	Sample	(Burks, Lodge, Jeppesen, and Lauridsen, 2002)

Variable	Metric/Unit	Hypothesis	Prediction	Level	Reference
Temperature	°C	Affects physiology and population ecology of zooplankton	Positive	Station and sampling day	(Burks, Lodge, Jeppesen, and Lauridsen, 2002)
Turbidity	NTU				(Burks, Lodge, Jeppesen, and Lauridsen, 2002)
78-day mean water residence time	Days	Longer residence time provides longer growing period for zooplankton within the reservoir	Positive	Reservoir and sampling day	(Korpelainen, 1986; Schwatz, and Ballinger, 1980)
78-day mean drawdown	m	Less habitat available for zooplankton as drawdown increases	Negative	Reservoir and sampling day	(Korpelainen, 1986; Schwatz, and Ballinger, 1980)
Distance from inflow	km	There would be greater biomass as distance from inflow increased due to currents concentrating plankton towards the outflow.	Positive	Reservoir and sampling day	
Station depth	m	Greater habitat availability for zooplankton.	Positive	Station and sampling day	

The monthly sampling dates spanned the complete algal growing season (May to October 2015). Temperature, PAR, turbidity and dissolved oxygen were measured over a vertical profile from surface to bottom using a Sea-Bird Electronics SBE19plusV2 CTD at C1 at the time that phytoplankton production measurements were done. The PAR data for the periphyton analysis was correlated with PAR that was continuously logged at a shore base station allowing the continuous measurements to be corrected for attenuation in water and used to calculate total accumulated PAR during incubation of the littoral periphyton samplers. Total accumulated PAR over the incubation period for each series was used in the periphyton analyses and mean daily PAR by station and sampling day was used in the zooplankton regression analyses. The mean was deemed an acceptable surrogate data by depth for the zooplankton analyses given the samples were taken from a single haul on a single sampling day and down to a maximum of 30 m (maximum depth for zooplankton hauls). Figure 2 shows the range in temperatures in Anderson, Carpenter and Seton lakes.

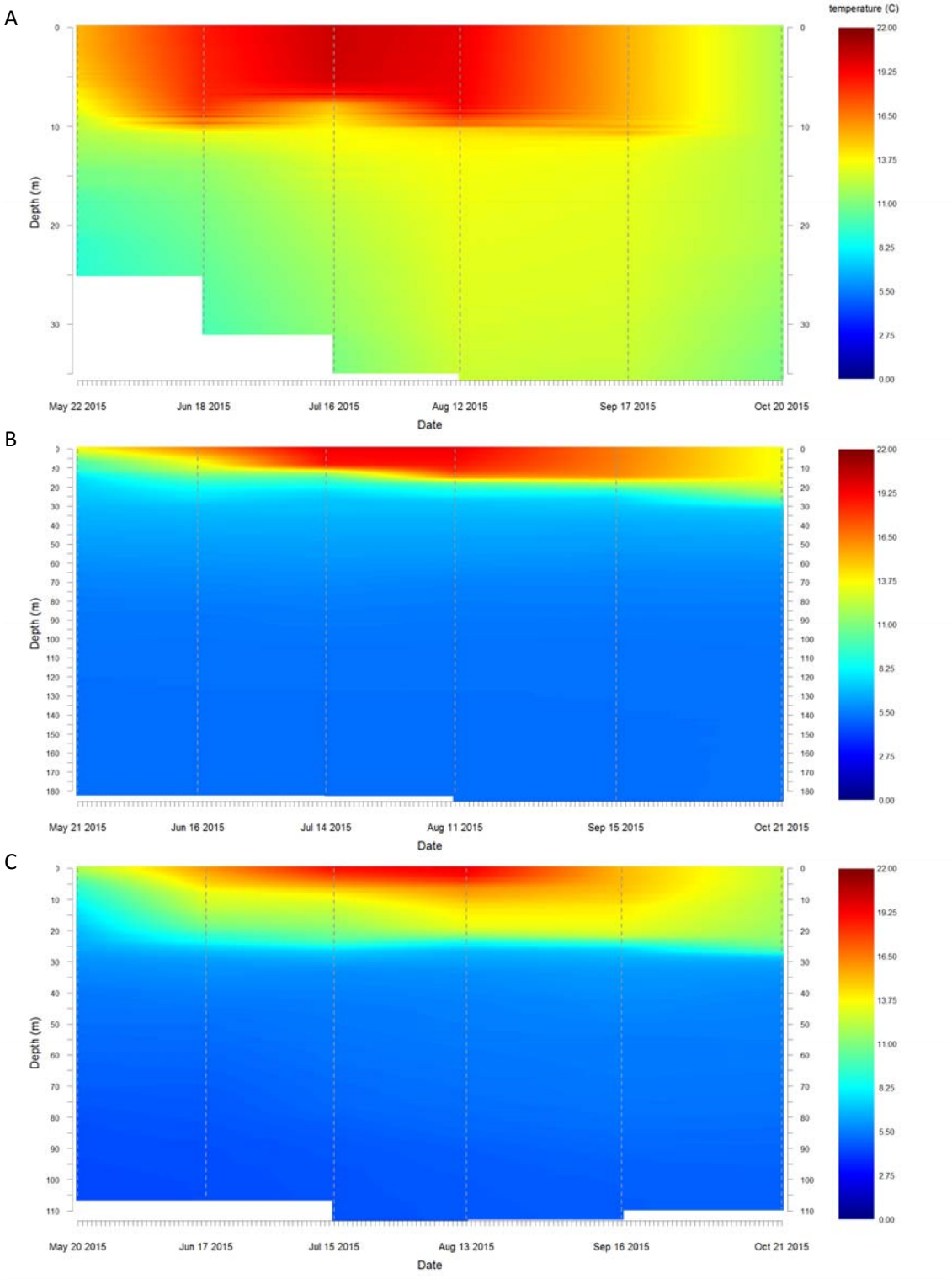

Figure 2. Temperature stratification in (A) Carpenter Reservoir at station C2, (B) Anderson Lake at station A1, and (C) Seton Lake at station S4 from May to October 2015. Note the difference in depths on the y-axis.

Temperature was also continuously measured at several depths along a thermistor chain installed at the trash boom, providing continuous temperature data for each depth that periphyton samplers were deployed in Carpenter Reservoir. Temperature by station, sampling day and depth measured by the Sea-Bird CTD were used for Anderson and Seton Lakes whereas temperature for Carpenter Reservoir was the mean temperature measured by the logger on the thermistor chain over the incubation period at each depth.

Water residence times for Carpenter Reservoir and Seton Lake were calculated as rate of outflow (data from BC Hydro) divided by reservoir volume, which was determined from a digital elevation model (DEM) developed by BC Hydro for this project. Water residence time for Anderson Lake was derived from bathymetric data collected in 1961 (Geen and Andrew, 1961). The amount of drawdown by month was calculated as the difference between the maximum height and the daily height of the reservoir or lake. For this report, the mean water residence time and mean drawdown were calculated using the daily values for 78 days prior to each sampling day, corresponding to the maximum reported lifespan of common zooplankton species (Korpelainen, 1986; Schwartz and Ballinger, 1980). Distance to inflow was the distance from the sampling station to the inflow source of each reservoir or lake. The inflow sources were the Gates Creek discharge in Anderson Lake, the discharge at Shalath in Seton Lake and the interface of the Middle Bridge River and reservoir in Carpenter. The distance to inflow was a constant value over the course of the sampling season for Anderson and Seton Lakes but varied by sampling date in Carpenter because of the change in water levels in the reservoir over time. The distance was calculated in Google Earth using the Ruler tool. The station depth was measured at each station on each sampling day using the depth sounder on the boat.

Soluble reactive phosphorus (SRP), dissolved inorganic nitrogen measured as the sum of ammonium (NH_4-N) and nitrate (NO_3-N) and pH were measured from one water sample collected from the surface and one from the hypolimnion using a VanDorn bottle each month, closely corresponding with the beginning and end of a periphyton sampling series and the dates of primary production measurements at C1. If Carpenter Reservoir was not stratified, a sample was collected from the reservoir surface and another from 2m off the bottom. These analyses were completed using standard methods at the ALS Canada Lab in Burnaby, B.C. Mean SRP and DIN were calculated by station and sampling day for the periphyton and zooplankton regression analyses.

See Table 5 for the mean values for each of the environmental variables used in the periphyton and zooplankton analyses.

Table 5. Mean environmental variables by lake for 2015 used in the periphyton and zooplankton regression analyses.

Reservoir/ Lake	Station	Station Depth (m)	Distance to Inflow (km)	Mean Water Residence Time (days)	Mean Draw-down (m)	DIN (μg/L)	SRP (μg/L)	Daily PAR (μMol/m^2)	Accumulated PAR (μMol/m2)	Temperature (°C)	Turbidity (NTU)	Chl a 0.20 um filter size (μg/L)	Chl a 0.75 um filter size (μg/L)
Anderson	A1	206.2	11.7	1592.54	1.29	40.12	1.01	205.08	308,629,582	12.60	2.32	1.18	0.93
	A2	196.4	17.7	1592.54	1.29	47.86	1.00	212.40	201,319,510	12.64	0.45	0.66	0.76
Carpenter	C2	37.5	44.1	80.03	7.80	15.28	1.19	78.07	521,565,699	13.44	9.31	0.97	0.80
	C6	26.4	30.7	80.03	7.80	16.09	1.23	103.31	-	13.07	14.27	1.28	0.87
Seton	S4	119.4	9.4	232.56	0.28	30.73	1.01	117.89	150,666,404	12.06	4.09	1.27	1.07
	S5	110.0	14.9	232.45	0.28	27.88	1.00	76.46	269,772,432	11.86	3.14	1.01	1.04

2.3.5 Analytical approach for periphyton and zooplankton production

We used multiple regression analyses to show the relative importance of habitat attributes that cumulatively contribute to change in periphyton and zooplankton production. This approach provides equations that can be used to describe change in periphyton and zooplankton production as a function of variation among habitat attributes selected *a priori*. Regression analysis also retains the original units of measure and allows quantitative prediction of the dependent variable with estimated error.

The regression model that was fit to the data collected from the field had the following form:

$$y_i = \beta_0 + \beta_1 x_{i1} + \beta_2 x_{i2} \ldots . + \beta_j x_{ij} + \varepsilon_i$$

Equation 3

where

y_i is the value of algal production for an ith observation,

$x_{1\ldots j}$ is the value of independent variable 1 and j is the number of independent variables,

β_0 is the intercept when all predictor variables (e.g. variables describing habitat attributes) have a value of zero,

β_1 is the regression slope for y on x_1 when all other predictor variables (other x's) are held constant,

β_2 is the regression slope for y on x_2 when all other predictor variables (other x's) are held constant,

β_j is the regression slope for y on x_j when all other predictor variables (other x's) are held constant, and

ε_i is unexplained error associated with the $i$the observation.

We conducted four separate analyses, two for periphyton production and two for zooplankton production as example analyses for this report. We constructed separate models for periphyton growth on stony substrates (polystyrene balls) and sand substrates (sand pails) and two separate models for zooplankton production, one including phytoplankton biomass (as a predictor variable) sampled with a 0.20 μm filter and the second for phytoplankton biomass sampled with a 0.75 μm filter (see section 2.3.3 of this report for a detailed description). We hypothesized that zooplankton would have a different response to different size classes of phytoplankton. These were labeled as $\text{zooplankton}_{0.20\ \mu\text{m filter}}$ and $\text{zooplankton}_{0.75\ \mu\text{m filter}}$.

For the polystyrene and sand pail samples, we calculated the mean for two replicates taken from two stations, at each depth, during each of three incubation

periods over the course of the sampling season in Carpenter Reservoir, Anderson and Seton Lakes, which resulted in 85 data points for the polystyrene analysis and 18 for the sand pails (Carpenter only). Zooplankton samples were the total biomass collected in a 30m haul (or from the reservoir bottom in the case of Carpenter) from each lake, station and month, which resulted in 32 observations.

We checked for multicollinearity among the environmental variables using variance inflation factors (VIF) and correlation coefficients (Zuur, Ieno, and Elphick, 2010). The combination of variables used in each of the periphyton and zooplankton regressions were not highly correlated (VIF scores < 3.5 and correlation coefficients < 0.6) so we did not need to exclude any variables from the regression analyses. Periphyton biomass, measured as chlorophyll-a, and zooplankton biomass were log-transformed to model the exponential accrual that algae exhibits over time and to satisfy assumptions of normality.

We generated a list of models with various combinations of biotic and abiotic variables identified in Table 3 and Table 4, limiting the number of parameters in each model to approximately one for every 10 data points, to avoid spurious results due to overfitting (Harrell, 2001). This approach generated 40 models for the polystyrene analysis, 27 models for the sand pail analysis, and 57 models for each zooplankton analyses. We used Akaike's information criterion for small sample sizes (AICc) to evaluate support for each model/competing hypothesis (Akaike, 1974; Burnham and Anderson, 2002). We relied on ΔAICc, model weights (w_i), evidence ratios (ER) and adjusted r^2 to aid in the interpretation of model rankings. Delta AICc is the difference in AICc values between model *i* and the top ranked model, w_i is the probability that model *i* is the best model given the model set and ER is $w_{top\ model}/w_i$, which indicates the likelihood that the top model is better than model *i.*

All regression analyses were performed in R (R Development Core Team, 2011).

2.4 Questions 3 & 4: Is light penetration in Carpenter Reservoir impacted by changes in reservoir operations and can suspended sediment transport into Seton be altered by changes in Carpenter Reservoir operation?

2.4.1 CE-QUAL-W2 model overview

Simulation modeling supported with empirical data will be used to answer questions 3 and 4 after all years of work. Over that time we will explore the effect of a wide range of reservoir operation and natural inflow scenarios on PAR, temperature, nutrient concentrations, and water residence time that are predictors of algal production (Section 2.3.4) using a hydrodynamic simulation model. Output of PAR, temperature, and nutrient concentrations from that model will be input into the regression models described in Section 2.3.5 to predict algal production among scenarios of reservoir operation and natural inflow. The following paragraphs describe the modeling approach.

The simulation model will be CE-QUAL-W2, a hydrodynamic and water quality model for rivers, lakes, reservoirs and estuaries. CE-QUAL-W2 laterally averages calculations (across channel) with segments along the length of the water body, and bins from the surface to the bottom. This structure makes CE-QUAL-W2 particularly suited for modelling long and narrow water bodies such as Carpenter Reservoir. Lateral averaging reduces the model to 2-dimensions, capturing the important physics along the length of the reservoir while ensuring the run time for the model is reasonable for a desktop computer. This also makes it possible to explore a wide range of reservoir operation scenarios. CE-QUAL-W2 has been widely used, having been applied to over 200 reservoirs in the United States, and more than 100 other reservoirs worldwide (http://www.ce.pdx.edu/w2/). The source code for CE-QUAL-W2 is publicly available, and is currently being developed and maintained at Portland State University (http://www.ce.pdx.edu/w2/) for the US Army Corp of Engineers. In addition, CE-QUAL-W2 is widely accepted in the scientific literature, making it ideal for our purposes.

CE-QUAL-W2 solves laterally averaged equations of fluid flow for conservation of mass, and conservation of momentum along the length of the reservoir. The model assumes that the reservoir is well mixed across channel, a reasonable assumption in a narrow reservoir like Carpenter Reservoir. The model will solve transport equations for temperature, conductivity, turbidity, and nutrients in Carpenter Reservoir. Conductivity is not a predictor of algal production but it is needed for solving mass transport equations. Turbidity is a measure of optical properties of water by light scattering. It can be correlated with PAR that will be a predictor of algal production (Section 2.3.1) and used in place of PAR for modelling purposes. Hence, three of the predictors of algal production that are described in Section 2.3.4 (PAR, temperature, nutrient concentration) will be turbidity, temperature, and nutrient concentration in CE-QUAL-W2. Values of turbidity in output from CE-QUAL-W2 will be approximately converted to PAR as input into the regression models described in Section 2.3.5 or prediction of algal production in the second part of simulation modeling described above in this section.

2.4.2 Input data

CE-QUAL-W2 requires data describing the physical and chemical state of the reservoir over time periods when it will be run. The time will be May through October in each of 2015 and 2016. This duration covers the time from lowest water surface elevation and volume (early spring) to highest water surface elevation and volume (fall) and the time of most annual algal production. Data describing wide ranging habitat conditions allows for diverse reservoir management scenarios to be run after the model is compiled. Several measurements were made in 2015 to set up and calibrate CE-QUAL-W2 and they will be repeated in 2016 to support testing of the model or provide data for further calibration if found necessary during model development. Existing chemical data from 1995 and 1996 (Perrin and MacDonald 1999) were accessed and appended to the new data collected in 2015.

A basic tool for setting up and running CE-QUAL-W2 is a digital elevation model (DEM) of the reservoir. The DEM supports calculations of water volumes in the whole reservoir and in various segments and bins for given water surface elevations. The production of a DEM was completed by BC Hydro as part of this study.

The physical and chemical measurements within the reservoir were completed among stations situated along the longitudinal axis. Detailed measurements were made at each of the 10 stations shown in Figure 1 during each of the monthly sampling episodes when water depth was a minimum of 10m at a given station. The stations overlapped those established for earlier nutrient budget studies (Perrin and MacDonald 1999), thus providing consistency between data sets. The measurements were as follows:

Tributary water quality

The water quality of tributaries to Carpenter Reservoir was sampled monthly from May to October 2015. The area draining to Carpenter Reservoir can be divided into five major components:

1. Drainage area to La Joie Dam 26.7%
2. Hurley River 18.2%
3. Gun Creek 15.9%
4. Tyaughton Creek 20.5%
5. Other local drainage 18.7%

Of these components, the outflows from the first four were sampled, representing 81.3% of the total drainage. In addition, two smaller tributaries that contribute to the balance of the local drainage were also sampled, one from the north side of Carpenter Reservoir, Marshall Creek, and one from the south side, Keary Creek.

Sampling of the Middle Bridge River was done at three locations:

- Middle Bridge River above the Hurley, sampling below La Joie dam but above the confluence with the Hurley River;
- Middle Bridge River below the Hurley; and
- Middle Bridge River at Confluence, sampled after the Middle Bridge River has crossed the drawdown zone and enters the wetted reservoir.

Data were also collected from the outflows from Carpenter Reservoir, and from the Upper Bridge River for comparison.

Continuous turbidity monitoring in tributaries

A turbidity recorder was moored in the Bridge River above Carpenter Reservoir (UTM 10U 511,946 Easting 5,634,532 Northing). The recorder consisted of a RBR Virtuoso, connected to a Seapoint optical backscatter sensor (OBS). In 2015 the OBS was deployed without a without a wiper; a wiper was added to the deployment in 2016. The OBS was placed face up at the highest point to reduce fouling. Data was recorded every 2 minutes.

Meteorological data

In 2015, three sources of meteorological data were available near Carpenter Reservoir:

1. BC Hydro sensors at Terzaghi Dam: This station provides hourly wind speed, wind direction and air temperature.
2. Limnotek station at Terzaghi Dam: This station was setup close to the BC Hydro sensors and consisted of a Hobo Micro Station Data logger (H21-002) with PAR (S-LIA) and Solar Radiation (S-LIB) sensors. An Onset Hobo Pro (U23) was used to measure air temperature and relative humidity.
3. BC Wildfire Service Fivemile site: This weather station is approximately half way up the reservoir (50° 54’ 39” N, 122° 41’ 20” W, elevation 865 m), and records wind speed and direction, air temperature and relative humidity.

Monthly Sea-Bird profiles

Profiles were collected using a Sea-Bird Electronics SBE19plusV2 CTD (conductivity, temperature, depth) profiler. This instrument, designed for oceanographic work, provides high accuracy (0.005 °C), high resolution (0.0001 °C) and stable temperature. The particular design of the conductivity cell gives rise to unprecedented accuracy and stability at low conductivity, with excellent results in fresh water. As the

profiler is lowered through the water column, it collects four samples a second which are recorded internally for upload after the survey. The profiler was equipped with a WETlabs EC0 combined fluorometer and turbidity meter, a Photosynthetically Active Radiation (PAR) sensor, and a SBE43 dissolved oxygen sensor.

Surveys of the reservoir were conducted monthly from May to October 2015, with Seabird profiles collected at up to 10 stations along the 50 km length of the reservoir, providing a snapshot of the reservoir each month, and giving a detailed view of the gradients along the reservoir.

At each station, the Seabird profiler was lowered on the sunny side of the boat to record light data. The Secchi depth was measured at each station. The Secchi depth was the mean of the depth at which the disk disappeared on the way down, and the depth it reappeared on the way up.

Mooring

The mooring consisted of a line with temperature recorders attached to the Carpenter Trash boom upstream of the Bridge 1 and 2 intakes. The mooring was attached to the boom at the location with greatest depth (UTM 10U 551,263 Easting 5,624,112 Northing). The mooring was deployed from 16 April to 20 October 2015.

The line consisted of 1.8 m of ¼" galvanized chain at the top, and 5/8" Samson Quik-Splice for the remainder, a 12 strand single braid polyolefin rope with low stretch (specific gravity 0.94, weight 11.9 kg/100 m). At the bottom of the mooring, was attached 20 lbs of steel to stabilize the line.

The depths of the temperature recorders are given in Table 6. Most of the temperature recorders were Onset U22-001 Hobo Water Temp Pro v2 (HWTP) loggers with accuracy of ±0.2 °C and resolution of 0.02 °C. The Onset HWTPs recorded every 20 minutes. Also included were two high accuracy RBR Solo T recorders, with accuracy ±0.002 °C, resolution of <0.05 m°C, and recording every 3 seconds. At the bottom of the mooring a RBR Solo D depth recorder was included to measure movement of the mooring, recording every 6 seconds.

Table 6. Mooring in Carpenter Reservoir, 16 April to 20 October 2015.

Depth (m)	Instruments (16 Apr - 20 Oct 2015)
0.5	HWTP 1068-5988
1	RBR Solo T 75933
2	HWTP 1068-5976
3	HWTP 1068-5977
5	HWTP 1068-5978
7	HWTP 1068-5979
10	HWTP 1068-5980

Depth (m)	Instruments (16 Apr - 20 Oct 2015)
15	HWTP 1068-5981
20	RBR Solo T 76651
~20[(1)]	HWTP 1068-5982
25[(2)]	
27[(3)]	RBR Solo T 76652
	RBR Solo D 78474
30 [(2)]	RBR Virtuoso 54153 with Seapoint turbidity 14839

(1) Tied up near 20 m from 16 April to 18 June; these data not used.

(2) From 18 June to 20 October.

(3) From 16 April to 22 May; removed for service from 22 May to 18 June.

The mooring line included an RBR Virtuoso turbidity recorder, connected to a Seapoint optical backscatter sensor (OBS) with a Zebra Hydro Wiper. Data was recorded every 2 minutes. The turbidity recorder was at the same depth at the Solo T and Solo D at the bottom of the mooring (Table 6). On 23 April 2015, the bottom Solo T sensor, along with the Solo D and turbidity recorder were deployed at 27 m depth, just above the bottom (28.5 m). After deployment, the water level in Carpenter Reservoir declined slightly. On the first sampling trip on 22 May 2015 (day 142) the mooring was inspected and the bottom sensors were found to have dragged along the bottom. The instruments were undamaged except for the wiper arm, which was bent. The bottom three instruments were removed for service, a replacement wiper arm was built, and the instruments were reattached at 30 m during the following sampling trip on 18 June 2015 (day 169). The mooring was pulled up to the surface each month to inspect the turbidity sensor; data during these times were removed. The depth recorder data showed brief periods when the bottom of the mooring was shallower than expected; this could have resulted from the log boom shifting to a shallow location, or from drag on the mooring as the boom moved from one location to another. Data during the worst cases were removed.

Upon removal of the main mooring line on 20 October 2015, three temperature recorders were attached to the log boom for the winter. The recorders were hung from individual lines, consisting of chain to 1 m and 3/8” static cord below 1 m, anchored with a 10 lb steel weight ring (Table 7).

Table 7. Mooring in Carpenter Reservoir, 20 October 2015 to 13 April 2016.

Depth (m)	Instruments 20 Oct 2015 – 13 Apr 2016
0.5	HWTP 1011-0014
5	HWTP 1011-0083
10	HWTP 1011-0084

2.4.3 CE-QUAL-W2 Modelling

The model was run from spring through to fall, to simulate the evolution of the biologically productive season. The model was started on the date of the first sampling trip, 22 May 2015 (day 142), and was ended on the date of the last sampling trip, 20 October 2015 (day 293).

The model requires initial conditions to specify the state of the reservoir at the start of the model run. Initial conditions for temperature and conductivity were determined from the Seabird profiles on 22 May 2015. The initial concentration of TSS and nutrients were determined from the bottle samples collected on 22 May 2015.

As the model runs through a computational grid (Figure 3), it requires boundary conditions such as river inflow and meteorological data. The model has been setup with inflow from Bridge River, inflow from the local drainage, outflow to the Bridge River powerhouses, and outflow from Terzaghi Dam. The local inflow is distributed along the length of the reservoir based on drainage area.

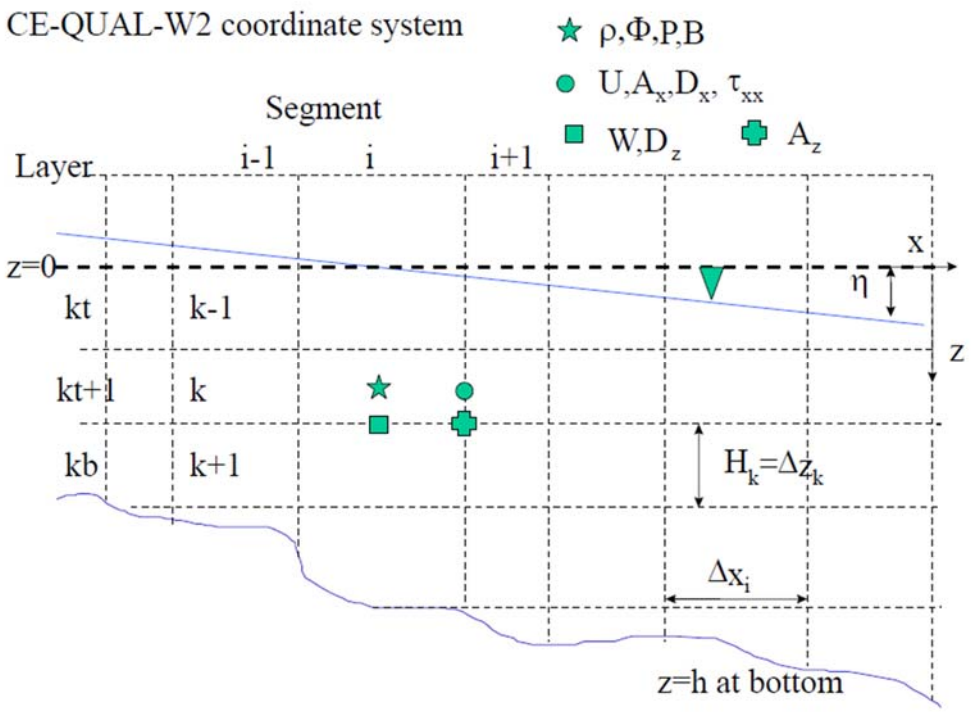

Figure 3. CE-QUAL-W2 computational grid. Width (B), density (ρ), pressure (P) and water quality state variables (Φ) are defined at cell centers. Horizontal velocity (U), longitudinal eddy viscosity (A_x) and diffusivity (D_x), and longitudinal shear stress (τ_{xx}) are defined at the right hand side of the cell. Vertical velocity (W) and vertical diffusivity (D_z) is defined at the bottom of the cell, and the vertical eddy viscosity is defined at the lower right corner of the cell. Adapted from Cole and Wells (2015).

2.4.4 Model Bathymetry

As described earlier, 10 sampling stations were located along the length of Carpenter Reservoir. Based on the sampling stations, and in consultation with B.C. Hydro, the reservoir was divided into 13 reservoir segments. In most cases, there was one segment for each sample station, and in some cases there were two. The stations associated with each segment in CE-QUAL are shown in Table 8, and a plan view of the segments is shown in Figure 4.

Each segment was divided into vertical layers. The model was setup with 109 layers of 0.5 m depth each. In the deepest segment next to the dam (#14), there were 107 active layers (layer 2 to 108), and layers 1 and 109 were boundary layers used by the model (Figure 5). Farthest from the dam, segment #2, had 17 layers, with 15 active layers (layers 2 to 16) and 2 boundary layers (layer 1 and 17) (Figure 6). A side view of Carpenter Reservoir showing all layers in each active segment is shown in Figure 7.

Table 8. Stations and model segments

Station	CE-QUAL Segment	Comment
-	1	Boundary segment for the model (inactive)
C10B	2	Segment with inflow from Bridge River
C10A	3	
C9	4	
C8	5	
C7	6	
C6B	7	
C6A	8	
C5	9	
C4	10	
C3	11	
C2B	12	
C2A	13	Segment with outflow to Bridge powerhouses
C1	14	Segment adjacent to Terzaghi Dam
-	15	Boundary segment for the model (inactive)

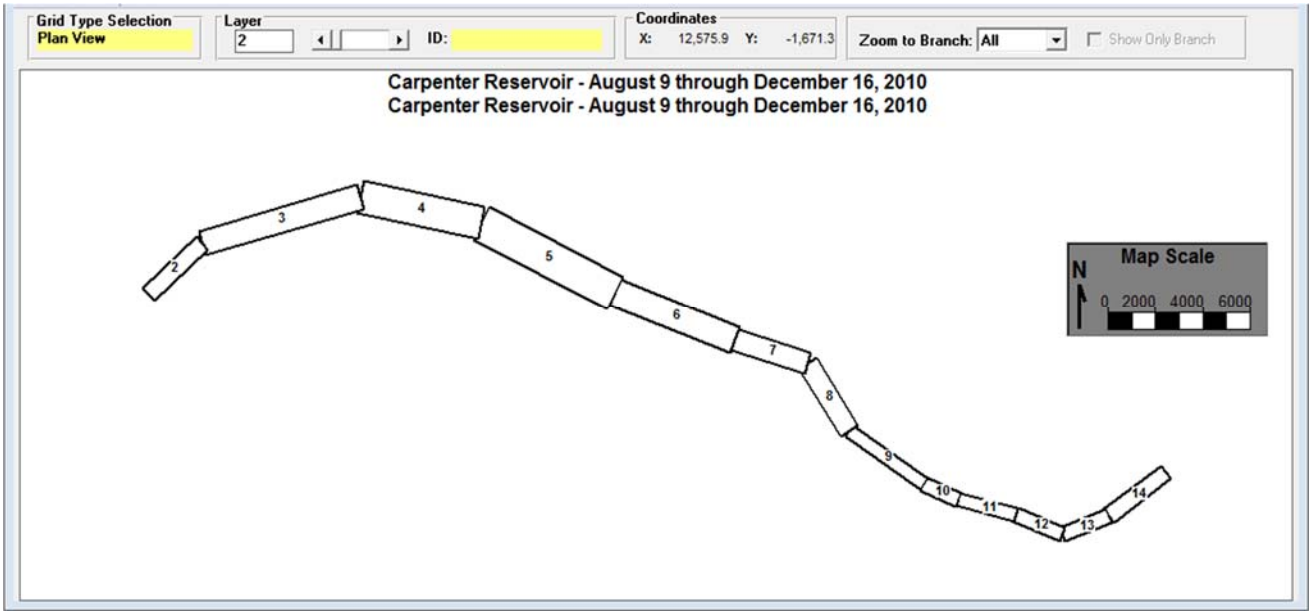

Figure 4. Plan view of model segments. The Bridge River flows into Segment 2. Terzaghi Dam is located at the east end of Segment 14. Segments 1 and 15 (not shown) are inactive boundaries for use by the model.

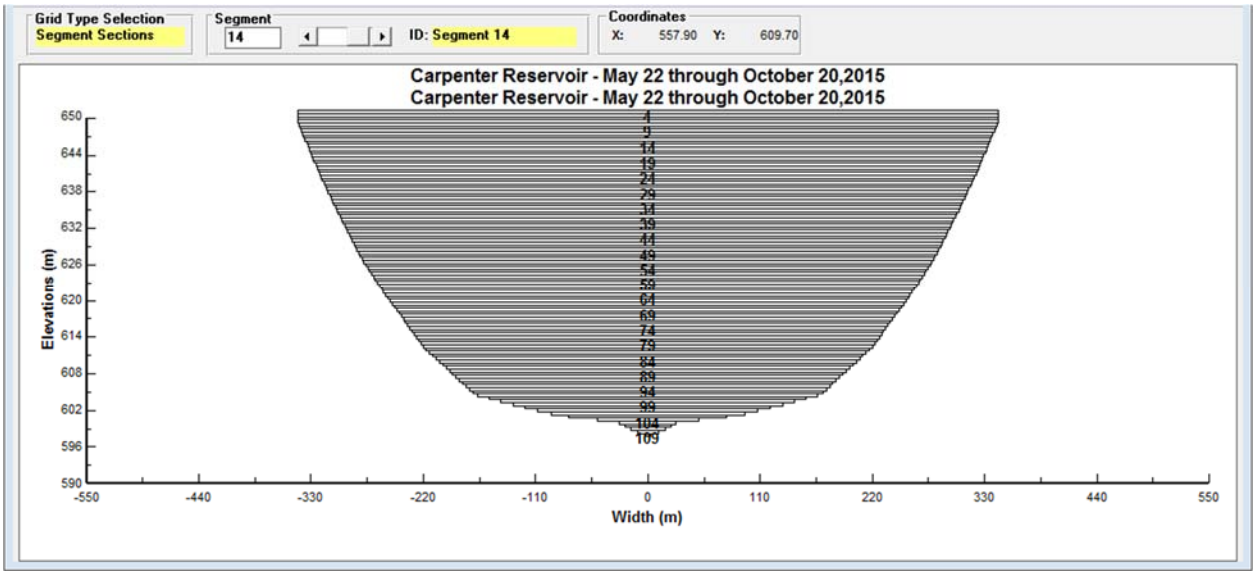

Figure 5. Cross channel profile of Segment 14, the last active segment before Terzagi Dam. Shown are 107 active layers of 0.5 m each (layers 2 to 108). Layer 1 and 109 are inactive boundaries for use by the model. The top elevation of first active layer #2 is 651 mASL and the bottom elevation of the last active layer #108 is at 597.5 mASL. The bottom elevation of the bottom active layer is 597.5 mASL.

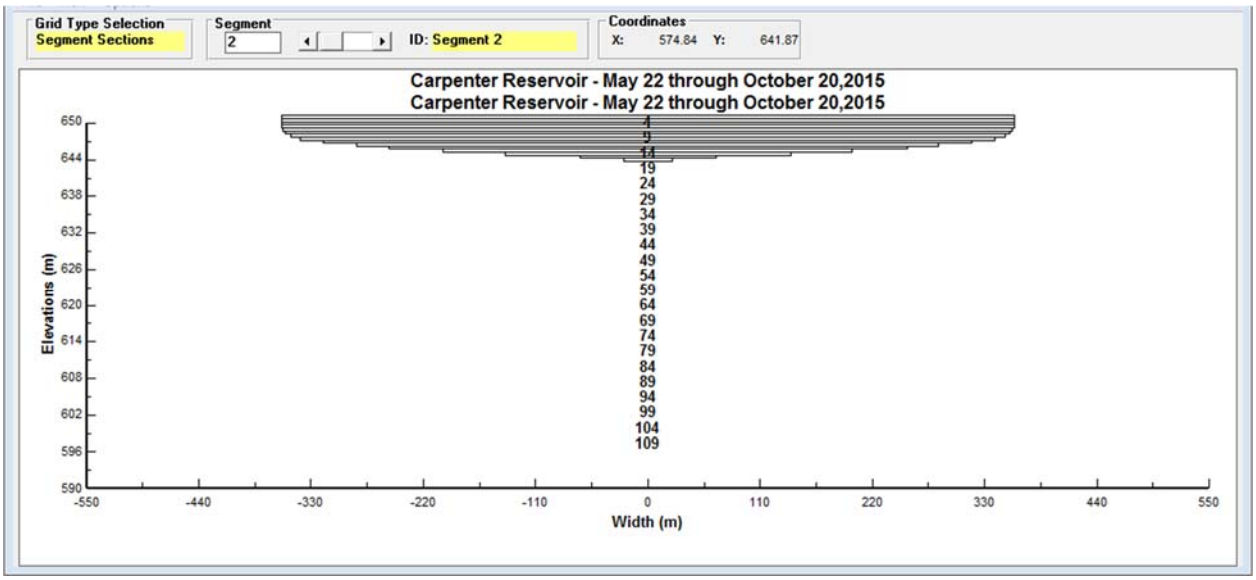

Figure 6. Cross channel profile of Segment 2, the shallowest active segment of the reservoir which received inflow from the Bridge River. The top elevation of first active layer #2 is 651 mASL and the bottom elevation of the last active layer is 643.5 mASL.

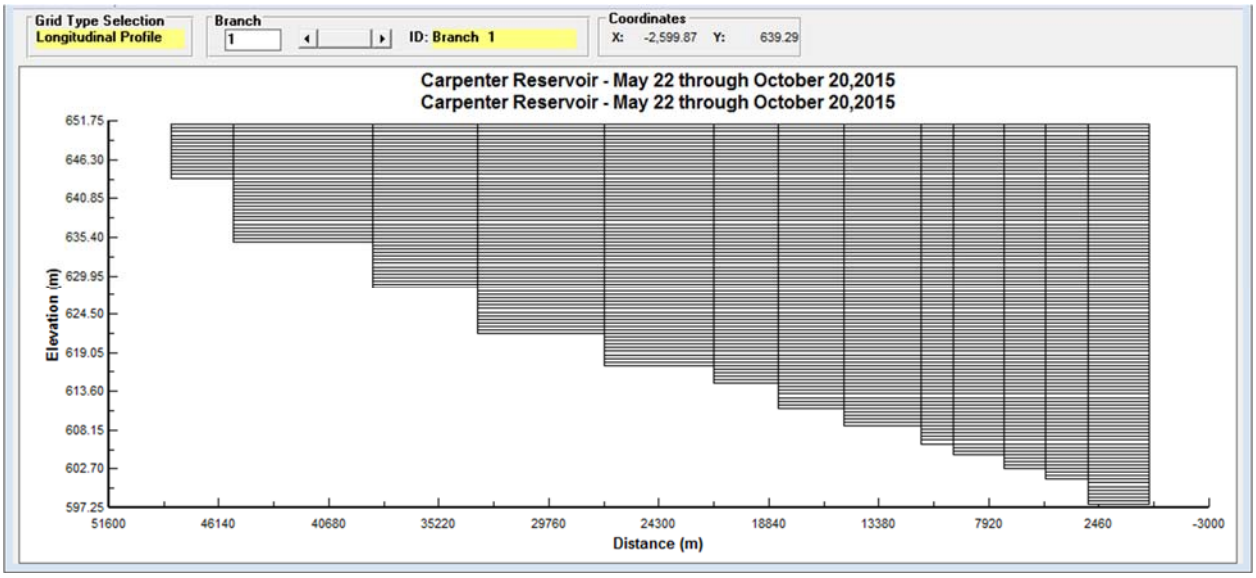

Figure 7. Side view of Carpenter Reservoir showing the 13 active segments along the length of the reservoir and the 108 active layers. The Middle Bridge River enters on the left, and Terzaghi Dam is adjacent to the deepest segment on the right.

2.4.5 Model setup and analysis scripts

It is important to make it convenient to both setup the model and read the output due to the large number of model runs. CE-QUAL-W2 requires all inputs as text files in a specific format that are time consuming to create. The output of CE-QUAL-W2 is also written to text files. We have begun writing routines in MATLAB to create the input files for, and read the output data from CE-QUAL-W2. MATLAB is a widely used scientific and engineering programming environment for data analysis and plotting.

3 RESULTS AND DISCUSSION

3.1 Overview

Data from the 2015 sampling season is the first in a three-year study to answer four questions about what environmental variables and reservoir activities affect productivity in Carpenter Reservoir. The following sections detail preliminary results from Carpenter Reservoir and include data from Anderson and Seton Lakes, where appropriate, to enhance the statistical power and biological interpretation of the results.

3.2 Question 1: Is light the primary factor regulating productivity of the littoral habitat in Carpenter Reservoir

3.2.1 Stony substrate

3.2.1.1 Community composition

Periphyton found on polystyrene balls in Carpenter Reservoir were comprised of 64%, 71% and 86% chlorophytes during spring, summer and fall incubation periods, respectively (Table 9; Figure 8A; Greens). The chlorophytes in these samples were predominantly *Spirogyra* spp. Diatoms were also prevalent in all three time series making up 12-33% of the total biovolume of periphyton. *Melosira* sp., *Nitzschia* sp., *Cymbella* sp., *Achnanthes* sp. and *Stauroneis* sp. were among the most common species found throughout the sampling period.

Table 9. Periphyton biovolume, measured as $\mu m^3 \times 10^9 \bullet m^{-2}$ by lake, substrate and incubation period (series) separated by major taxa. SD is the standard deviation when the mean of two samples was calculated.

Lake	Substrate	Series	Blue Green	Diatoms	Chlorophytes	Chryso - Cryptophytes	Dinoflagellates	Euglenoids	Total Mean Biovolume	SD
Carpenter	Polystyrene balls	Spring	72	1,398	2,651	-	-	-	4,121	529
		Summer	40	1,003	2,651	-	-	-	3,694	-
		Fall	13	1,038	7,085	-	25	51	8,212	-
Anderson		Spring	92	1,272	-	-	-	-	1,364	932
		Summer	21	451	1,444	-	-	-	1,916	-
		Fall	76	2,306	4,629	-	-	-	7,011	-
Seton		Spring	34	823	7	-	-	-	864	23
		Summer	95	1,437	1,609	-	-	-	3,142	294
		Fall	358	1,986	3,153	430	-	-	5,927	3,561
Carpenter	Sand pails	Spring	-	-	-	93	-	-	93	131
		Summer	-	54	-	-	-	-	54	76
		Fall	-	57	4	387	-	-	447	481

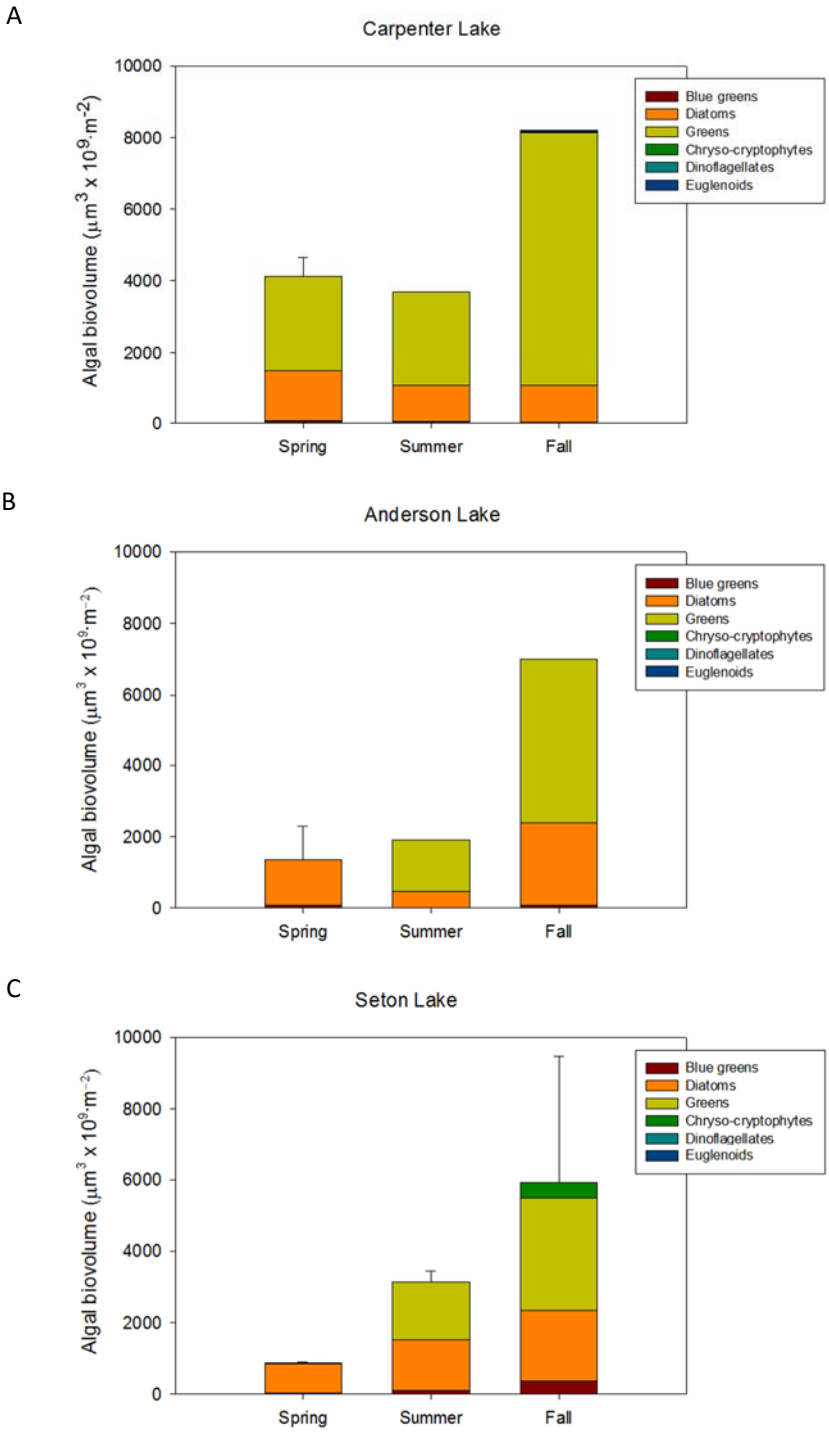

Figure 8. Algal biovolume by group found on polystyrene balls during each incubation period in (A) Carpenter Reservoir, (B) Anderson Lake and (C) Seton Lake. Standard deviations (error bars) were included where the mean of two samples was calculated.

The bulk of spring samples from both Anderson and Seton Lakes were comprised of diatoms (93% and 95%, respectively) with *Flagilaria* sp. *Nitzschia* sp. *Cymbella* sp. *Achnanthes* sp. and *Diatoma* sp. being the most abundant (Table 9; Figure 8B & C). A shift in composition occurred between spring and summer in both lakes where chlorophytes, specifically *Spirogyra* sp., became more abundant in the samples making up 75% and 51% of the periphyton community in Anderson and Seton Lakes, respectively. The remainder of the samples were composed of diatoms. This trend continued in Anderson Lake with a slight increase in blue-green algae, predominantly *Aphanisomenon* sp. In Seton Lake, while chlorophytes and diatoms still dominated the community, the biovolume of *Cryptomonas* sp., a chryso-cryptophyte, and blue-green algae, namely *Aphanisomenon* sp. increased (Figure 8B & C).

The chryso-cryptophytes, dinoflagellates and euglenoids identified from the polystyrene samples in Carpenter Reservoir and Seton Lake were likely not part of the samples as they are all free-living flagellated organisms, common to pelagic habitat (Table 9). These individuals were probably gathered from the water column as the polystyrene balls were pulled from the moorings.

3.2.1.2 Regression analysis

Periphyton biomass, measured as chlorophyll-a, growing on polystyrene balls was higher in areas with greater accumulations of photosynthetically active radiation, warmer water and higher concentrations of dissolved inorganic nitrogen as shown by the top model in the AICc analysis (Table 10),

$$logChlorophyll\text{-}a = -0.58 + 2.08 \times 10^{9} * PAR + 0.05 * Temperature + 7.58 * DIN - 1.17 \times 10^{-10} * PAR:Temperature$$

Table 10. Results from the model selection process for the top 10 of 40 models using AICc for periphyton production on polystyrene balls anchored in the littoral habitat. *k* is the number of parameters in each model including the intercept and error terms, logLik is the log-likelihood, adjusted r^2 is the r^2 of the linear regression model adjusted for the number of variables in the model, ΔAICc is the difference between the top model AICc value and subsequent model AICc values, w_i is the model weight for each model and ER is the evidence ratio for each model, which measures the likelihood that the top model is better than model *i.* The dashed line highlights the models with ΔAICc <2. PAR is photosynthetically active radiation, DIN is dissolved inorganic nitrogen measured as the sum of NH_4-N and NO_3-N, and SRP is soluble reactive phosphorus measured as PO_4-P.

Model	*k*	logLik	Adjusted r^2	ΔAICc	w_i	ER
PAR * Temperature + DIN	6	6.30	0.38	0.00	0.30	1.00
PAR * Temperature	5	4.88	0.37	0.51	0.23	1.29
PAR * Temperature + DIN - SRP	7	6.67	0.38	1.64	0.13	2.27
PAR * Temperature + DIN + Turbidity	7	6.37	0.38	2.26	0.10	3.09
PAR * Temperature - SRP	6	5.04	0.36	2.51	0.09	3.50
PAR * Temperature - Turbidity	6	5.02	0.36	2.56	0.08	3.59
PAR * Temperature + DIN - SRP + Turbidity	8	6.72	0.37	4.00	0.04	7.37
PAR * Temperature - SRP - Turbidity	7	5.23	0.36	4.53	0.03	9.62
PAR + Temperature - SRP	5	-2.73	0.24	15.73	0.00	2602.72
PAR + Temperature + DIN - SRP	6	-2.02	0.24	16.63	0.00	4084.94

This top model had an r^2 of 0.38 and was 1.29 and 2.27 times (ER) more likely than the next two models in the model set. Chlorophyll-a increased significantly with accumulated PAR to approximately 2.5 x 10^8 μMol/m^2 and showed signs of saturation between 3 and 4 x 10^8 μMol/m^2 (Figure 9A). Chlorophyll-a continuously increased with temperature between 6 and 20 °C and with dissolved inorganic nitrogen between 0.01 and 0.03 mg/L (Figure 9B & C).

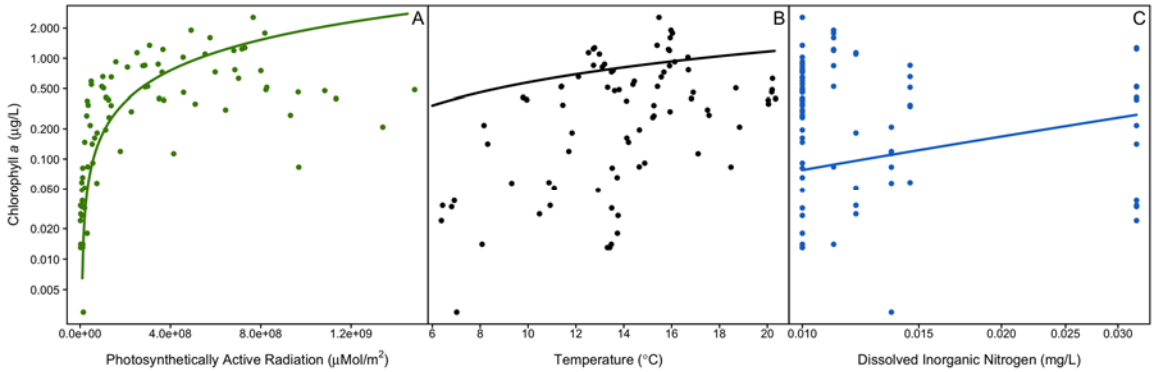

Figure 9. Relationship between chlorophyll-a, (A) photosynthetically active radiation (PAR), (B) water temperature and (C) dissolved inorganic nitrogen (DIN). The y-axis is log-transformed as is the x-axis for dissolved inorganic nitrogen but the data points are all untransformed so that units can be read from the figures. The model lines are derived from the intercept and coefficients from the top model selected by AICc and show the main effect of the environmental variable of interest while maintaining all other variables at their mean value.

There was a significant interaction between PAR and temperature such that the effect of temperature declined with increasing PAR and vice versa. Figure 10 shows a peak in chlorophyll-a concentration at values of PAR greater than 1.5 x 10^9 μMol/m^2 and water temperature less than 10 °C. A smaller peak also exists at PAR less than 5 x 10^8 μMol/m^2 and water temperature above 18 °C. The interaction between PAR and temperature may reflect the inherent seasonality between the two variables such that an increase in water temperature may lag behind increasing accumulated PAR in the spring and remain high into the fall as accumulated PAR declines with decreasing daylight.

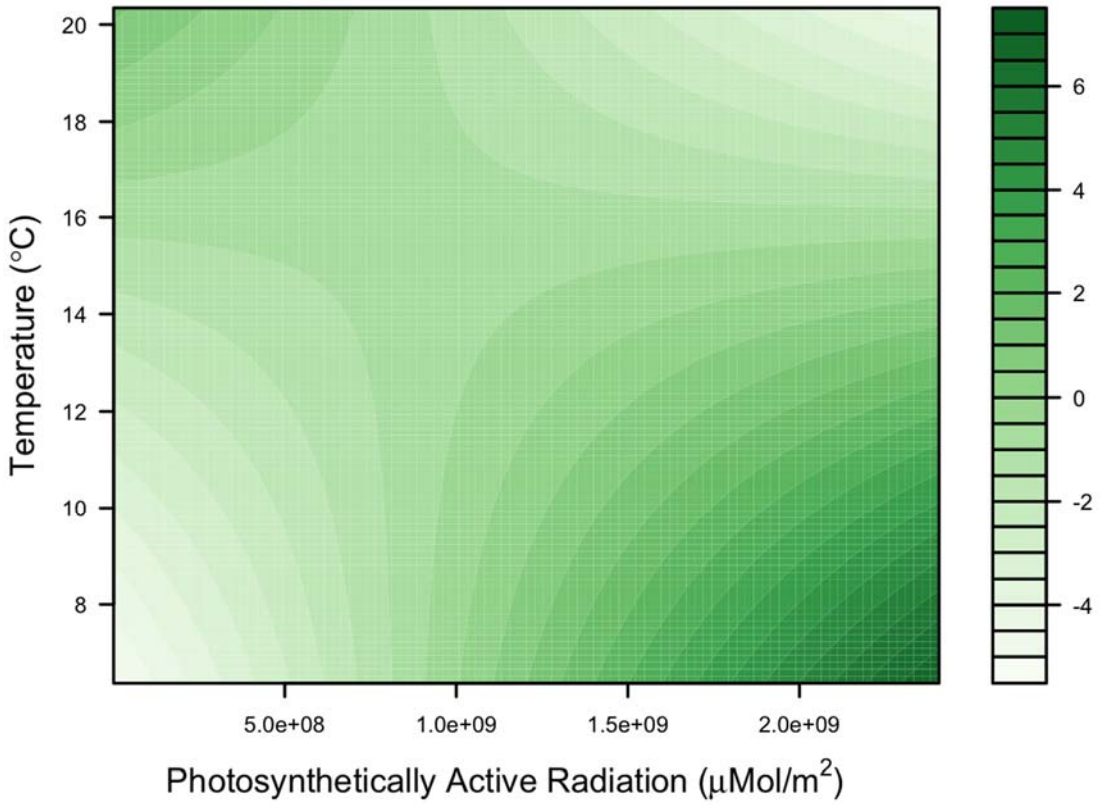

Figure 10. The combined effect of PAR and water temperature on chlorophyll-a concentration on polystyrene balls in the littoral habitat.

Interestingly, we did not see a peak in chlorophyll-a concentration at high temperatures and elevated levels of accumulated PAR as we might have expected based on the physiology of these organisms (Lamberti and Steinman, 1997). However, we know that Spirogyra spp. was the dominant species present on the polystyrene balls and that their biovolume increased throughout the 2015 growing season. Based on a study by Berry and Lembi (2000) certain forms of these chlorophytes are sensitive to high temperature and PAR. Consequently, the low chlorophyll-a concentration observed in Figure 11 might be a result of intolerance for these conditions.

Notably, the top ten models all included PAR and temperature suggesting these variables were primary factors regulating periphyton growth on the polystyrene balls in the 2015 growing season.

3.2.2 Sand substrate

3.2.2.1 Community composition

The periphyton community composition on sand was completely different and less dense than the community found on polystyrene balls in Carpenter Reservoir. Periphyton in the spring was entirely made up of *Cryptomonas* sp., a chryso-cryptophyte (Table 9; Figure 11. While in the summer, the community shifted to 100% diatoms dominated by *Stauroneis* sp. and some *Rhopalodia* sp. The community in the fall was approximately 5x larger than either of the previous seasons and was comprised primarily of *Cryptomonas* sp. (87%). The remaining portion was a combination of *Cymbella* sp. and *Stauroneis* sp., both diatom species. Chryso-cryptophytes are flagellated organisms suggesting that the individuals identified in the sand samples were likely from entrainment during the removal of the samples from the moorings. During analysis, we did not see any benthic algae actually attached to the sand particles but rather they were all free-living forms. This finding in part explains the low biomass observed in the sand samples compared to the polystyrene samples.

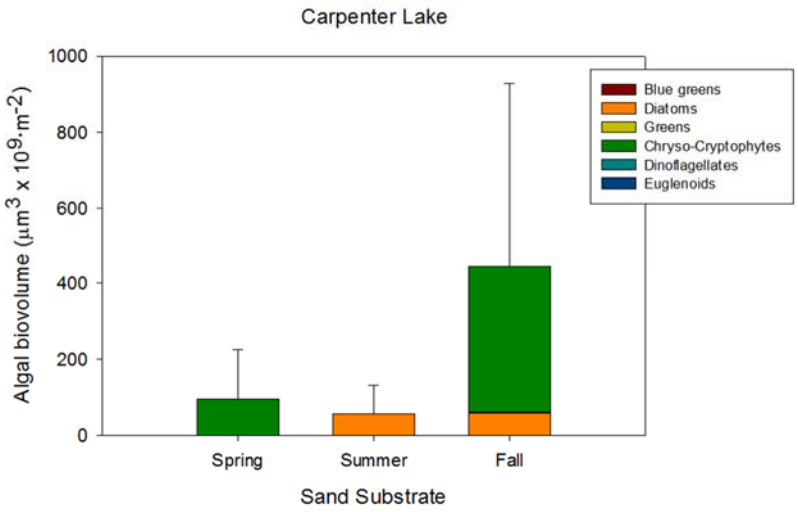

Figure 11. Algal biovolume, by group, found on sand substrate during each incubation period in Carpenter Reservoir. Error bars were included where the mean of two samples is shown.

3.2.2.2 Regression analysis

The top four models for periphyton growth on sandy substrates had similar log-likelihoods, ΔAICc and evidence ratios but the amount of variation described by these models varied from 53% to 59% (Table 11). Given that the third model performed similarly to the other models with ΔAICc < 2, the magnitude and direction of the coefficients were similar among models and this model described the greatest amount of

variation in the data (59%), we selected the third model as the best descriptor of periphyton growth on sandy substrates,

*logChlorophyll-a = -4.13 + 514.77 * DIN – 0.12 * Turbidity – 0.03 * Temperature.*

This model showed that chlorophyll-a increased with higher concentrations of dissolved inorganic nitrogen but declined with increasing turbidity and water temperature (Table 11; Figure 12).

Table 11. Results from the model selection process for the top 10 of 27 models using AICc for periphyton production in sand pails. *k* is the number of parameters in each model including the intercept and error terms, logLik is the log-likelihood, Adj. r^2 is the r^2 of the linear regression model adjusted for the number of variables in the model, ΔAICc is the difference between the top model AICc value and subsequent model AICc values, w_i is the model weight for each model and ER is the evidence ratio for each model, which measures the likelihood that the top model is better than model *i.* The dashed line highlights the models with ΔAICc <2. SRP is soluble reactive phosphorus measured as PO_4, DIN is dissolved inorganic nitrogen measured as the sum of NH_4 and NO_3 and PAR is photosynthetically active radiation.

Model	*k*	logLik	Adj. r^2	ΔAICc	w_i	ER
Temperature - SRP	4	11.96	0.54	0.00	0.25	1.00
DIN - Turbidity	4	11.84	0.54	0.24	0.22	1.13
DIN - Turbidity - Temperature	5	13.57	0.59	0.72	0.17	1.43
DIN - Turbidity - SRP	5	13.48	0.59	0.90	0.16	1.57
Temperature - SRP - PAR	5	12.13	0.52	3.59	0.04	6.01
Temperature - SRP - Turbidity	5	12.06	0.52	3.73	0.04	6.45
Temperature - SRP + DIN	5	11.97	0.51	3.92	0.03	7.09
DIN - Turbidity + PAR	5	11.89	0.51	4.08	0.03	7.69
DIN	3	8.15	0.35	4.26	0.03	8.42
DIN + Temperature	4	8.84	0.35	6.26	0.01	22.86

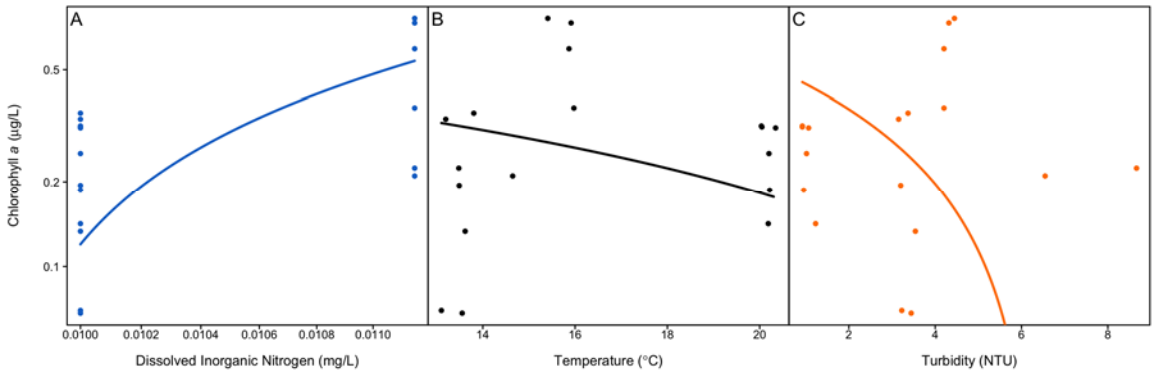

Figure 12. Relationship between chlorophyll-a, (A) dissolved inorganic nitrogen (DIN), (B) water temperature and (C) turbidity. The y-axis is log-transformed but the data points are all untransformed so that units can be read from the figures. The model lines are derived from the intercept and coefficients from the third model selected by AICc and show the main effect of the environmental variable of interest while maintaining all other variables at their mean value.

In this experiment, sand pails were deployed in Carpenter only as the other two lakes do not have sand bottoms. Sand offers less stability and surface area per particle for periphytic growth and can subsequently alter the metabolism in a system (Marcarelli, Huckins, and Eggert, 2015). Common disturbance in the reservoir may result from wave action in the littoral habitat but any effect of disturbance would be incorporated into the design of this experiment using sand pails.

Based on these results, periphyton growth, as measured by chlorophyll-a, increased with dissolved inorganic nitrogen suggesting this community is nitrogen-limited. This is likely the case for all primary producers in these lakes as previous studies have identified Carpenter, Anderson and Seton as oligotrophic or ultraoligtrophic, meaning concentrations of dissolved nutrients accessible to primary producers are low (Limnotek, 2016) although shifts between nitrogen and phosphorus deficiency may occur between Carpenter Reservoir and Seton Lake in relation to changes in molar N:P supply ratios. For Carpenter Reservoir the present model shows that the sand periphyton community is sensitive to change in inorganic N concentration. This finding means that change in DIN concentration would be expected to have influence on areal biomass of algae on sand substrata. Potential changes in DIN concentration may originate from atmospheric sources (to be examined in 2016) and from fluxes in transport of nitrogen from upstream and terrestrial sources (Allan and Castillo, 2007a). Further insight into the role of nitrogen on the algal assemblages having an affinity to sand will be further examined with the addition of data in 2016.

The top model also showed that temperature and turbidity affected chlorophyll-a concentration on sand. While we expected that increased turbidity would have a negative effect on attached chlorophyll-a accrual as seen by Haven et al. (2001), it is interesting that temperature also had a negative effect, given it had a positive effect on chlorophyll-a concentration on the polystyrene balls. There is however, considerable variation in chlorophyll-a concentration with temperature and turbidity (Figure 12), which makes it difficult to discern a pattern in either direction. Additional data from 2016 will help resolve this uncertainty.

3.3 Question 2: Is light the primary factor regulating productivity of pelagic habitat in Carpenter Reservoir?

3.3.1 Overview

This section focuses on zooplankton biomass. There were two regressions used to model zooplankton in the pelagic habitat: one having phytoplankton biomass as an independent variable filtered on 0.20 μm filter ($zooplankton_{0.20\ \mu m\ filter}$) and a second from phytoplankton on 0.75 μm filter ($zooplankton_{0.75\ \mu m\ filter}$). The 0.20 μm filter would capture phytoplankton > 0.20 μm while the 0.75 μm filter would capture larger phytoplankton > 0.75 μm. We were testing the hypothesis is that zooplankton would respond differently to different phytoplankton size classes.

3.3.2 Community composition

Zooplankton biomass increased 10 fold from May to June at station C2 in Carpenter Reservoir to a peak biomass of 3,399 mg dry weight/m^2 (Table 12; Figure 13). Biomass declined back to spring values by October when the last sample was collected. There was a one-month lag in biomass at station C6 compared to C2 whereby peak biomass (3,504 mg dry weight/m^2) occurred in August and was 100x greater than in May at the same station. Throughout the season, the zooplankton community was dominated by cladocerans at both stations. *Daphnia* spp. made up 90% or more of the cladocerans present except in May when half the cladocerans were *Leptodora* sp. and half were *Daphnia* spp. At both stations, cyclopods peaked in June, making up approximately 35% of the zooplankton community, of which 95% or more were *Cyclops* spp. Peak calanoid biomass occurred in July and August at stations C2 and C6, respectively, making up approximately 20% of the samples and comprised primarily of *Acnathodiaptomus* spp.

Table 12. Mean zooplankton biomass measured as mg dry weight/m^2 by station, month and group. SD is the standard deviation around the mean.

Lake	Station	Month	Cladocera	Cyclopoid	Calanoid	Total Mean	SD
Carpenter	C2	May	178	141	19	338	24
		June	662	425	143	1,229	225
		July	2,417	266	715	3,399	321
		August	1,775	110	310	2,195	504
		September	1,297	71	113	1,480	353
		October	227	70	17	314	4
	C6	May	12	20	5	36	4
		June	332	202	29	564	79
		July	1,927	139	263	2,329	83
		August	3,021	77	406	3,504	644
		September	643	84	191	918	113
		October	127	43	32	203	10
Anderson	A1	May	795	1,136	20	1,951	212
		June	3,365	545	30	3,940	673
		July	4,775	373	38	5,185	568
		August	2,915	591	56	3,562	669
		September	847	601	8	1,457	8
	A2	May	872	1,271	12	2,155	181
		June	3,029	539	22	3,590	342
		July	1,311	328	53	1,691	79
		August	1,533	666	42	2,241	151
		September	1,732	724	3	2,459	114
Seton	S4	May	28	797	49	873	42
		June	383	629	28	1,040	51
		July	633	232	34	898	30
		August	753	211	64	1,028	146
		September	1,044	128	21	1,194	13

Lake	Station	Month	Cladocera	Cyclopoid	Calanoid	Total Mean	SD
	S5	May	26	574	82	682	4
		June	802	610	70	1,481	126
		July	892	289	14	1,195	77
		August	718	200	49	968	152
		September	723	189	16	927	50

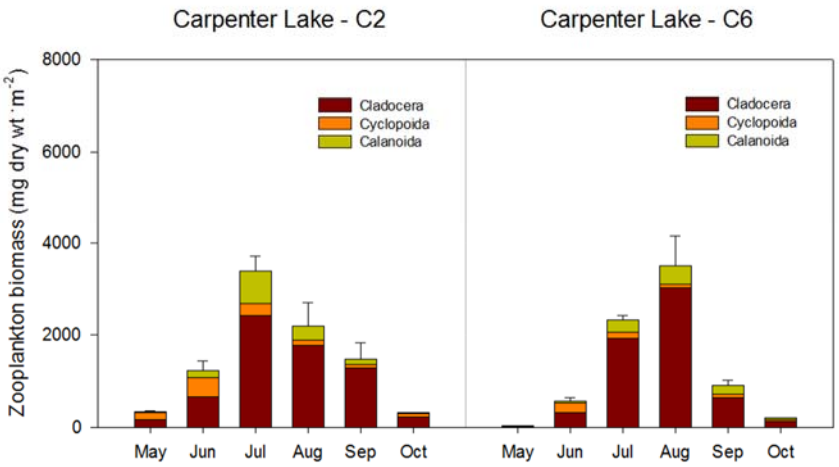

Figure 13. Zooplankton biomass by month and station in Carpenter Reservoir. Error bars were included when the mean of two samples was calculated.

The zooplankton community in Anderson Lake was similar to Carpenter Reservoir with some notable differences. Total biomass was 1.5x to 60x (May, C6 vs. A2) higher in Anderson compared to Carpenter (Table 12, Figure 14). Cyclopoida biomass was also higher throughout the sampling season at both stations in Anderson, with few calanoids (Figure 14). Peak cyclopoid biomass occurred in May at stations A1 and A2, with 1,136 and 1,271 mg dry weight/m^2, respectively. The proportion of cyclopoids declined in the middle of the season and rebounded by October to near spring values (Figure 14). *Cyclops* spp. made up 91% or more of the total cyclopoids present. However, as in Carpenter, the zooplankton community was largely made up of cladocerans with 95% or more of those being *Daphnia* spp (Table 12; Figure 14). The only exception was at A1 in September, where 30% of the community was Eubosmina spp.

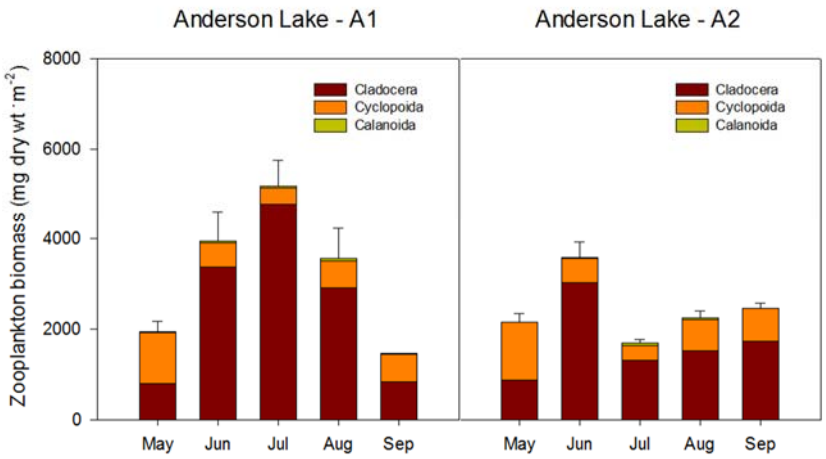

Figure 14. Zooplankton biomass by month and station in Anderson Lake. Error bars were included when the mean of two samples was calculated.

Total monthly biomass at both stations in Seton were remarkably similar from month to month and lower in the summer compared to Carpenter and Anderson (Table 12; Figure 15). The majority of the community in May was comprised of cyclopoids (91% and 84% at S4 and S5, respectively) and the bulk of these individuals were *Cyclops* spp. However, *Daphnia* spp. (Cladocera) quickly dominated the zooplankton community making up 70% or more of the samples from July to September. Calanoids were present throughout the season but made up 12% or less of the total community.

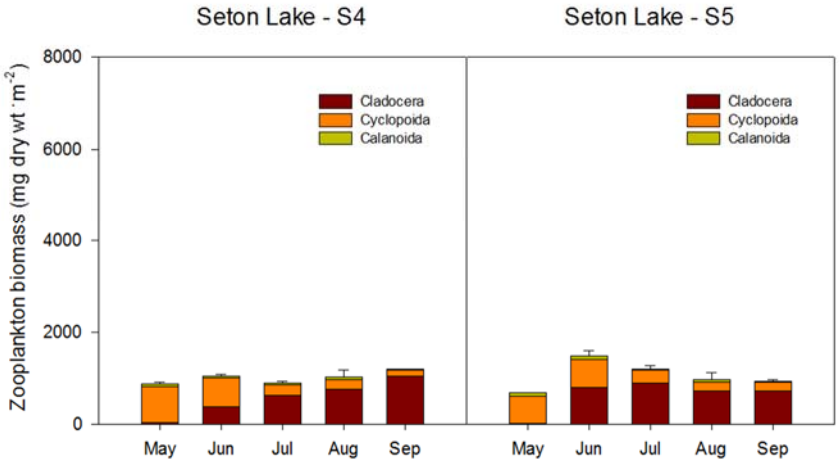

Figure 15. Zooplankton biomass by month and station in Seton Lake. Error bars were included when the mean of two samples was calculated.

3.3.3 Regression analysis for zooplankton$_{0.20\ \mu m\ filter}$

There was more zooplankton biomass at stations with warmer water, less turbidity, longer water residence time and lower phytoplankton biomass as measured by chlorophyll-a from 0.20 μm filters.

$$logZooplankton_{0.20\ \mu m\ filter} = 6.94 + 0.13 * temperature - 0.07 * turbidity + 3.37x10^{-4} * mean\ water\ residence\ time - 0.56 * chlorophyll\text{-}a_{0.20\ \mu m\ filter}.$$

The r^2 for this model was 0.63 and was considered to be 1.44, 1.57 and 1.70 times better than the other three models with ΔAICc < 2, which contained just two or three of the above mentioned variables (Table 13). The effects of each environmental variable are clearly visible in Figure 16.

Table 13. Results from the model selection process for the top 10 of 57 models using AICc for zooplankton production in pelagic habitat using chlorophyll-a sampled with 0.20 μm filter size. *k* is the number of parameters in each model including the intercept and error terms, logLik is the log-likelihood, Adj. r^2 is the r^2 of the linear regression model adjusted for the number of variables in the model, ΔAICc is the difference between the top model AICc value and subsequent model AICc values, w_i is the model weight for each model and ER is the evidence ratio for each model, which measures the likelihood that the top model is better than model *i*. The dashed line highlights the models with ΔAICc <2.

Model	*k*	logLik	Adj. r^2	ΔAICc	w_i	ER
- Chlorophyll-a - Turbidity + Water Residence Time + Temperature	6	-26.73	0.63	0.00	0.17	1.00
- Chlorophyll-a - Turbidity	4	-30.03	0.57	0.73	0.12	1.44
- Chlorophyll-a - Turbidity + Water Residence Time	5	-28.70	0.59	0.90	0.11	1.57
- Chlorophyll-a - Turbidity + Temperature	5	-28.79	0.59	1.07	0.10	1.70
- Chlorophyll-a - Turbidity + Temperature + Station Depth	6	-27.52	0.61	1.59	0.08	2.22
- Chlorophyll-a + Temperature + Station Depth	5	-29.25	0.58	1.99	0.06	2.70
- Chlorophyll-a - Turbidity + Station Depth	5	-29.51	0.57	2.52	0.05	3.52
- Chlorophyll-a - Turbidity + Water Residence Time + Distance to Inflow	6	-28.35	0.59	3.23	0.03	5.04
- Chlorophyll-a - Turbidity + Distance to Inflow	5	-29.93	0.56	3.34	0.03	5.32
- Chlorophyll-a - Turbidity + Water Residence Time - Station Depth	6	-28.54	0.58	3.63	0.03	6.13

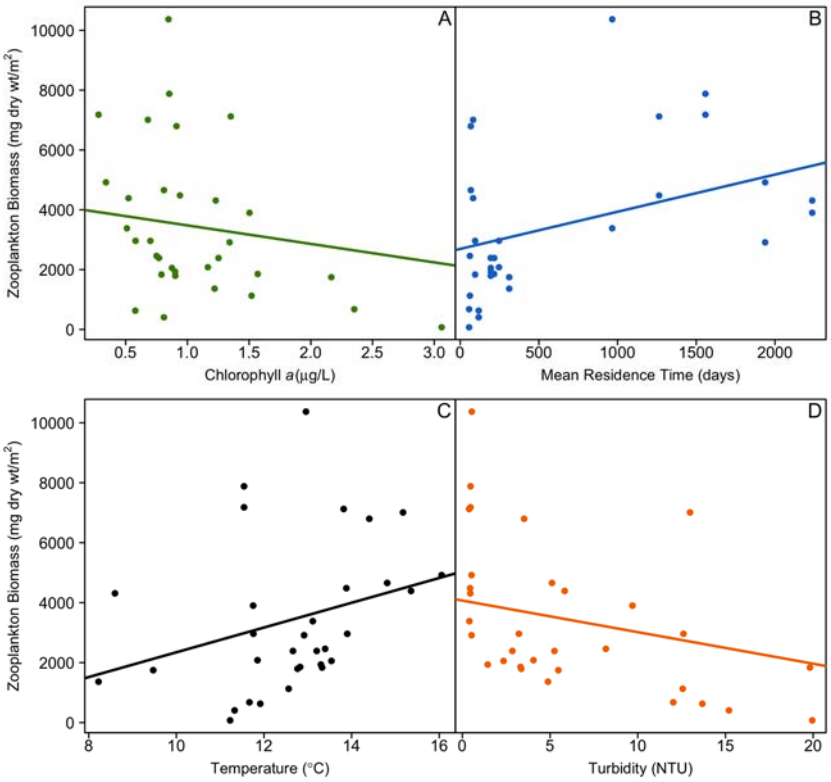

Figure 16. Relationship between zooplankton biomass (A) chlorophyll-a*0.20 µm filter*, (B) mean water residence time, (C) water temperature and (D) turbidity. The model lines are derived from the intercept and coefficients from the top model selected by AICc and show the main effect of the environmental variable of interest while maintaining all other variables at their mean value.

While there is considerable variation in zooplankton biomass at low levels of chlorophyll-a, zooplankton biomass was inversely related to phytoplankton biomass, which is what we would predict if grazing by zooplankton alone strongly affected phytoplankton biomass. That is, as zooplankton biomass increases, so would the amount of phytoplankton they consume. This relationship between herbivores and plants has been shown in a variety of habitats but is particularly strong in aquatic systems (Cyr and Face, 1993). It is not consistent among lakes, however, and in many cases zooplankton and phytoplankton biomass are positively related where top down control of phytoplankton is not a factor determining phytoplankton biomass (Shuter and Ing 1997).

There was a positive relationship between mean water residence time and zooplankton biomass as seen in other studies on zooplankton (e.g. Basu, and Pick, 1996). The longer the water resided in the lake or reservoir the more zooplankton biomass that was present. Residence time ranged from approximately 2.5 months (80 days ± 9) in Carpenter Reservoir to almost 8 months (233 days ± 22) in Seton Lake and just over 4 years (1593 days ± 228) in Anderson Lake. For this analysis we used a

shifting 78-day mean based on the day zooplankton was sampled. This 78-day mean corresponds to the mean lifespan of common zooplankton species (Korpelainen, 1986; Schwartz and Ballinger, 1980); a water residence time less than this would potentially flush developing zooplankton from the system. This is particularly relevant in Carpenter Reservoir given that the mean water residence time at the beginning of the zooplankton growing season is typically less than 78 days (minimum mean recorded value = 56 days in May 2015). The low residence time in the reservoir would have important implications for pelagic food web interactions. Water residence time lower than time needed for cladocerans and cyclopoids to fully develop and reproduce would strongly limit availability of zooplankton as food for pelagic fish, potentially forcing a shift to food produced in benthic habitats. This kind of response was shown by Wu and Culver (1992), albeit for a different food web than in Carpenter, but still relevant with respect to potential shifts in trophic interactions caused by change in limitation of zooplankton production.

As with periphyton on stony substrates in the littoral habitat, zooplankton biomass increased with water temperature and decreased with turbidity. Temperature ranged between 8 and 16 °C, within the range of maximum lifespans reported for common *Daphnia* spp. (Korpelainen, 1986), which make up the majority of these samples (Figure 13 to Figure 15). We would expect temperature to have a negative effect on zooplankton biomass if it were to increase beyond 24 °C (Korpelainen, 1986). Turbidity measures the amount of light scatter, which results from of organic (e.g. plankton, detritus) and inorganic (e.g. silt and clay) suspended solids in the water column (Jeppesen, Jensen, Søndergaard, and Lauridsen, 1999). Turbidity may not directly affect zooplankton production but rather phytoplankton production and result in less food for zooplankton. Future analysis of phytoplankton biovolume data will enhance the interpretation of the zooplankton data. However, these current findings further highlight the importance of temperature and turbidity in regulating biological production in these systems. Further analysis in 2016 is needed to confirm these relationships.

3.3.4 Regression analysis for zooplankton$_{0.75\ \mu m\ filter}$

When only the larger size class of phytoplankton was considered in the analysis, it was no longer an important variable describing zooplankton biomass. In this case, zooplankton biomass increased with water temperature and mean water residence time but declined with increasing turbidity as seen in Figure 17 and shown by the top model in Table 14,

$$logZooplankton_{0.75\ \mu m\ filter} = 5.46 + 0.21 * temperature - 0.09 * turbidity + 3.37x10^{-4} * mean\ water\ residence\ time.$$

The r^2 for this model was 0.56 compared to the third model, which included chlorophyll-a and had an r^2 of 0.57. This result shows that the larger size fraction of chlorophyll-a had

a limited effect on zooplankton biomass and suggests that zooplankton were feeding more regularly on the smaller size fraction of phytoplankton.

Table 14. Results from the model selection process for the top 10 of 57 models using AICc for zooplankton production in pelagic habitat using chlorophyll-a sampled with 0.75 μm filter size. *k* is the number of parameters in each model including the intercept and error terms, logLik is the log-likelihood, Adj. r^2 is the r^2 of the linear regression model adjusted for the number of variables in the model, ΔAICc is the difference between the top model AICc value and subsequent model AICc values, w_i is the model weight for each model and ER is the evidence ratio for each model, which measures the likelihood that the top model is better than model *i*. The dashed line highlights the models with ΔAICc <2.

Model	*k*	logLik	Adj. r^2	ΔAICc	w_i	ER
Temperature - Turbidity + Water Residence Time	5	-30.14	0.56	0.00	0.16	1.00
Temperature - Turbidity	4	-31.83	0.52	0.55	0.12	1.31
Temperature - Turbidity + Water Residence Time - Chl a	6	-28.98	0.57	0.74	0.11	1.45
Temperature - Turbidity - Chl a	5	-30.77	0.54	1.26	0.09	1.88
Temperature - Turbidity + Station Depth	5	-30.88	0.54	1.47	0.08	2.08
Temperature - Turbidity + Station Depth + Distance to Inflow	6	-29.47	0.56	1.71	0.07	2.35
Temperature - Turbidity + Water Residence Time + Distance to Inflow	6	-29.57	0.56	1.90	0.06	2.59
Temperature - Turbidity - Chl a + Station Depth	6	-29.74	0.55	2.24	0.05	3.07
Temperature - Turbidity + Distance to Inflow	5	-31.57	0.51	2.87	0.04	4.19
Temperature - Turbidity + Water Residence Time - Station Depth	6	-30.12	0.54	3.01	0.04	4.51

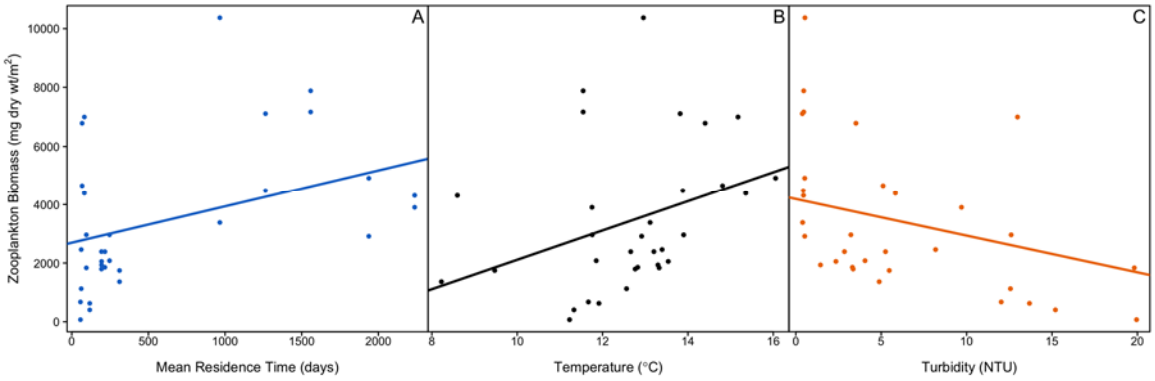

Figure 17. Relationship between zooplankton biomass, (A) mean water residence time, (B) water temperature and (C) turbidity. The model lines are derived from the intercept and coefficients from the top model selected by AICc and show the cumulative effect of all the variables on zooplankton biomass.

3.4 Question 3: Is light penetration in Carpenter Reservoir impacted by changes in reservoir operations?

3.4.1 Flow

3.4.1.1 Outflow from Lajoie Dam

Outflow from Lajoie Dam is shown in Figure 18. The average outflow for 1961-2015 was 40.9 $m^3 \cdot s^{-1}$. The mean outflow was relatively uniform throughout the year with small increases in February-March and August-September. The year to year variability in the outflow was greatest in August, at which time brief periods of high flows are not unusual. In 2015, the outflow from Lajoie Dam generally followed the average, but with significantly above average flow from March to mid April, and from mid July through August (red, Figure 18 b).

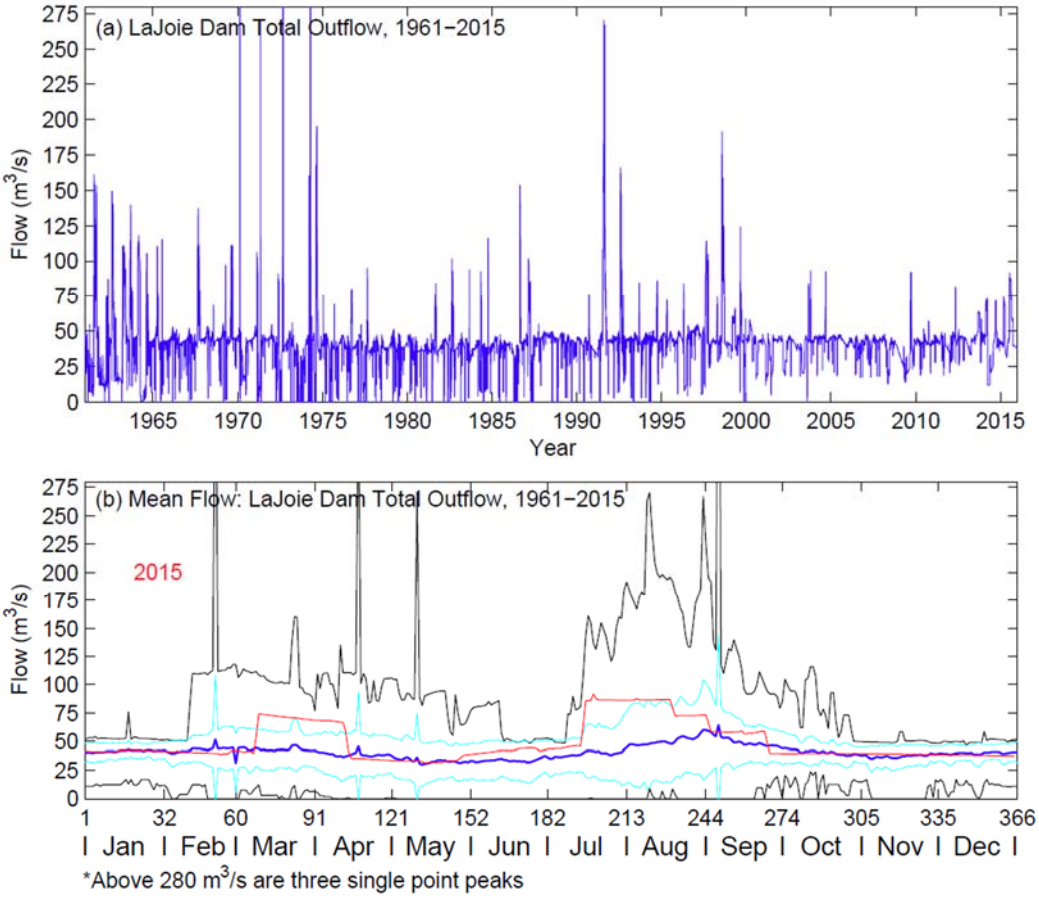

Figure 18. (a) Daily total outflow from Downton Reservoir at Lajoie Dam, 1961-2015. (b) Total outflow from Lajoie Dam averaged over 1961-2015 for each calendar day. Mean (blue line), maximum and minimum (black lines) and mean ± one standard deviation (cyan lines). The total outflow in 2015 is shown in red. In (a) there are three offscale peaks consisting of a single point each.

3.4.1.2 Local inflow

The local inflow to Carpenter Reservoir includes all drainage and tributaries downstream of Lajoie Dam. The average from 1961-2015 was 50.6 $m^3 \cdot s^{-1}$. The local inflow shows a strong seasonal signal dominated by a peak of snowmelt in June (Figure 19). This peak shows a long tail through July and August driven by glacial melt. In 2015, freshet was early with above average flows in May and early June, but below average inflows from mid-June to the end of August (red, Figure 19 b). Flow in fall 2015 was generally average, though there were three large peaks resulting from rainstorms.

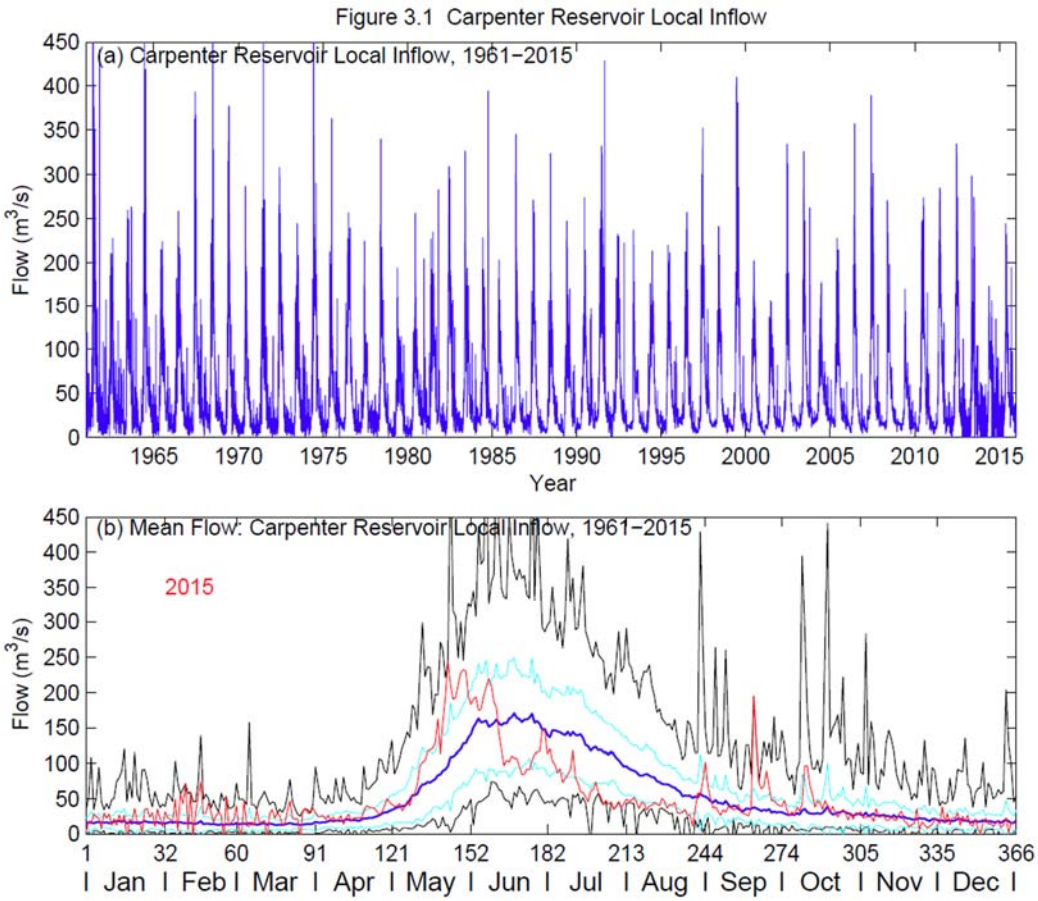

Figure 19. **(a)** Daily local inflow to Carpenter Reservoir, 1961-2015. **(b)** Daily local inflow to Carpenter Reservoir, averaged over 1961-2015. Mean (blue line), maximum and minimum (black lines) and mean ± one standard deviation (cyan lines). The local inflow in 2015 is shown in red.

3.4.1.3 Outflow to Bridge 1 and 2 Powerhouses on Seton Lake

The vast majority of water (96%) exits Carpenter Reservoir through two tunnels to the Bridge powerhouses on Seton lake. The flow to Seton Lake for 1961-2015

averaged 87.4 $m^3 \cdot s^{-1}$. The flow is highest through winter, with another small peak in August-September (Figure 20 b). In 2015, the outflow was generally average, except for mid-June to mid-July when it was significantly higher than average.

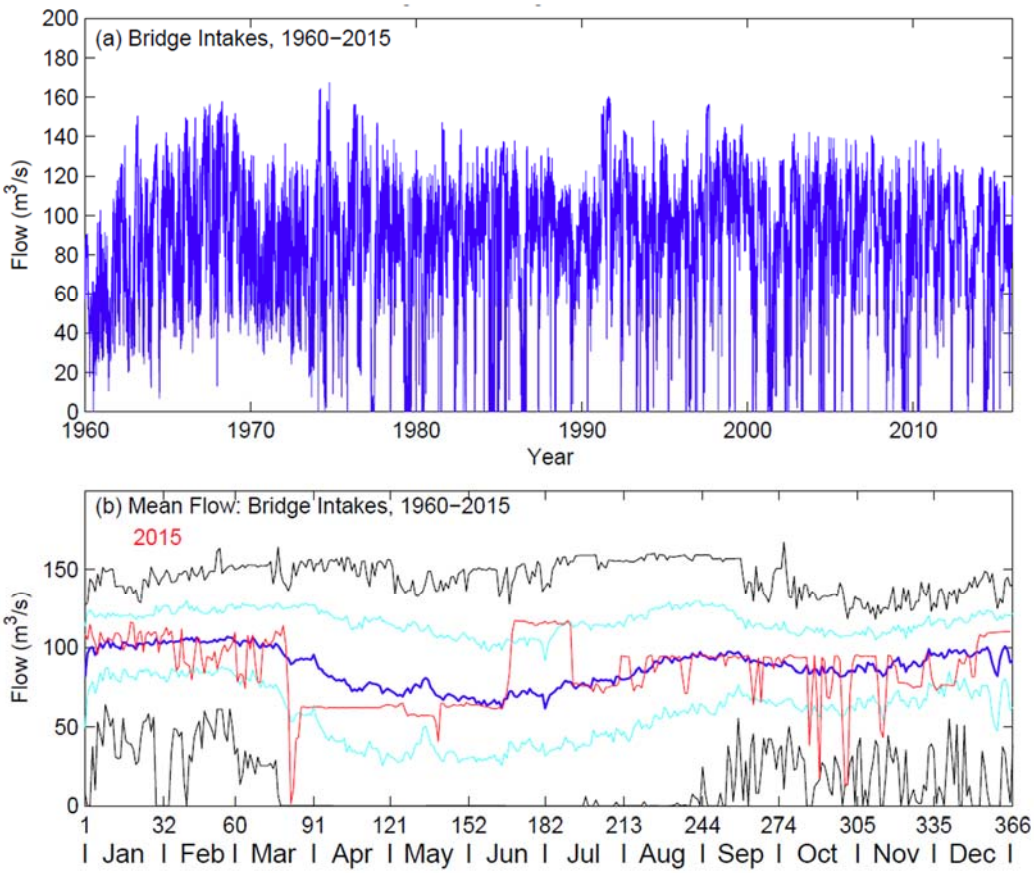

Figure 20. **(a)** Daily local outflow to Bridge powerhouses, 1961-2015. **(b)** Outflow to the Bridge powerhouses, averaged over 1961-2015. Mean (blue line), maximum and minimum (black lines) and mean ± one standard deviation (cyan lines). The outflow in 2015 is shown in red.

3.4.1.4 Water level

Water level in Carpenter Reservoir is shown in Figure 21. The water level also shows a strong seasonal cycle, with water level declining through fall and winter to sustain power generation, reaching a minimum in May, and rising rapidly through spring with storage of freshet inflow (Figure 21 b). There is also inter-annual variability in the maximum water level, and this variability can go in cycles with periods of relatively high water level (eg. 1982-1985), alternating with periods of relatively low water level (e.g. 2007-2009, Figure 21 a). The water level in 2015 was generally average, except for above average water level from April to June, and slightly above average water levels in the fall (Figure 21 b).

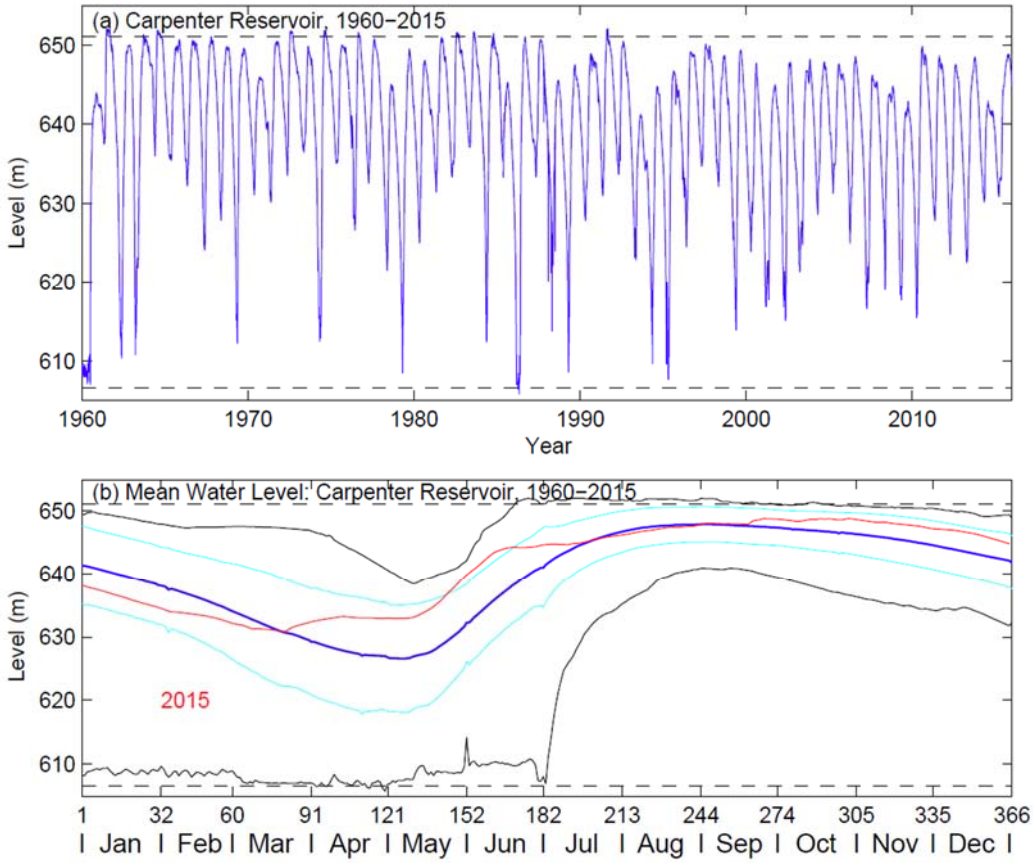

Figure 21. **(a)** Water level, Carpenter Reservoir, 1960-2015. **(b)** Average water level, Carpenter Reservoir, 1960-2015. Mean (blue line), maximum and minimum (black lines) and mean ± one standard deviation (cyan lines). The water level in 2015 is shown in red. The dash line mark the normal minimum (606.55 m ASL) and maximum (651.08 mASL).

3.4.1.5 Flow climatology

The mean outflow from Lajoie Dam from April to October (the biologically productive season) is shown in Figure 22. During 2015, the outflow from Lajoie Dam was significantly higher than average, in contrast to 2014, which had relatively low outflow (Figure 22). In 2015, the local flow was average, while in 2014 is was significantly below average (Figure 23). In 2015, the water level was somewhat above average from April to October, while it had been close to average for the previous five years (Figure 24). These data will be used to select scenarios with extremes in climate and operating conditions in running CE-QUAL. For example, April to October in 1991 had both very high outflow from Lajoie Dam (Figure 22) and high local flow (Figure 23).

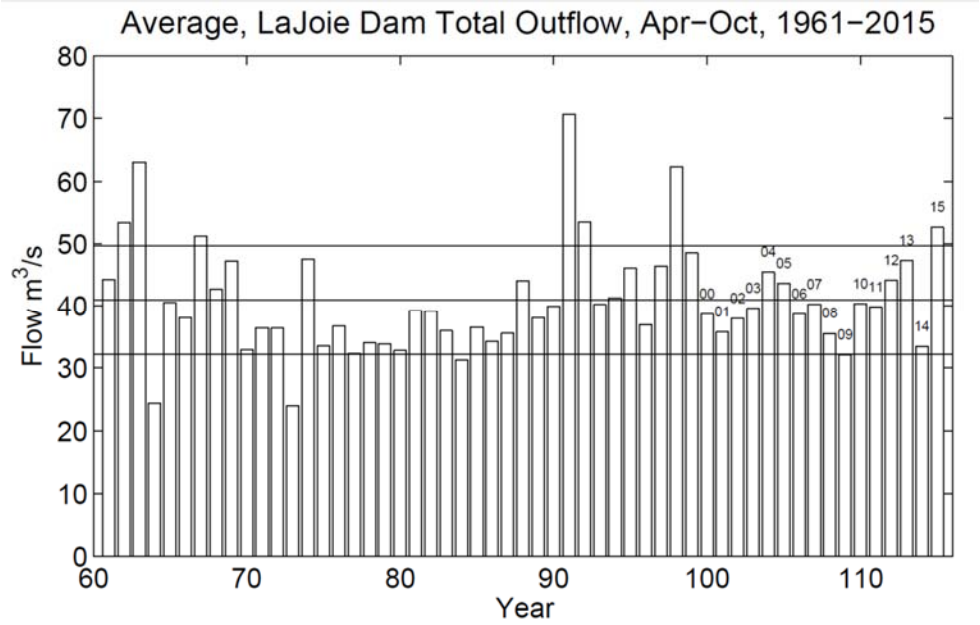

Figure 22. Average outflow from Lajoie Dam, April to October, 1961 to 2015. The black lines show the mean and the mean ± one standard deviation.

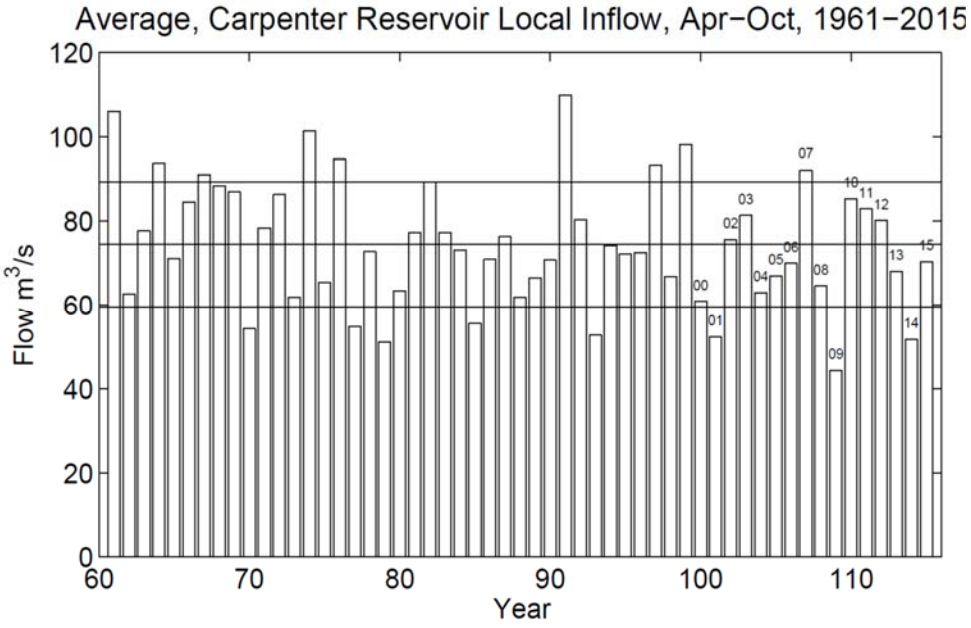

Figure 23. Average local inflow to Carpenter Reservoir, April to October, 1961 to 2015. The black lines show the mean and the mean ± one standard deviation.

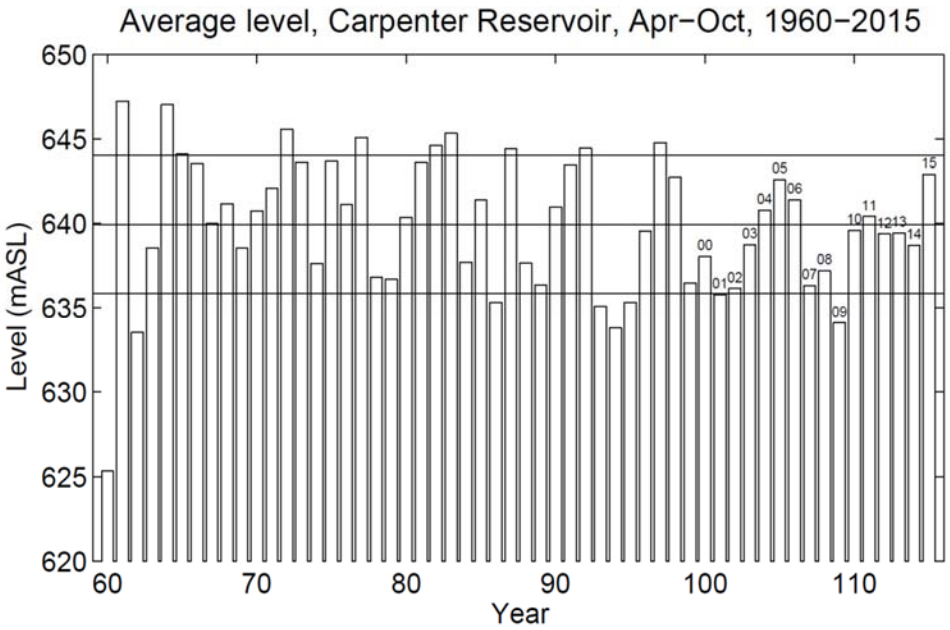

Figure 24. Average water level, Carpenter Reservoir, April to October, 1961 to 2015. The black lines show the mean and the mean ± one standard deviation.

3.4.2 Tributary temperature

The temperature of the outflow from Lajoie Dam (red, Figure 25 a) was relatively steady between 7 and 10 °C. In contrast the temperature of the Hurley River showed strong seasonal, weekly and daily variations (green, Figure 25 a). The mixing of the Hurley River into the outflow of the Lajoie Dam resulted in an intermediate temperature (blue, Figure 25a).

The temperatures of the other two major inflows to Carpenter Reservoir, Gun and Tyaughton Creeks, are shown in Figure 25b. The temperatures of three smaller tributaries are shown in Figure 25c, and vary from warmer (Sucker Creek) to colder (Girl Creek).

Given low TSS and TDS observed in Carpenter Reservoir tributaries, temperature is the key parameter in determining the plunge depth into the reservoir (e.g. Pieters and Lawrence 2011). If the tributary is cold, and entrainment during plunging is low, then the tributary can plunge into the hypolimnion, and if the tributary is warm, it will enter the epilimnion. If the tributary temperature is intermediate it can slot in at the thermocline. In the summer, the tributary temperature can vary by over 5 °C in the course of a day, and the plunge depth will vary accordingly.

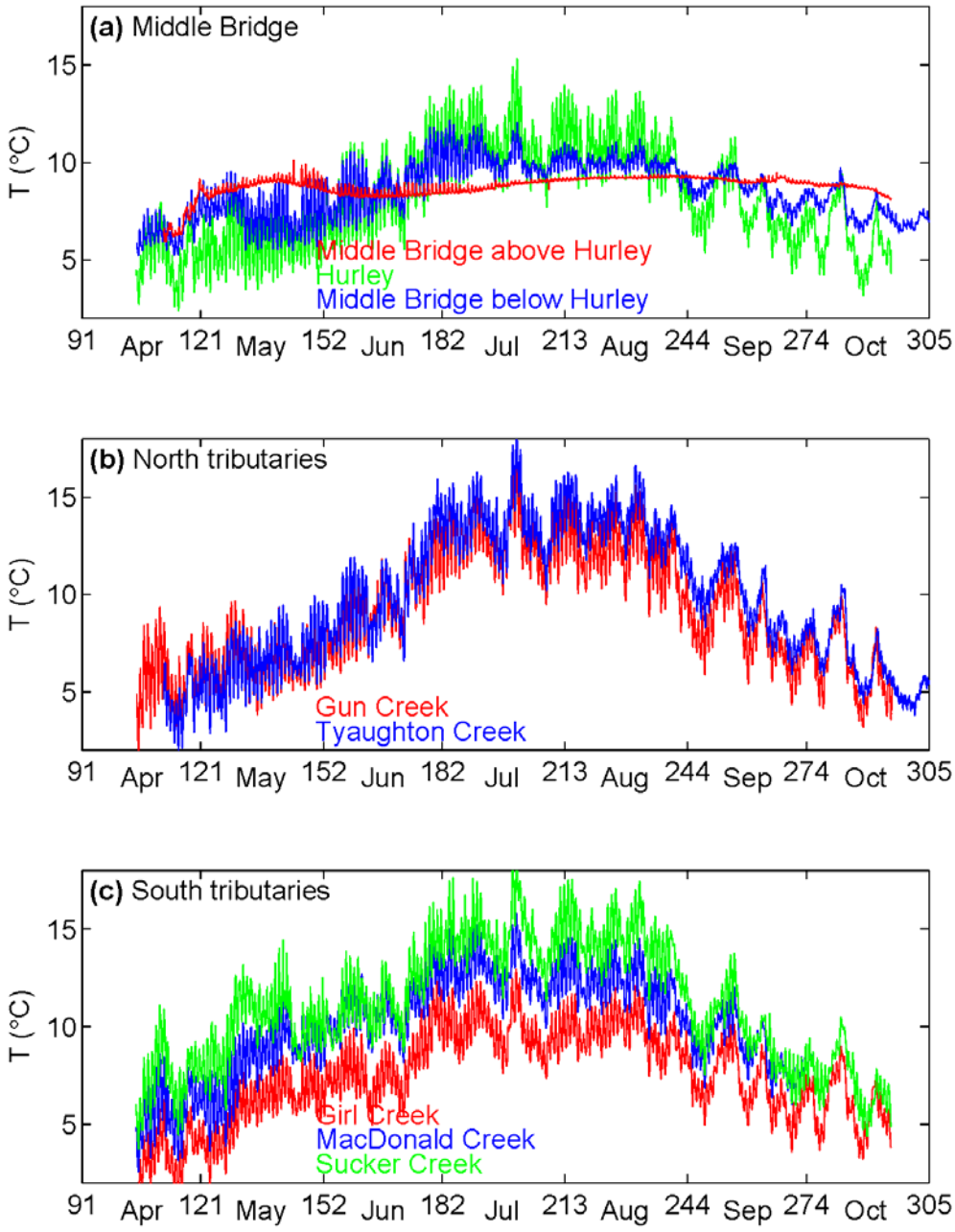

Figure 25. Tributary temperature for (a) Middle Bridge inflow (b) tributaries to the north side of Carpenter Reservoir, and (c) tributaries to the south side.

3.4.3 Tributary water quality

Total suspended solids (TSS) and turbidity data are shown for the Upper Bridge, Middle Bridge and Hurley Rivers in Figure 26, and for the other tributaries to Carpenter Reservoir in Figure 27. TSS and turbidity are important measures related to the penetration of light which is controlled by glacial fines in Carpenter Reservoir. In the tributary samples without an upstream reservoir - Hurley, Gun, Truax, Tyaugton,

Marshall and Keary – the TSS and turbidity were well correlated, the May sample at the start of freshet was elevated, and subsequent samples were low (Figure 26f and Figure 27a-e). In contrast, TSS and turbidity in the Upper and Middle Bridge River, and in the Bridge Tailrace show little correlation (Figure 26b-e and Figure 27f).

Total suspended solids and turbidity are complementary but different physical measurements. Total suspended solids require laboratory analyses: a filter is weighed, a water sample is passed through the filter, the filter is dried and weighed again, and the solids content is determined as the difference in the filter weights. The results have poor resolution at low suspended solids, and for small particles.

In contrast, turbidity, which measures the amount of scattered light, is easy to measure with an optical sensor in the field. However, the amount of scattered light depends on the size, shape, color and texture of the particles, which make turbidity an indirect measure.

Even a reservoir-specific relationship between TSS and turbidity usually shows significant scatter, and Carpenter Reservoir is no exception. For the local tributaries, there is a reasonable relationship between TSS and turbidity, though the fit is mainly controlled by the highest reading (blue, Figure 28). However, there is little correlation between TSS and turbidity for the other samples (red, Figure 28).

In a lentic environment, particles of all sizes are transported downstream. In a lotic environment, such as in the reservoirs, the larger particles that contribute mass to TSS settle, while the small (<2 µm) glacial particles that contribute to light scattering remain suspended. For example, the settling rate for particles of 1 µm diameter is ~ 1 m/month. Because light scattering is a key process in Carpenter Reservoir, determining the depth of the photic zone (the depth at which photosynthesis can occur), turbidity is used in place of TSS in the CE-QUAL-W2 model, and settling of the turbidity has been set to zero.

Figures for other parameters (TDS and nutrients) are given in APPENDIX A.

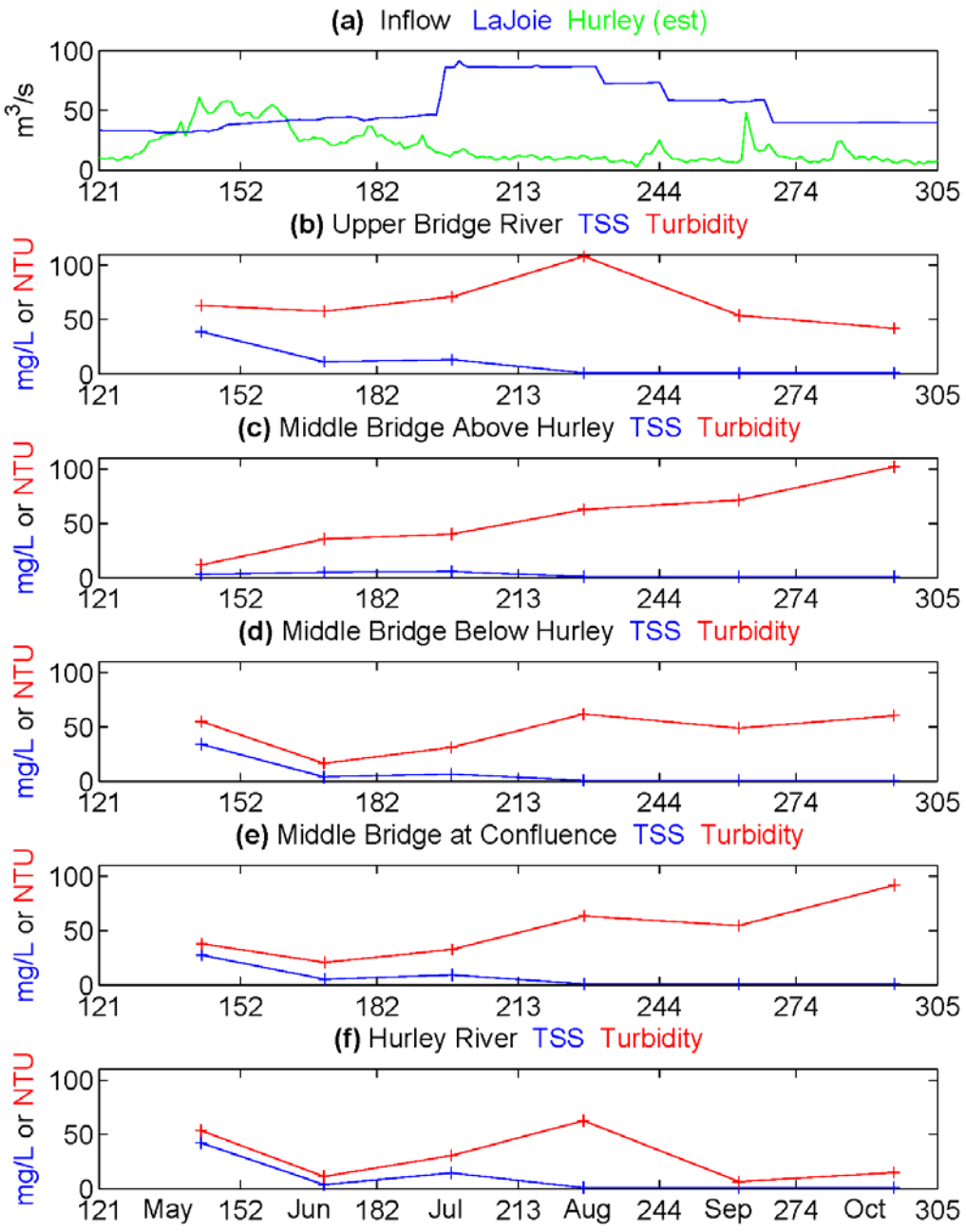

Figure 26. (a) Outflow from Lajoie Dam, and inflow from the Hurley River (estimated as 25% of the local flow). (b-f) Total suspended solids (TSS) and turbidity, May to October, 2015.

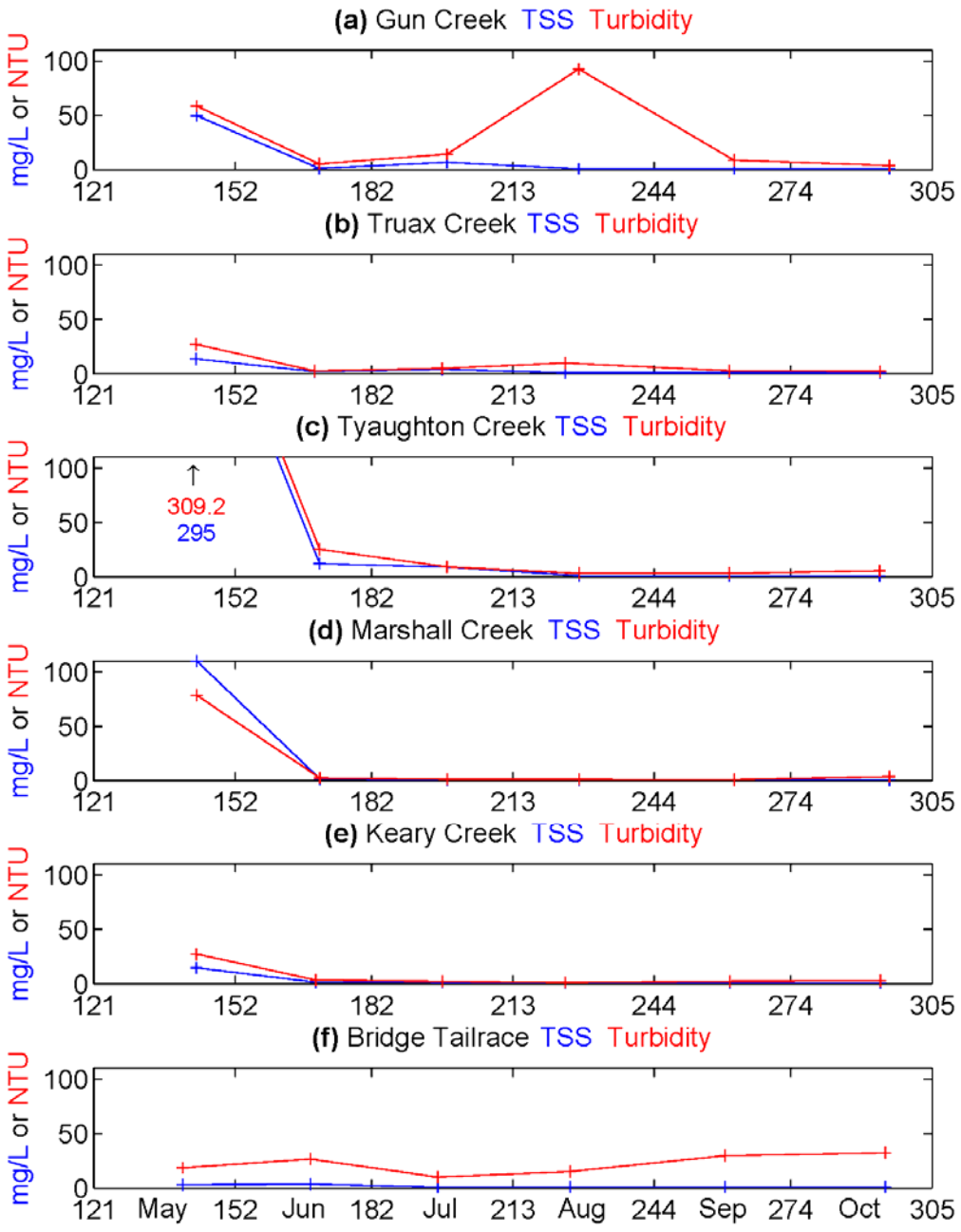

Figure 27. (a-f) Total suspended solids (TSS) and turbidity, May to October, 2015.

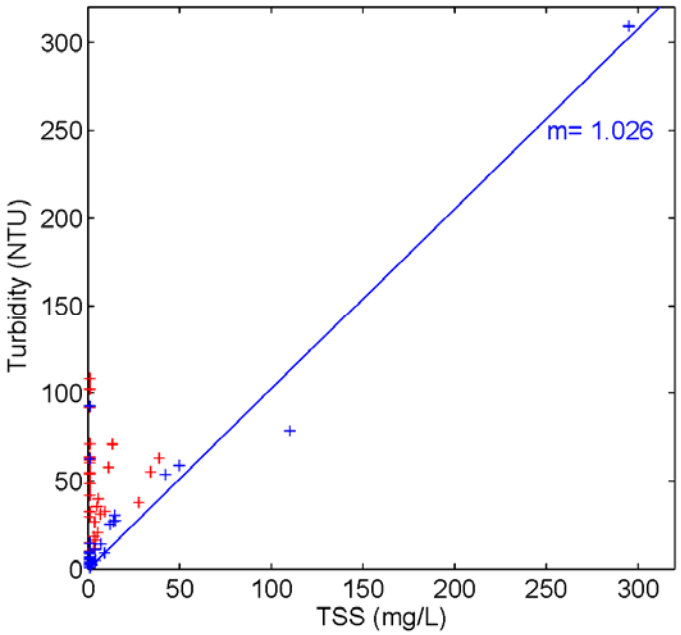

Figure 28. Turbidity versus total suspended solids (TSS) for tributaries to Carpenter Reservoir, 2015. **RED** – Samples from Upper and Middle Bridge Rivers and the Bridge Tailrace. **BLUE** – Samples from Hurley River and, Gun, Truax, Tyaughton, Marshall and Keary Creeks. The blue line gives the fit through zero to the blue data.

3.4.4 Continuous turbidity monitoring in the Middle Bridge River

Data from the turbidity recorder moored in the Middle Bridge River are shown in Figure 29c. The sensor was deployed without a wiper. At the time of the spot readings, the sensor face was cleaned (except for 22 October 2015 when the water was too deep to recover the mooring). An increase in the readings after cleaning (e.g. in May and September) suggests fouling may have reduced the readings at times. To correct this problem the turbidity recorder was deployed with a wiper in 2016.

Turbidity in the Middle Bridge River above the Hurley represents outflow from La Joie Dam, and this turbidity increased steadily throughout the observation period. The turbidity measured in the Hurley River shows more variability, being higher at the start of freshet, and lower after freshet has peaked and in the fall. Note, however, there are two fall peaks in the estimated Hurley flow, one in September (just before turbidity sampling) and one in October. At the same time as these peaks in Hurley flow, the turbidity logger also recorded large increases in turbidity, which suggests they may originate from mobilization of sediments in the Hurley.

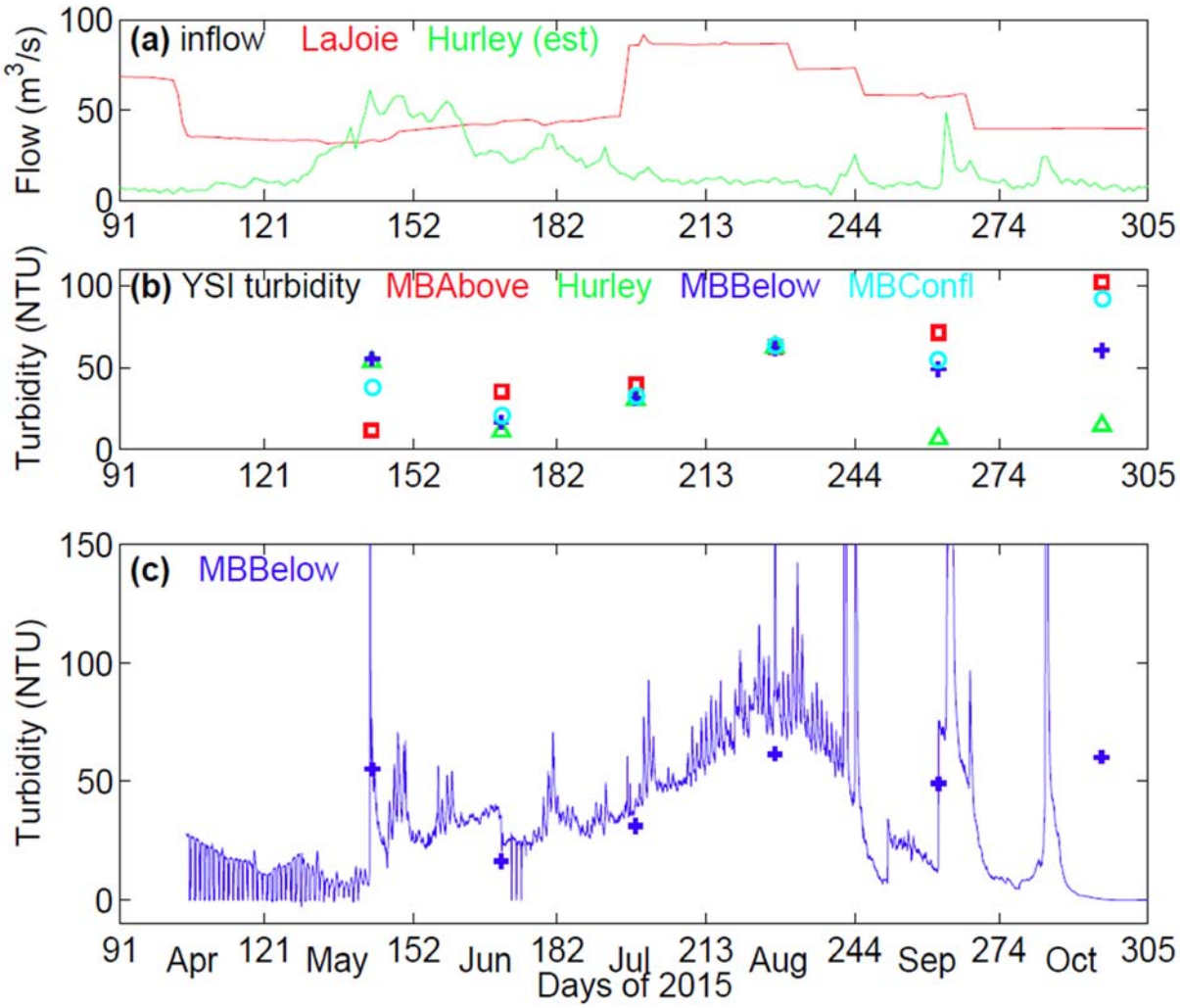

Figure 29. **(a)** Inflow, **(b)** YSI turbidity, and **(c)** hourly average turbidity from inflow to the top of Carpenter Reservoir, 14 April to 22 October, 2015. **MBAbove** marks the Middle Bridge River above the Hurley; **MBBelow** marks the Middle Bridge Below the Hurley, and **MBConf** marks the Middle Bridge at confluence with Carpenter Reservoir. Flow in the Hurley was estimated as 25% of the local flow.

3.4.5 Meteorological data

Meterological data from both Terzaghi Dam and the Forest Service Filemile site, located about half way up Carpenter Reservoir, are shown in Figure 30. The winds at Terzaghi Dam are relatively high, often reaching over 10 m/s (36 km/h). In contrast the winds at Fivemile are modest, generally less than 10 m/s (Figure 30a).

The air temperature is shown in Figure 30b; the three temperature records are generally consistent with each other. There were 31 days with temperature > 30 °C, and, in particular, 15 consecutive days from 26 June to 10 July 2015, with a maximum of 37 °C on 27 June 2015.

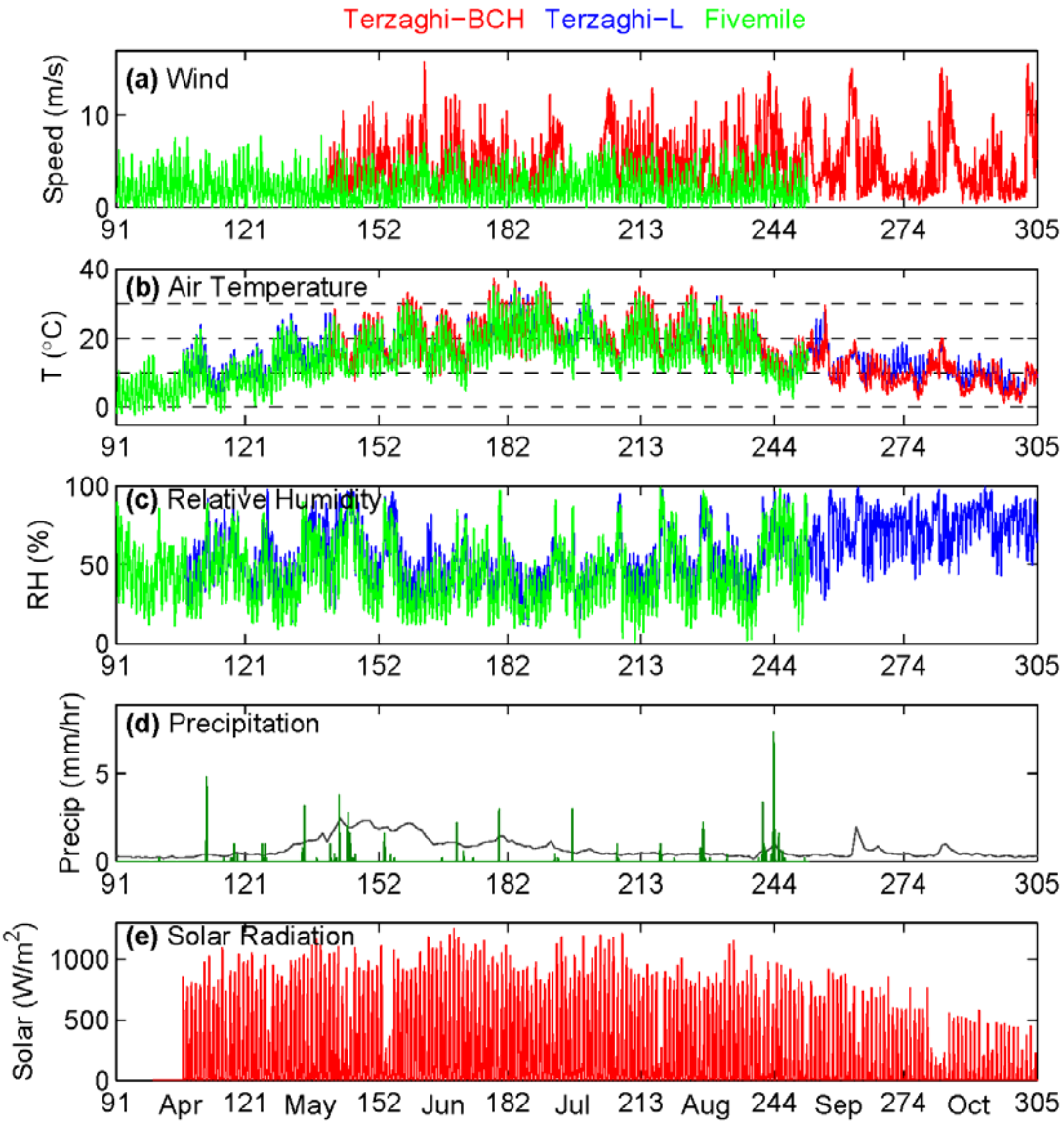

Figure 30. (a) Wind speed, (b) air temperature, (c) relative humidity, (d)precipitation and (e) solar radiation data available for Carpenter Reservoir, hourly, April to October 2015. The grey line in (d) is local inflow, $(m^3/s)/100$.

3.4.6 Monthly Sea-Bird profiles

On 22 May 2015, the surface of Carpenter Reservoir was 15 °C and the temperature stratification consisted of a broad gradient to the bottom (Figure 31a). By 18 June 2015, a typical two-layer stratification was observed, with a surface mixed layer (epilimnion), a sharp thermocline between 12 and 14 m, and a cooler deep water (hypolimnion) below 14 m. On 16 July and 12 August 2015, the surface layer was close

to 20 °C. By 17 September 2015, the surface layer had cooled to 15 °C. By 20 October, the surface layer had deepened to over 25 m and cooled to 12 °C, just above the temperature of the deep water, 11 °C. Fall turnover would be expected shortly after this last profile.

The conductivity at 25 °C (C25) declined from May to September 2015, particularly in the deep water as a result of freshet inflow (Figure 31b).

After May, the turbidity in the epilimnion was generally low (<2 NTU), while the turbidity in the hypolimnion remained elevated, up to 35 NTU (Figure 31c). The turbidity of the surface layer rose in October, possibly the result of mixing with more turbid water at depth, and of shallower plunging of turbid inflows.

The dissolved oxygen was high (Figure 31d) and close to saturation (Figure 31e), as would be expected for an oligotrophic and low residence time system. On 16 July, when the thermocline was in the photic zone, there was a small peak in oxygen (>120 % saturation) at the thermocline, and a corresponding small peak in chlorophyll fluorescence (Figure 31f), both suggestive of localized productivity.

Chlorophyll fluorescence was generally low (<2 µg/L) which is consistent with an oligotrophic system. In May, there was a broad peak to 1.7 µg/L at the base of the photic zone, suggestive of a spring bloom (Figure 31f). In the remaining months the fluorescence was a little lower with smaller peaks near the 1% light level.

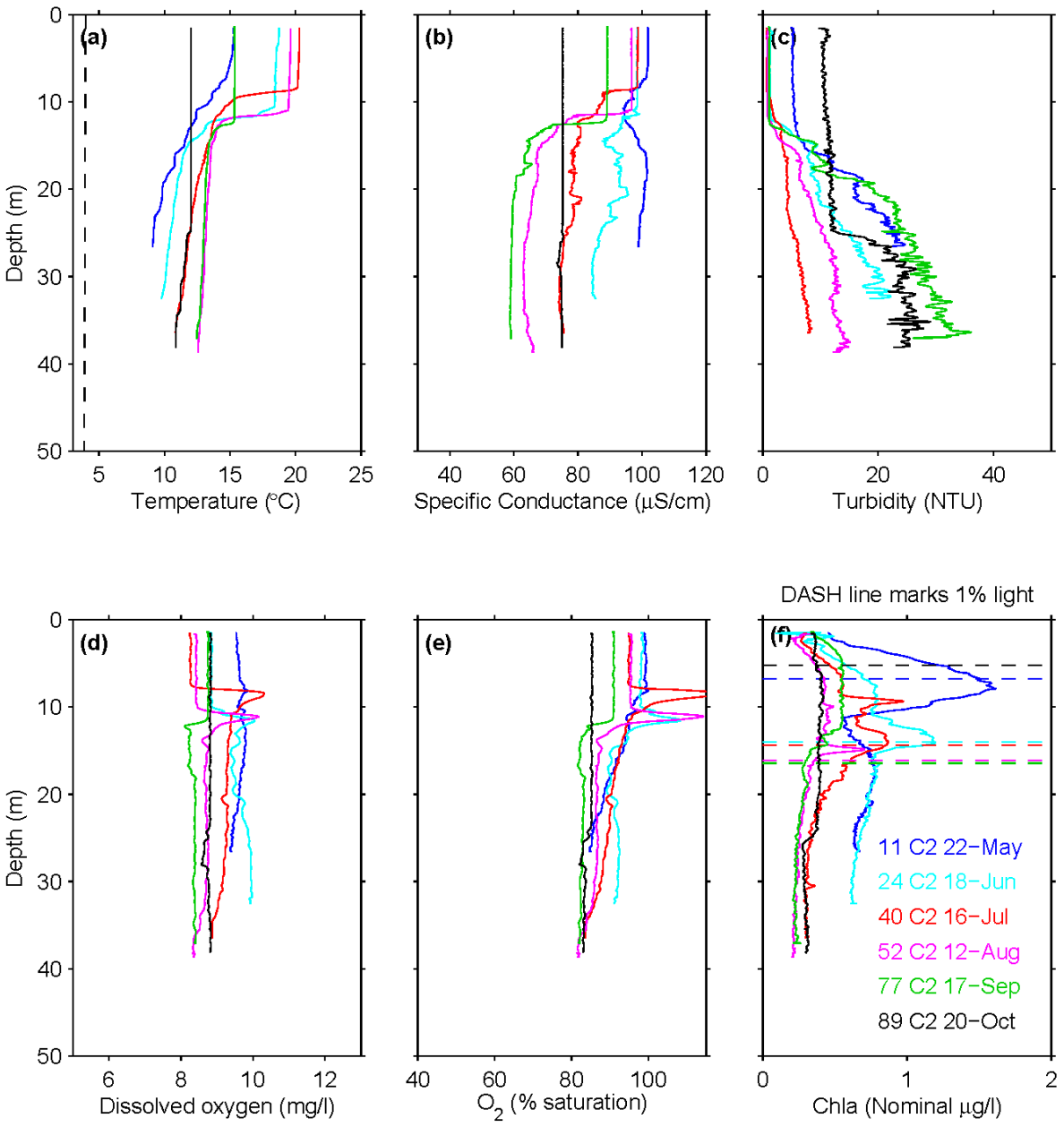

Figure 31. (a) Temperature, (b) conductivity, C25, (c) turbidity, (d) dissolved oxygen, (e) dissolved oxygen as percent saturation, and (f) nominal chlorophyll profiles collected at Carpenter Reservoir station C2, May to October, 2015. The legend in the last panel gives the cast number, station and date. In (f), the dashed lines mark the bottom of the photic zone (the 1% light level).

3.4.7 Mooring

3.4.7.1 Temperature, April to October 2015

The water temperature data measured by the instruments hung from the trash boom in 2015 are shown in Figure 32, along with wind speed, air temperature and solar radiation and inflow, shown for reference.

The water temperature is shown as both a line plot (Figure 32e) and a contour plot (Figure 32f). In the line plot, each line of a given color plots the temperature at a given depth. In the contour plot, the color represents a given temperature. Note, the contour program interpolates data between the measured depths. For example, the contour plot shows a smooth gradient between the data from the sensors at 10 m and 15 m depth. However, from the Seabird profiles, through most of the summer there is a sharp gradient in temperature at the thermocline, located at 12-14 m depth (Figure 31a); this is not resolved in the contour plot. Figure 32f used the same data as shown in Figure 2 but greater smoothing of the data was done in Figure 2 to clearly show the thermocline for purposes of description in that section of the report. Additional sensors were added to the 2016 mooring to better measure the thermocline. From 22 May to 18 June 2015, the deepest temperature sensors were removed for repair of the turbidity wiper.

At the start of the mooring period on 16 April 2015, the reservoir had just begun to stratify with temperature ranging from 5.5 to 7.4 °C. The reservoir reached maximum stratification during the exceptionally hot period from 26 June to 10 July 2015, with a surface layer temperature well above 20 °C and temperature at 0.5 m peaking at 24.9 °C during a period of low wind on 3 July 2015 (day 184). The temperature of the deep water also increased over the summer, reaching a maximum of about 13 °C in late August 2015.

In September, the surface layer cooled steadily and deepened to 15 m on 20 September 2015 (day 263). By mid-October, little stratification remained with temperature ranging from 11.3 to 12.2 °C on 20 October 2015.

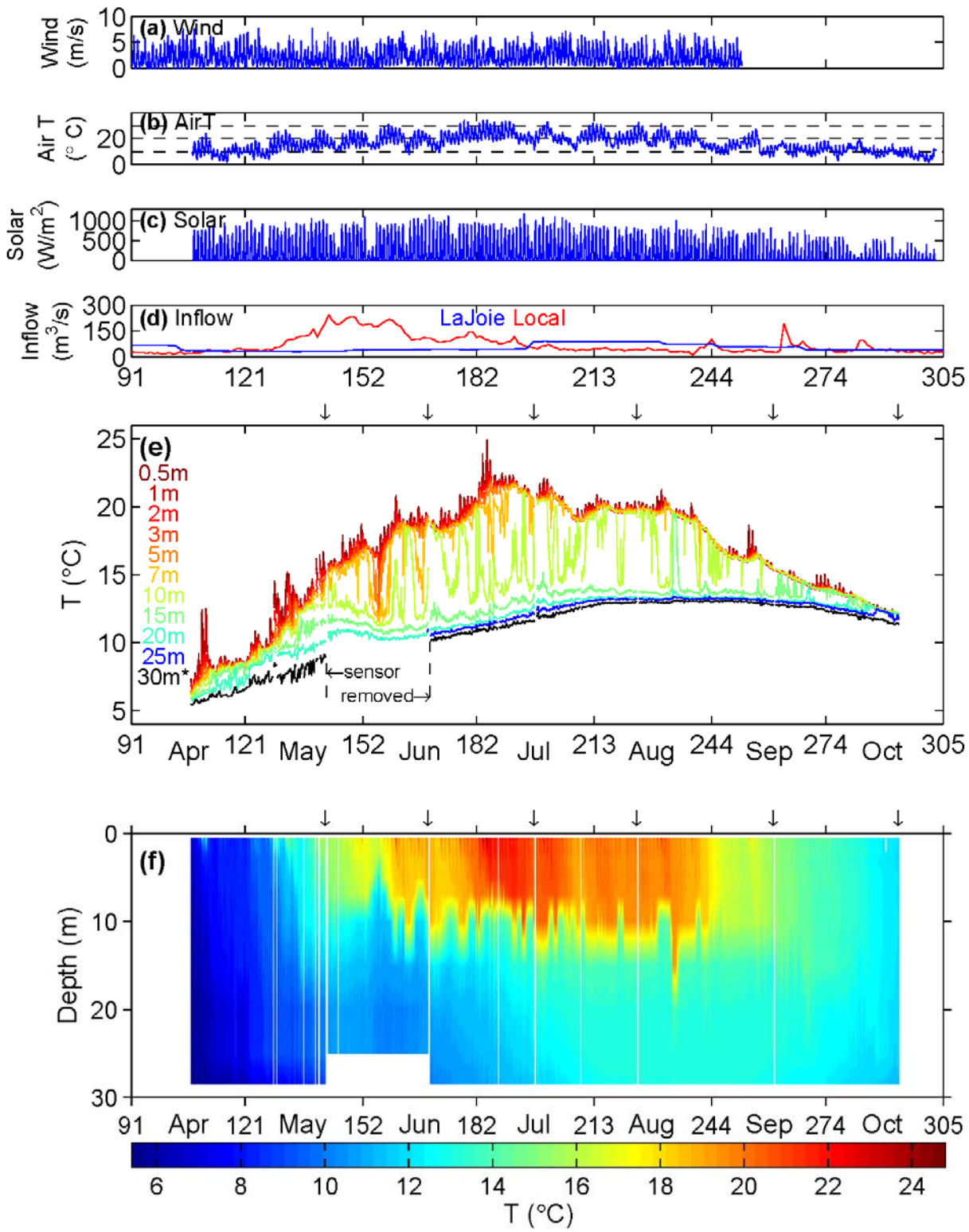

Figure 32. (a) Wind speed at Fivemile, (b) air temperature at Terzaghi Dam, (c) solar radiation at Terzaghi Dam, (d) inflows and (e,f) water temperature at log boom in Carpenter Reservoir, 16 April to 20 October 2015. From 22 May to 18 June, the deepest sensor was removed for repair of the turbidity wiper. Arrows mark the times of the sampling surveys.

3.4.7.2 Turbidity, April to October 2015

A continuous record of turbidity was collected at ~ 30 m depth from the mooring attached to the log boom in Carpenter Reservoir, see Figure 33. The data show that the turbidity is high through April and May (30 to 40 NTU), and that the turbidity declines in June and July to a minimum of 7 NTU in mid-July, after which time the turbidity rose again to 30 to 40 NTU by mid-September.

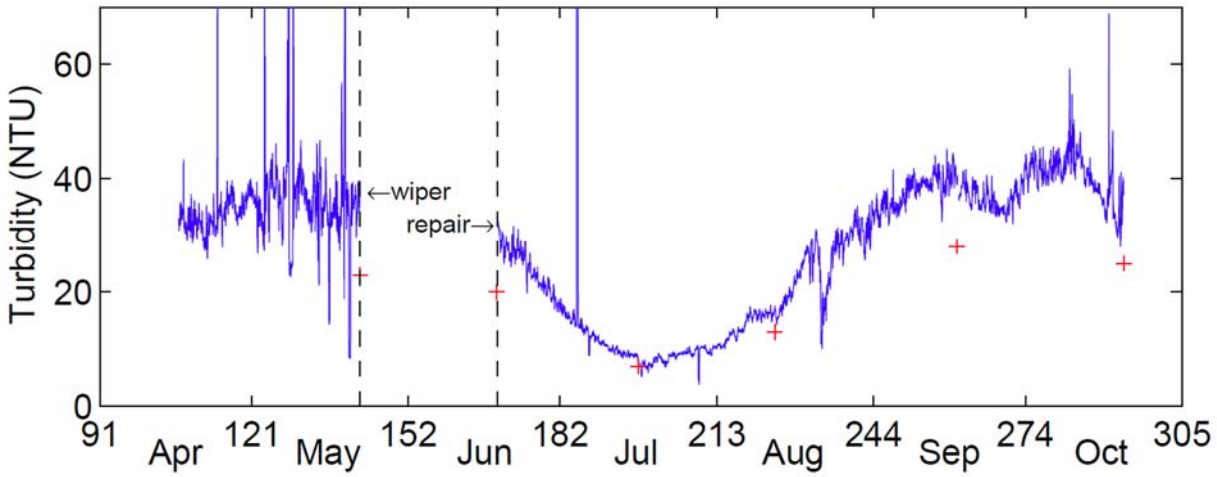

Figure 33. Turbidity data recorded at the log boom in Carpenter Reservoir, 16 April to 20 October, 2015. The recorder was at 27.5 m depth before 18 June 2015, and at 30 m depth thereafter. The red + signs give the turbidity measured at 30 m by the Seabird at Station C2.

3.4.7.3 Temperature, October 2015 to April 2016

On 20 October 2015, the mooring hanging from the trash boom in Carpenter Reservoir was replace with three temperature recorders at depths of 0.5, 5 and 10 m for the winter. When the temperature sensors were installed, the top 10 m were well mixed at 12 °C. Based on the data from the previous mooring removed on 20 October 2015, there was little temperature stratification and fall turnover likely began in late October. The top 10 m cooled steadily and remained well mixed throughout the fall; during this time both wind and cooling contributed to mixing.

The reservoir reached the temperature of maximum density (T_{MD} = 3.98 °C), on 24 December 2015 (day 358), after which it alternated between brief periods of mixing and reverse stratification. Below T_{MD}, cooling gives rise to less dense and stable water, which resists mixing by the wind. The data suggests ice-on was likely complete around 3 January 2016 (day 368) when the water stopped cooling, and a period of relatively steady temperature began.

Relatively steady water temperature ended around 6 February 2016 (day 402), when the 0.5 m sensor began to warm; the 0.5 m sensor reached the temperature of the 5 m sensor on 8 February 2016 (day 404), and that of the 10 m sensor on 14 February 2016 (day 410). From this merging of temperatures, it is hard to pinpoint when ice-off occurred, though it likely happened in late February.

From late-February through March, the top 10 m of the reservoir warmed; during this time both wind and warming contributed to mixing. There was a strong diurnal cycle at 0.5 m, with strong cooling at night (stable) and occasional warming during the day (unstable). The top 10 m reached T_{MD} on 30 March 2016 (day 455). As the surface continued to warm, there were periods of stable temperature stratification and periods of mixing. Whether the stratification observed at the end of the record is the beginning of the permanent summer stratification will be known when data is uploaded from the moorings currently in the reservoir.

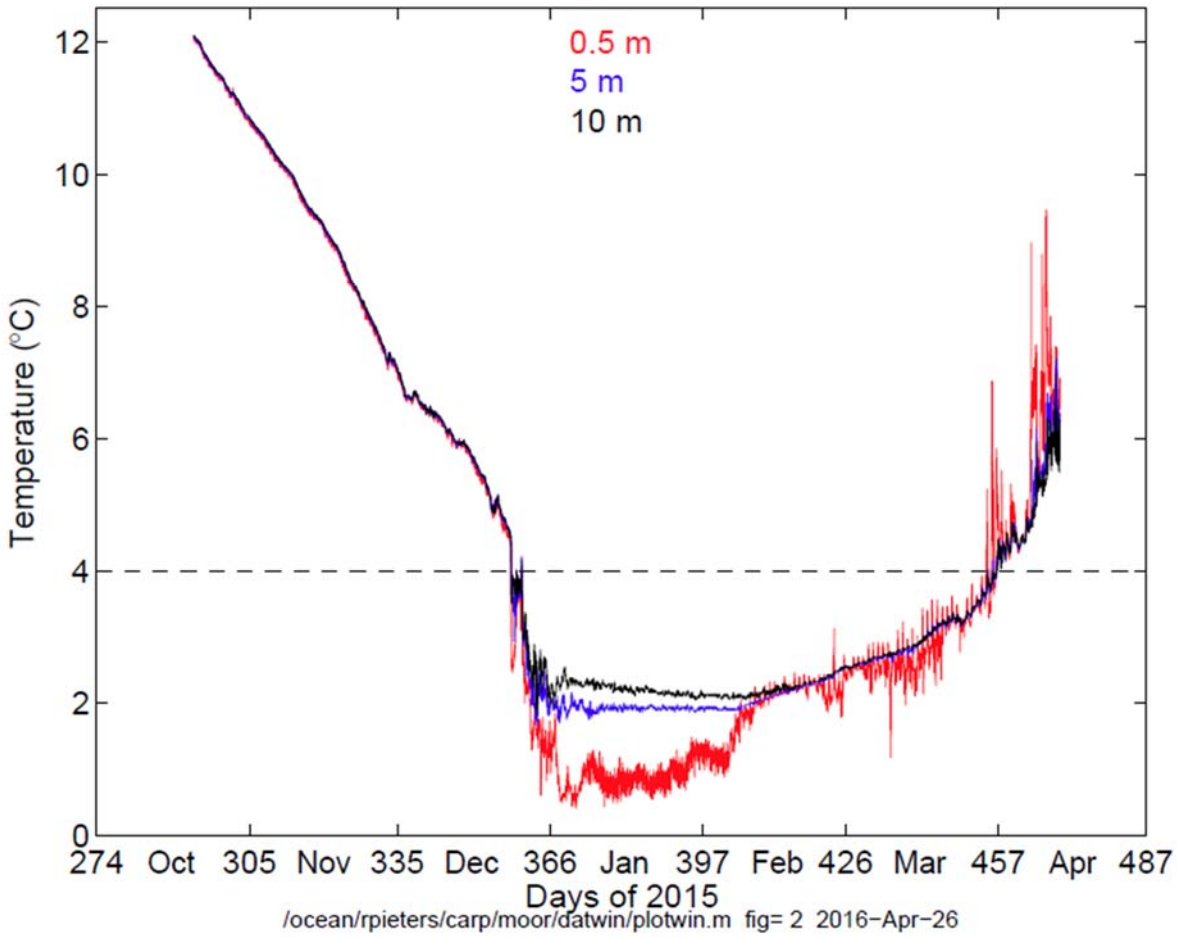

Figure 34. Temperature at 0.5, 5 and 10 m at the trash boom in Carpenter Reservoir, 20 October 2015 to 13 April 2016. The dash line marks the temperature of maximum density.

3.4.8 CE-QUAL-W2 Model

The model CE-QUAL-W2 was run for a period of 22 May to 20 October 2015, corresponding to the dates of the first and last sampling in the reservoir.

The model was initialized with water temperature, TDS and turbidity from the Seabird profile at station C2 on 22 May 2015, along with nutrients (PO_4, TDP, TP and NO_3) from the bottle samples on that date.

The model was forced with wind from the Fivemile site, along with air temperature, relative humidity, and solar radiation from Terzaghi Dam. For the examples shown here, the main inflow consisted of outflow from La Joie Dam plus estimated flow from the Hurley River (25% of the local flow). For turbidity, TDS and nutrients of the main inflow, the model used the data measured at the Middle Bridge River below the Hurley.

Tributary inflow was divided between segments as follows: 25% to segment 2 in order to approximate the inflow of Gun Creek; 25% to segment 4 in order to approximate the inflow of Tyaughton Creek; and the balance of 25% was divided equally between the remaining 12 active segments. The drainage areas to each segment are currently being determined by the Photogrammetry Section at BC Hydro, and these will be used to divide the tributary inflows in future model runs.

For these initial model runs, the water temperature, turbidity, TDS and nutrient concentrations for all tributary inflows were set to those of Gun Creek, which is generally representative of the other tributaries[1]. Flow weighted averages will be used in future model runs, and bootstrap error estimates will be used to bound the temperature, turbidity, TDS and and nutrient concentrations from the balance of the drainage.

As described above, the model was run with 15 inflows: the main inflow of the Middle Bridge River (La Joie outflow plus Hurley River) and 14 tributary inflows, one to each segment. The model was also setup with outflows from the tunnels to the Bridge powerhouses, and from Terzaghi Dam. Given inflow and outflows, the model computes the water level which is shown in Figure 35, which compares well with the measured water level.

[1] The exceptionally high turbidity of 92.7 NTU measured in Gun Creek in August was atypical of the low turbidity in all of the other local tributaries at this time, and, for this model run, was replaced with 3.2 NTU from Tyaughton Creek.

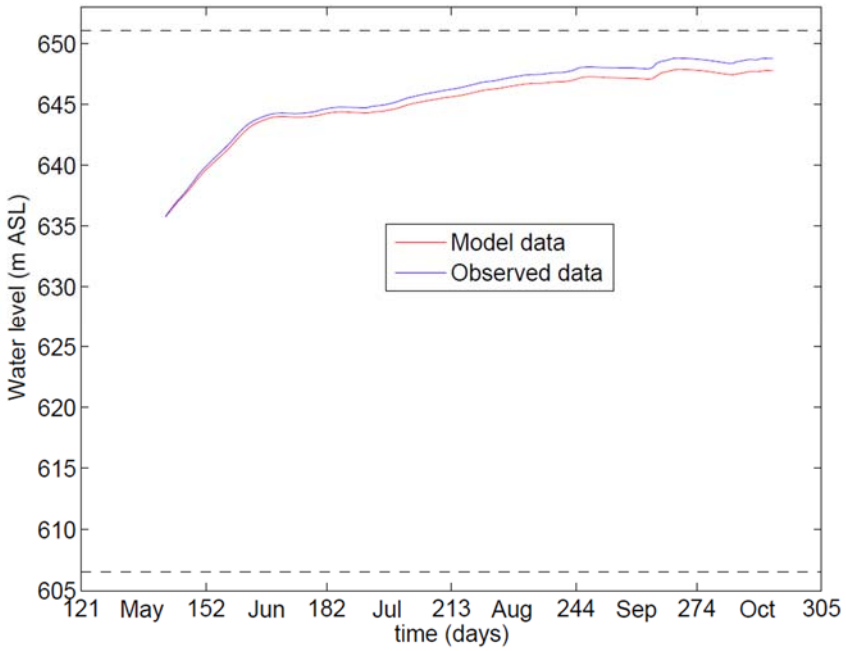

Figure 35. Observed (blue) and modelled (red) water level in Carpenter Reservoir, 16 April to 20 October 2015.

Water temperatures computed by the model are shown as both a line and contour plot in Figure 36, which can be compared with the moored data in Figure 32. Another way to compare the model and measured temperature is to plot the temperature data for individual depths as shown in Figure 37. The modelled temperature shows general agreement with the moored temperature. However, in the model the surface temperature is slightly warmer than observed, the thermocline is somewhat shallower, and the deep temperature remains cooler for the first half of the simulation. The next step includes a sensitivity analysis of the results to parameters such as tributary temperature and wind.

Both the moor and model data show oscillations in the depth of the thermocline, separating the warm epilimnion from the cooler hypolimnion. These oscillations have a period of 4 to 6 days, and likely results from prolonged variations of the wind on the surface of the reservoir. For example, wind from the west will push the warm surface layer toward Terzaghi Dam, deepening the layer of warm water in the vicinity of the dam. When the wind ends, the warm layer will become shallower again. Given limited wind data, the model is unlikely to accurately predict the details of these internal wave motions; the goal is to accurately model the seasonal evolution of the overall stratification.

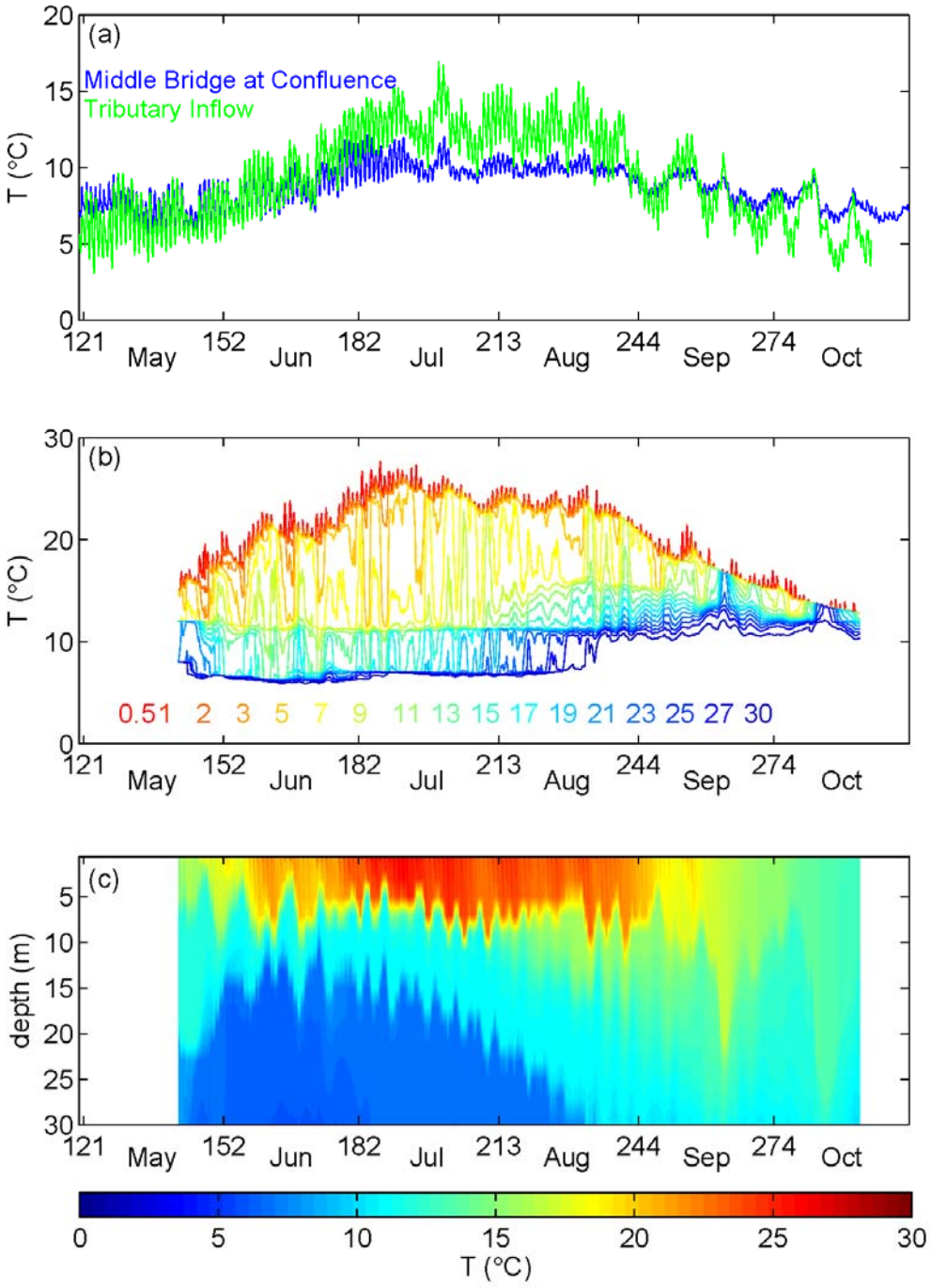

Figure 36. (a) Water temperature used for this main and tributary inflow to the model. (b) Line and (c) contour plots of modelled water temperature, segment 13 (station C2), Carpenter Reservoir, 22 May to 20 October 2015.

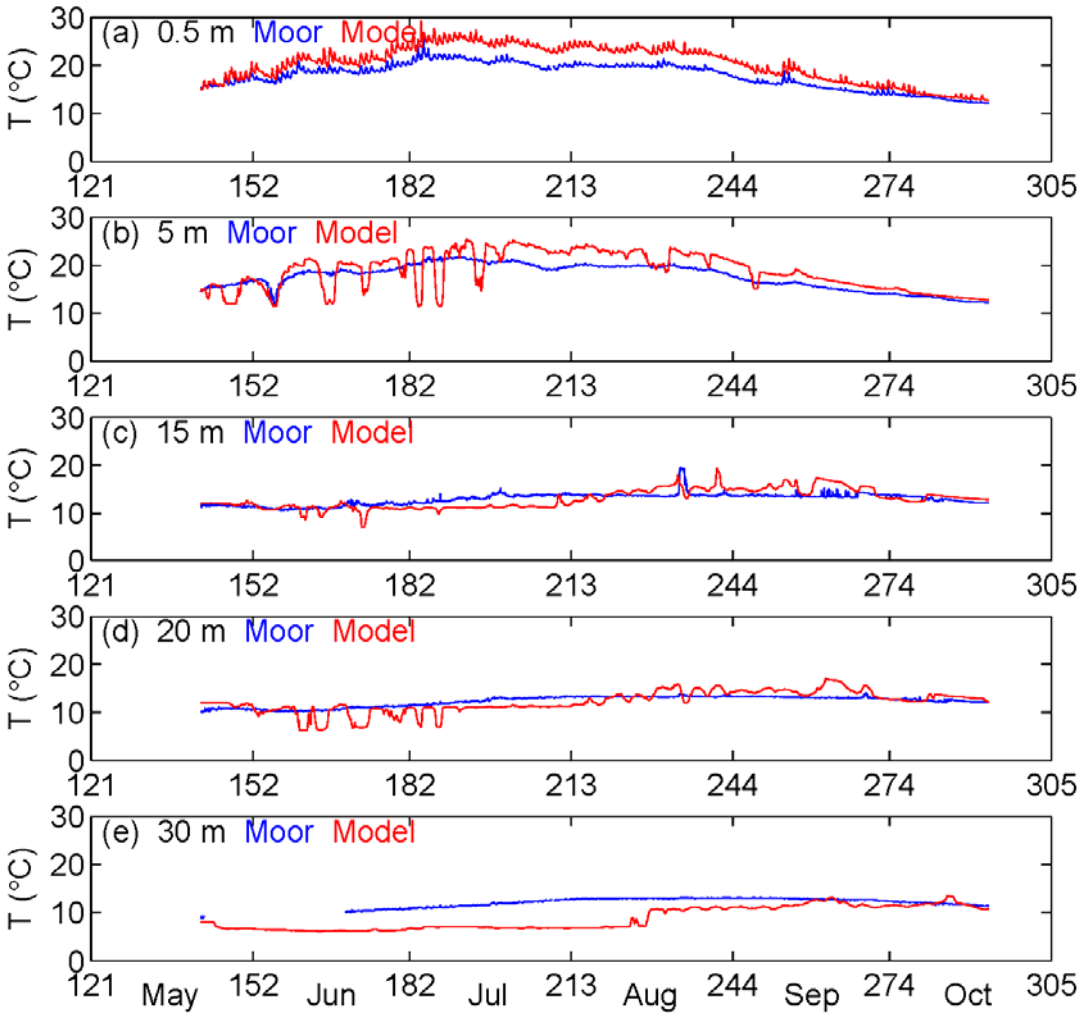

Figure 37. Comparison of the temperature measured at the log boom (blue) and the temperature from segment 13 (station C2) of the model (red) at depths of (a) 0.5, (b) 5, (c) 15, (d) 20 and (e) 30 m.

In what follows, the model results for turbidity, TDS and two nutrients (TDP and NO_3) are examined. The model output for turbidity is shown in Figure 38. The initial turbidity in the reservoir was 10 NTU. The turbidity in both the Middle Bridge River and the local tributary inflow were ~50 NTU at the start of the simulation, they both declined to ≤10 NTU in June, but then the turbidity in the Middle Bridge River rose again (Figure 38a).

The effect of these inflows can be seen in the reservoir: plunging of cold turbid inflow initially increased the turbidity of the deep water of the reservoir (below 15 m, June to mid-July, Figure 38b). During this time, the turbidity of the top 10 m was relatively unaffected. After mid-July the turbidity of the deepest water (<20 m) began to decline due to declining inflow turbidity. From August onward the picture is more

complex, with the turbidity of the surface layer beginning to increase slightly, and the turbidity increasing at mid-depth. The pattern of the declining and then rising turbidity of the deep water was observed in the Seabird profiles (Figure 31c). The next step is a detailed comparison of the model results to the monthly turbidity from the Seabird.

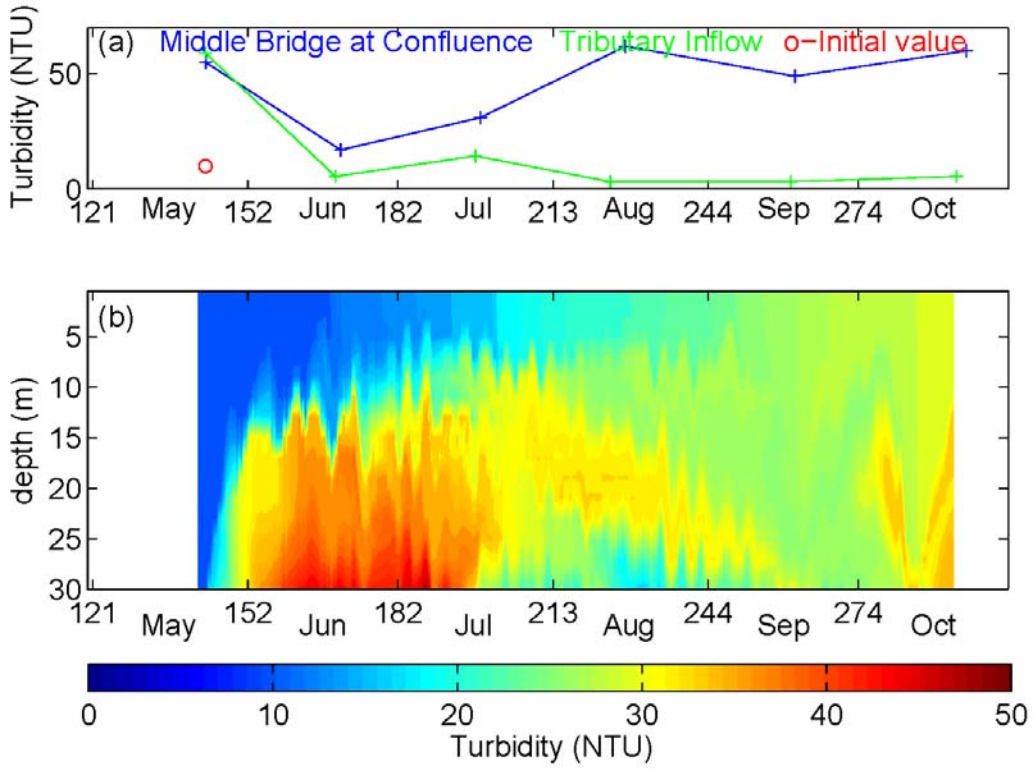

Figure 38. (a) Turbidity from the Middle Bridge River below the Hurley and from Gun Creek used by the model. (b) Modelled Turbidity at Station C2 in Carpenter Reservoir 22 May to 20 October 2015.

Total dissolved solids (TDS) is a measure of the dissolved ions of the water, and is a useful tracer given the contrasting TDS of the inflows. The initial TDS of the reservoir was 70 mg/L, the inflow from the Middle Bridge River had lower TDS (~40 mg/L), and the tributary inflow used here had rising TDS (≥70 mg/L), see Figure 39a.

In the reservoir, the TDS of the deep water generally declined reflecting the plunging of the cold and fresher inflow of the Middle Bridge River. The TDS of the surface water remained relatively steady through summer, and began to decline in the fall. Note the lens of fresh water around 10 m from mid-August to mid-September suggests that some of the fresher inflow from the Middle Bridge River slotted in at the

thermocline. The declining TDS of the deep water was also observed in the C25[2] from the Seabird profiles (Figure 31b).

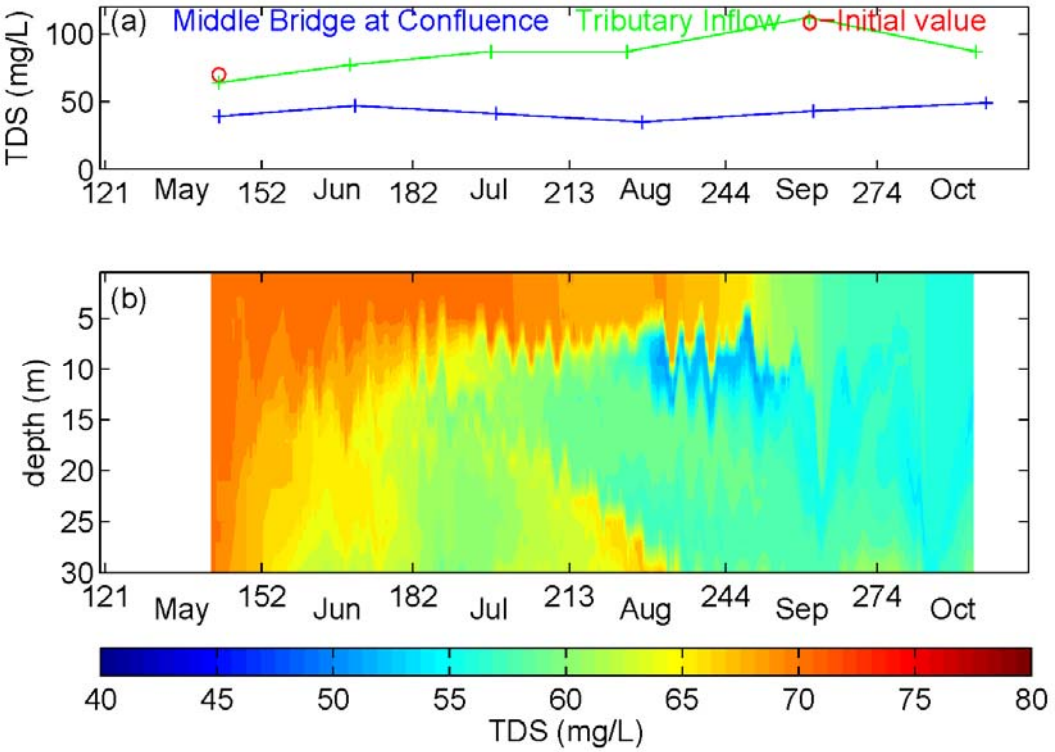

Figure 39. (a) Total dissolved solids (TDS) from the Middle Bridge River below the Hurley and from Gun Creek used by the model. (b) Modelled TDS at Station C2 in Carpenter Reservoir 22 May to 20 October 2015.

Total dissolved phosphorus (TDP) concentration from the model is shown in Figure 40. The initial TDP was at the detection limit of 2 µg/L; the tributary inflow was also at or close to the detection limit. TDP in the Middle Bridge was somewhat higher, reaching 4.7 µg/L in August 2015 (Figure 40a).

The effect of the higher TDP in the Middle Bridge River can be seen at depth, through June and July. During this time the TDP concentration in the surface layer remained relatively constant. In mid August, the lens of elevated TDP at 10 m again suggests insertion of the Bridge River inflow to the thermocline. In September and August, the TDP generally increased at most depths. This suggests that resupply of TDP to the surface layer does not occur until the fall, and that TDP from the Middle Bridge may 'short circuit' to the deep outlet without being available to the photic zone.

[2] Electrical conductivity, corrected to 25 °C (C25) is used to measure TDS; TDS[mg/L] ≈ 0.7 * C25 [µS/cm].

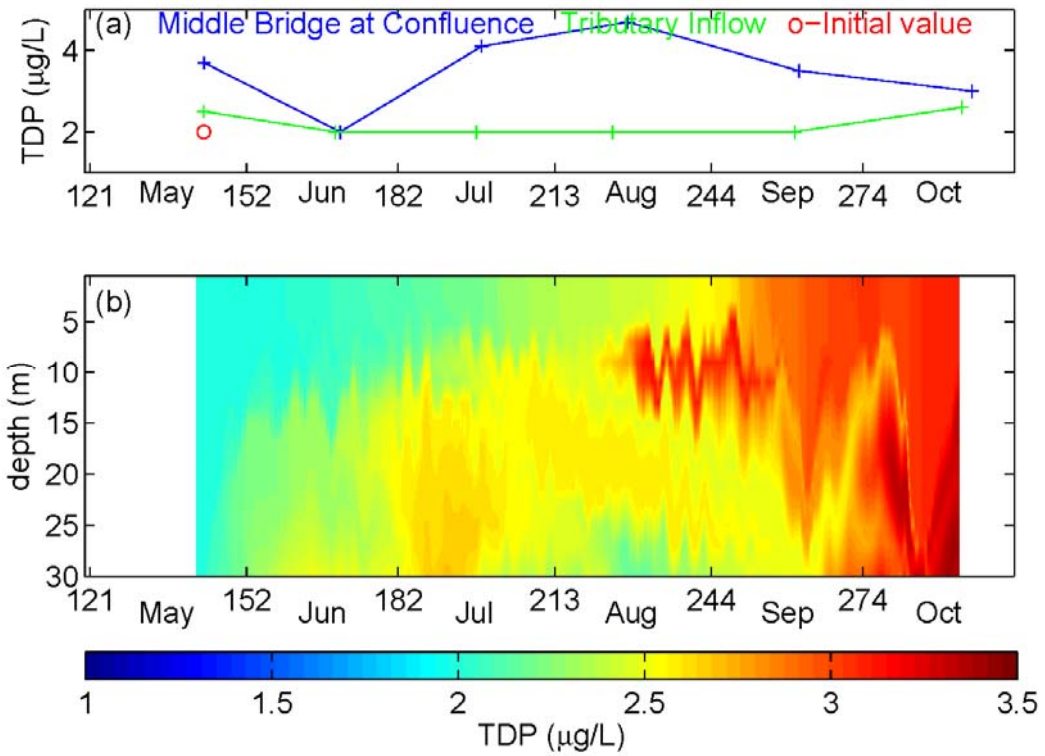

Figure 40. (a) Total dissolved phosphorus (TDP) from the Middle Bridge River below the Hurley and from Gun Creek used by the model. (b) Modelled TDP at Station C2 in Carpenter Reservoir 22 May to 20 October 2015.

The model results for nitrate (NO_3) are shown in Figure 41. The initial concentration of nitrate in the reservoir was very low (10 µg/L). The concentration of nitrate in the tributary inflow was also very low, and that in the Middle Bridge River was modestly higher or the first part of the summer (Figure 41).

Again the plunging of the Middle Bridge River inflow resulted in increasing nitrate at depth in June and early July, while nitrate in the surface layer remained relatively constant until mid August when it began to rise (Figure 41b). Again, nitrate in the inflow was not made available for early season productivity.

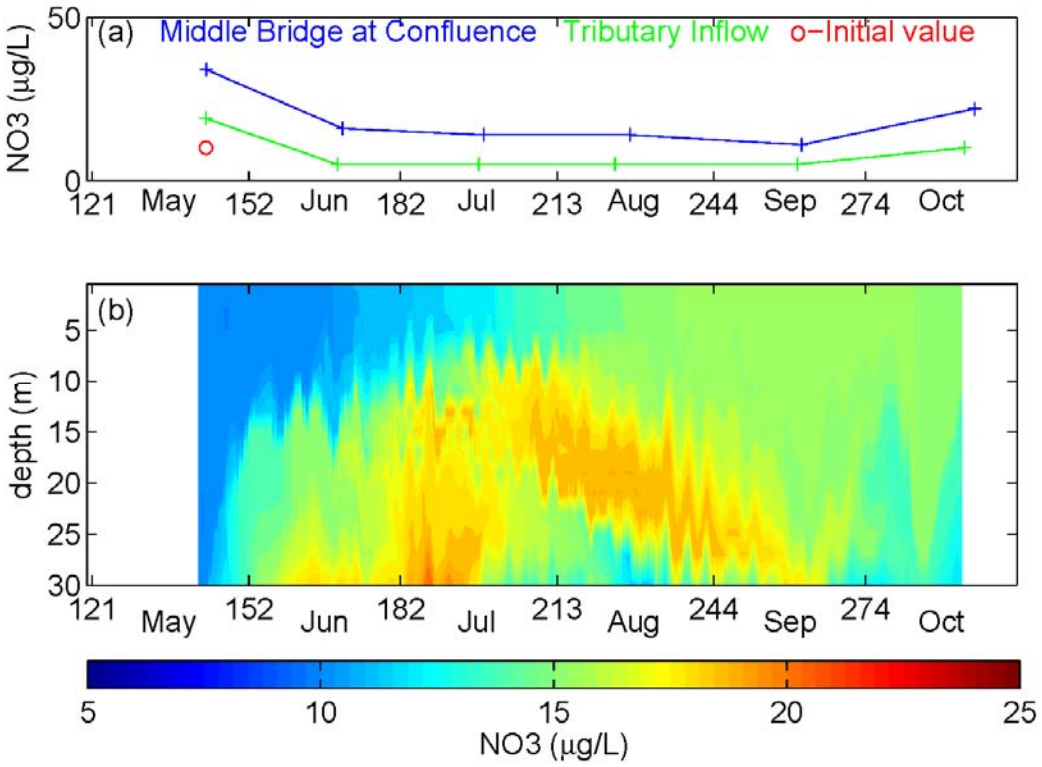

Figure 41. (a) Nitrate (NO_3) from the Middle Bridge River below the Hurley and from Gun Creek used by the model. (b) Modelled NO_3 at Station C2 in Carpenter Reservoir 22 May to 20 October 2015.

3.5 Question 4: Can suspended sediment transport into Seton be altered by changes in Carpenter Reservoir Operations?

Incorporating data collected in 2016 and 2017 into the analyses on the biological responses to environmental variables along with the integration of the CE-QUAL-W2 model will be required to fully answer this question.

4 CONCLUSIONS

The purpose of this project is to determine if light is the primary regulating factor for biological production in Carpenter Reservoir and how flow management decisions might affect PAR and other environmental variables. The results will ultimately inform how to best manage Carpenter Reservoir to benefit fish populations and their prey.

Based on our current findings, PAR is an important driver of littoral periphyton production on stony substrates. However, PAR did not describe as much variation in periphyton growing on sand or zooplankton biomass in the pelagic habitat. We will analyze the pelagic phytoplankton data this year, which is likely highly affected by PAR. Given that the smaller size class of phytoplankton was an important determinant in

zooplankton biomass, PAR may influence zooplankton production indirectly by influencing the biomass of phytoplankton.

Zooplankton biomass increased with water residence time, a measure that can be managed by increasing or decreasing the outflow in Carpenter Reservoir. As a cursory check, we looked at how change in water residence time would affect zooplankton biomass during the coolest and warmest months in the reservoir. Using Figure 42, we identified May-June as the coolest months and August-September as the warmest with mean temperatures of 11.13 °C and 13.90 °C, respectively.

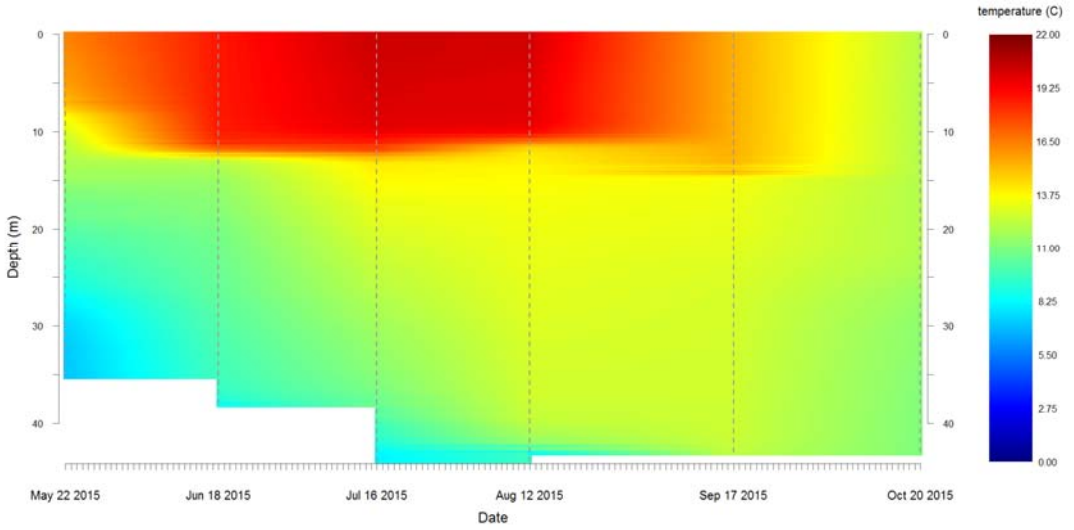

Figure 42. Temperature profile for Carpenter Reservoir by sampling date as indicated by the vertical dashed lines.

A doubling of mean water residence time from 57 days to 113 days resulted in a 4% increase in zooplankton biomass of 71 mg dry weight/m^2 for both temperature regimes (Figure 43). However, an increase in mean temperature from 11.13 to 13.90 °C resulted in a 77% increase in zooplankton biomass of 1,432 mg dry weight/m^2, regardless of mean water residence time. This is a substantial difference but this correlation may be due to the seasonal changes in species development rather than driven by environmental variables. This trend will need to be further explored in subsequent analyses.

From Figure 43 and the regression results in Sections 3.3.3 and 3.3.4 we can see that temperature had a much larger effect on zooplankton biomass than water residence time.

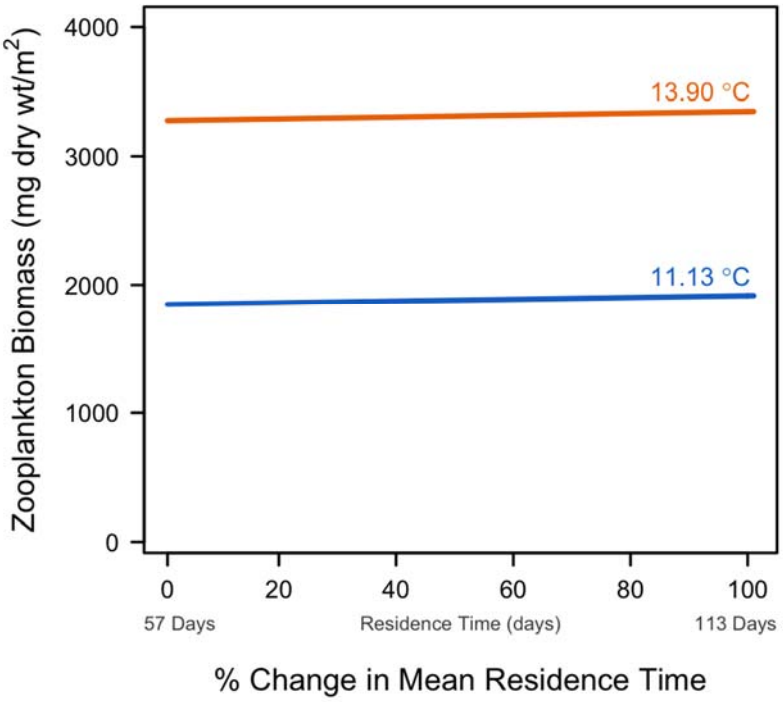

Figure 43. Zooplankton biomass as a function of percent change in mean residence time. The range extends from the minimum mean recorded residence time during the sampling period in 2015 (0% change or 57 days) to 100% change or twice as long (113 days).

We also found that water temperature, turbidity and dissolved inorganic nitrogen were significant determinants of periphyton and zooplankton production. These factors along with PAR are endpoints from the CE-QUAL-W2 model, which is performing well with the 2015 data. An emerging picture of links between physical and chemical attributes in the reservoir and biological production is as follows. Relatively warm water having low turbidity favouring zooplankton is restricted to the top 10m of the water column in May through September. Bottom water is cold and turbid in relation to inflows sinking according to density gradients, mainly in May through mid-July. After July, inflow turbidity declines as does the bottom turbidity in the reservoir but the bottom water remains cool. The change in inflow turbidity is likely related to declining flows and less erosion by glacial headwaters that leads to reduced transport of fines. As temperature rises among inflows late in the summer, some entrainment of inflow in reservoir surface waters is apparent with accompanying increasing turbidity. The strong influence of rising temperature over more of the water column than earlier in the growing season has a strong effect by favouring conditions for zooplankton despite the rising turbidity. Increasing concentrations of TDP and NO_3-N late in the growing season in Carpenter Reservoir resulted in increasing export to Seton Lake with peak transport of TDP in the fall (Figure 44) and peak DIN in the early summer, followed by more moderate increases

in the fall (Figure 45). These increases will favour phytoplankton and periphyton production with the boost in phytoplankton production favouring zooplankton. These interactions show that fall is an optimum time for biological production in Carpenter Reservoir and potentially Seton Lake. Combinations of suitable temperature and rising nutrient concentrations will drive metabolic activity. Light does not appear to be the main story of the modeling so far.

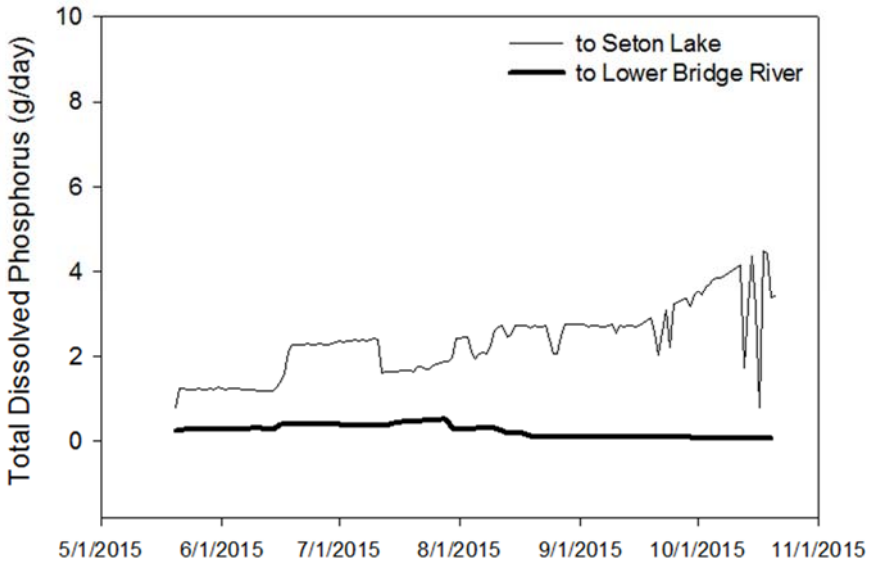

Figure 44. Total dissolved phosphorus (TDP) transport from Carpenter Reservoir to Seton Lake (thin line) and Lower Bridge River (bold line) from 1 May to 1 November, 2015.

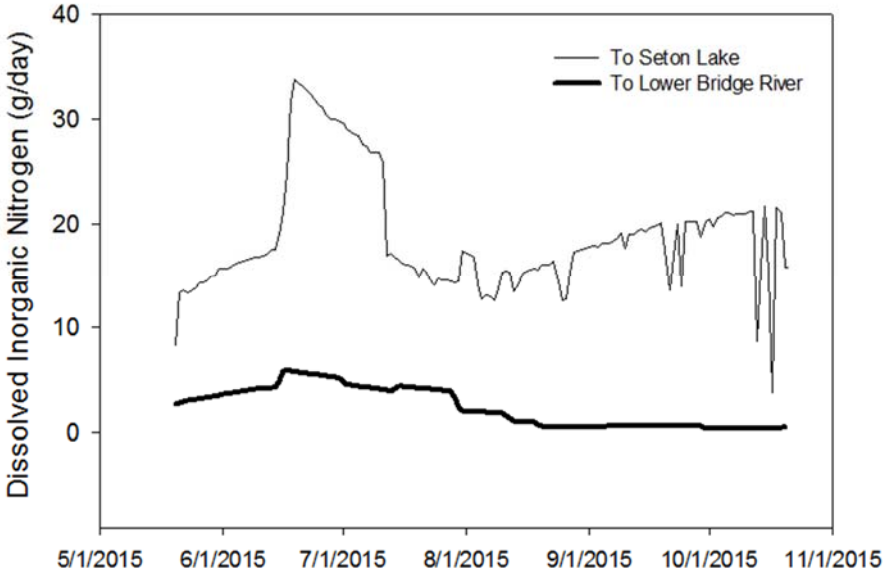

Figure 45. Dissolved inorganic nitrogen (DIN) transport from Carpenter Reservoir to Seton Lake (thin line) and Lower Bridge River (bold line) from 1 May to 1 November, 2015.

Further development of the modeling will include quantitative linking of CE-QUAL-W2 and the statistical models. This link will facilitate simulations to show implications of change in a water management strategy on biological endpoints including periphyton accrual that is an indicator of benthic production in littoral habitat and phytoplankton and zooplankton that are indicators of biological production in pelagic habitat. This approach can be particularly valuable in exploring potential change to biological production with respect to unforeseen events as is presently occurring with need to release more water this spring and for ongoing periods in face of safety precautions needed in the Bridge system (Ministry of Forest, Lands and Natural Resource Operations, 2016). The linked CE-QUAL-W2 and regression modelling will prove very useful in predicting changes to biological production in Carpenter Reservoir should similar or different scenarios occur in the future.

5 NEXT STEPS

5.1 Biological production and environmental variables

Periphyton, phytoplankton and zooplankton samples will continue to be collected in 2016 along with water chemistry, light, CTD profiles for PAR, turbidity, temperature and other measures of suspended and dissolved material to increase the dataset for and predictive power of the regression models. This new data will be collected from Carpenter Reservoir, Anderson Lake and Seton Lake.

5.2 CE-QUAL-W2 modelling strategy

The modelling strategy consists of the following steps:

1. **Model setup** CE-QUAL-W2 has been setup to simulate conditions during the productive season of 2015, and will be setup for a second year of field data collected in 2016.
2. **Model calibration** The next step is to undertake a systematic comparison of the model to the measured field parameters, including TDS, turbidity, PO_4, TDP, TP, and NO_3. A sensitivity analysis of important parameters, such as tributary temperature and wind, will also be undertaken. For example, using the warmer Sucker Creek for all local tributary temperatures gave better agreement to the measured temperature (Figure 46). The model will be calibrated by adjusting the tributary boundary conditions and model parameters to give the best results for 2015.
3. **Model validation** The model will be validated by comparing the results to the field data for 2016.
4. **Reservoir operation scenarios** The model will be used to simulate a variety of reservoir conditions (e.g. high flow year, low water level year) and a variety of reservoir operations. Data from CE-QUAL-W2 will be extracted for input into the empirical productivity model.

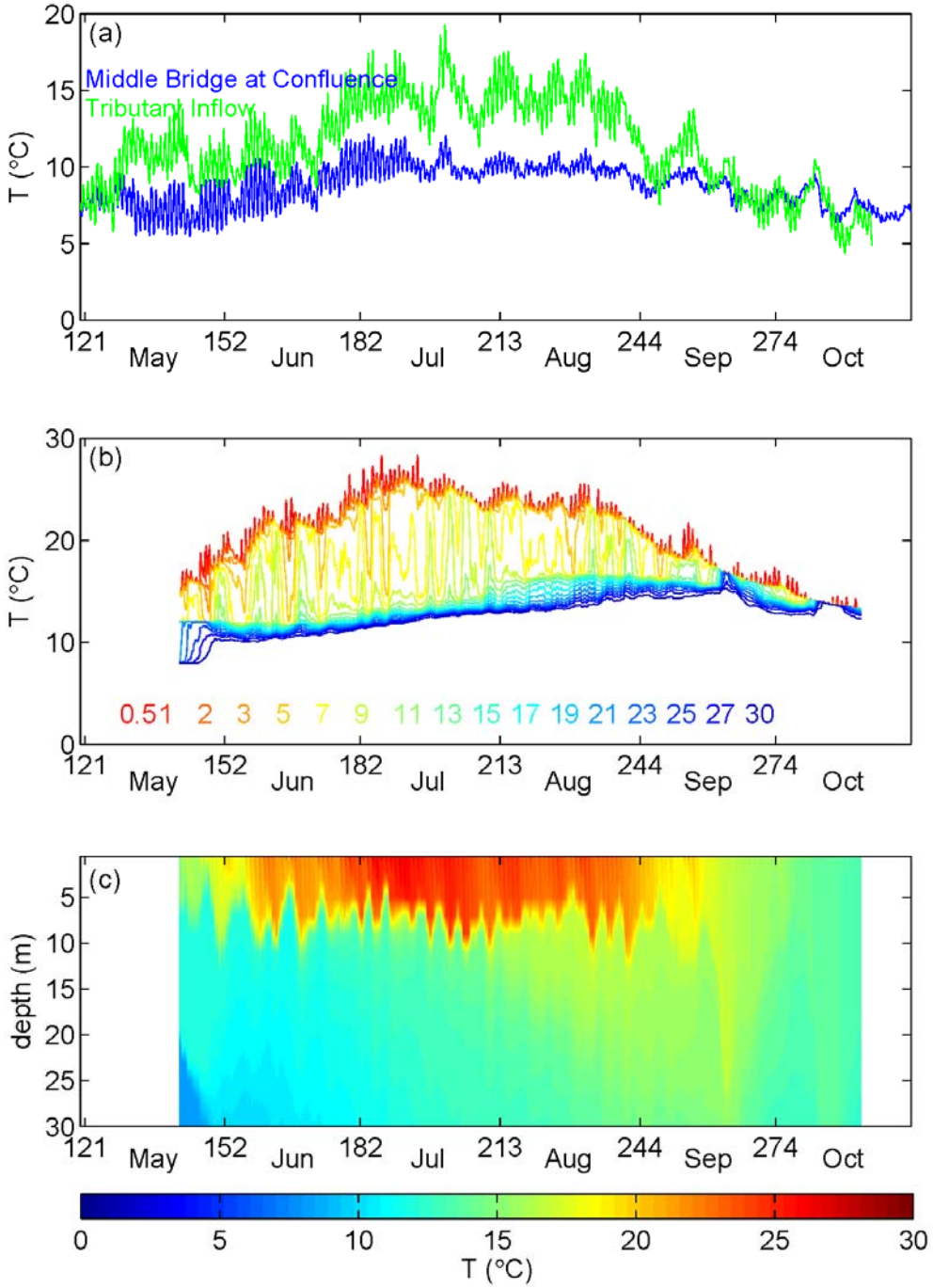

Figure 46. (a) Water temperature used for this main and tributary inflow to the model; the tributary inflow was set to the warmer temperature of Sucker Creek rather than Gun Creek. (b) Line and (c) contour plots of modelled water temperature, segment 13 (station C2), Carpenter Reservoir, 22 May to 20 October 2015. Compare with Figure MODT (model with Gun Creek) and Figure FIGMOOR.

6 LIST OF REFERENCES CITED

Armantrout, N.J. 1998. *Glossary of Aquatic Habitat Inventory Terminology*. American Fisheries Society. Bethesda, MD.

Akaike, H. (1974). New Look at Statistical Model Identification. IEEE Transactions on Automatic Control, AC19(6), 716–723.

Allan, J. D., and M. M. Castillo. 2007a. Nutrient dynamics. In Stream Ecology: structure and function of running waters (2nd ed.). Dordrecht, The Netherlands: Springer.

Allan, J. D., and M. M. Castillo. 2007b. Primary producers. In Stream Ecology: structure and function of running waters (2nd ed.). Dordrecht, The Netherlands: Springer.

Allan, J. D., and M. M. Castillo. 2007c. The abiotic environment. In Stream Ecology: structure and function of running waters (2nd ed.). Dordrecht, The Netherlands: Springer.

Basu, B. K., and F. R. Pick. 1996. Factors regulating phytoplankton and zooplankton biomass in temperate rivers. Limnology and Oceanography, 41(7), 1572–1577.

BC Hydro. 1995. Dam Safety Investigations. Terzaghi Dam deficiency investigation. Summary report and appendices. BC Hydro. Maintenance, Engineering and Projects. Report No. H2479.

Behrenfeld, M.J., E. Boss, D.A. Siegel, and D.M. Shea. 2005. Carbon-based ocean productivity and phytoplankton physiology from space. Global Biogeochemical Cycles. 19: 1-14.

Benke, A.C. and A.D. Huryn. 2006. Secondary production of macroinvertebrates. In F.R. Hauer and G.A. Lamberti (eds.). *Methods in Stream Ecology*. New York, NY: Academic Press. 691-710.

Berry, H. A., and C. A. Lembi. (2000). Effects of temperature and irrandiance on the seasonal variation of a Spirogyra (Chlorophyta) population in a midwestern lake (USA). Journal of Phycology, 36, 841–851.

Biggs, B.J.F. 2000. Eutrophication of streams and rivers: dissolved nutrient-chlorophyll relationships for benthic algae. *Journal of the North American Benthological Society* 19: 17-31.

Bothwell, M.L. 1988. Growth rate responses of lotic periphytic diatoms to experimental phosphorus enrichment: The influence of temperature and light. *Canadian Journal of Fisheries and Aquatic Sciences*. 45: 261-270.

Bothwell, M.L. 1989. Phosphorus – limited growth dynamics of lotic periphyton diatom communities: Areal biomass and cellular growth rate responses. *Canadian Journal of Fisheries and Aquatic Sciences*. 46: 1293-1301.

Bridge River WUP CC. 2003. Bridge River Water Use Plan Consultative Committee Report (WUP CC). Compass Resource Management and BC Hydro. A report produced for BC hydro Water Use Planning group. (Executive Summary available on website: http://www.bchydro.com/content/dam/hydro/medialib/internet/documents/environment/pdf/wup_bridge_river_executive_summary_pdf.pdf

Burks, R. L., D. M. Lodge, E. Jeppesen, and T. L. Lauridsen. 2002. Diel horizontal migration of zooplankton: costs and benefits of inhabiting the littoral. Freshwater Biology, 47, 343–365.

Burnham, K. P., and D. R. Anderson. 2002. Model selection and multimodel inference: a practical information-theoretic approach (2nd ed., pp. 1–515). New York, NY: Springer.

Canter-Lund, H. and J.W.G. Lund. 1995. *Freshwater Algae – Their Microscopic World Explored*. BioPress Ltd. Bristol, U.K.

Clarke, L.R. and D.H. Bennett. 2007. Zooplankton production and planktivore consumption in Lake Pend Oreille, Idaho. *Northwest Science* 81: 215-223.

Clarke, K.R., and R.N. Gorley. 2006. PRIMER v6: User Manual/Tutorial. PRIMER-E: Plymouth. UK.

Cloern, J.E., C. Grenz, and L. Vidergar-Lucas. 1995. An empirical model of the phytoplankton chlorophyll:carbon ratio – the conversion factor between productivity and growth rate. Limnology and Oceanography. 40: 1313-1321.

Cole T. M. and S. A. Wells. 2015. CE-QUAL-W2: A Two-Dimensional, Laterally Averaged, Hydrodynamic and Water Quality Model, Version 3.72, User Manual. Department of Civil and Environmental Engineering, Portland State University, Portland, Oregon. 797pp.

Cyr, H., and M. L. Face. 1993. Magnitude and patterns of herbivory in aquatic and terrestrial ecosystems. Nature, 361, 148–150.

Effron, B. and R. Tibshirani. 1993. An introduction to the bootstrap. Mongraphs on Statistics and Applied Probability No. 57. Chapman and Hall. London, U.K.

Geen, G.H. and F.J. Andrew. 1961. Limnological changes in Seton Lake resulting from hydroelectric diversions. International Pacific Salmon Commission Progress Report 8.

Goldman, J.C. and E.J. Carpenter. 1974. A kinetic approach to the effect of temperature on algal growth. Limnology and Oceanography. 19: 756-766.

Griffiths, R.P. 1999. Assessment of fish habitat and production in Carpenter Lake Reservoir relative to hydroelectric operations. Report prepared by R.P. Griffith and Associates for BC Hydro. 202p.

Guildford, S.J. and R.E. Hecky. 2000. Total nitrogen, total phosphorus, and nutrient limitation in lakes and oceans: Is there a common relationship? Limnology and Oceanography. 45: 1213-1223.

Harrell, F. E. 2001. Regression modelling strategies. New York, New York, USA: Springer.

Haven, K. E., J. Hauxwell, A. C. Tyler, S. Thomas, K. J. McGlathery, and J. Cebrian. 2001. Complex interactions between autotrophs in shallow marine and freshwater ecosystems: implications for community responses to nutrient stress. Environmental Pollution, 113, 95–107.

Healey, F.P. 1985. Interacting effects of light and nutrient limitation on the growth rate of *Synechococcus linearis* (Cyanophyceae). Journal of Phycology 21:134-146.

Ichimura, S., T.R. Parsons, M. Takahashi and H. Seki. 1980. A comparison of four methods for integrating ^{14}C-primary productivity measurements per unit area. J. Oceanogr. Soc. Jap. 36: 259-262.

Jeppesen, E., J. P. Jensen, M. Søndergaard, and T. Lauridsen. 1999. Trophic dynamics in turbid and clearwater lakes with special emphasis on the role of zooplankton for water clarity. Hydrobiologia, 408/409, 217–231.

Korpelainen, H. 1986. The effects of temperature and photoperiod on life history parameters of Daphnia magna (Crustacea: Cladocera). Freshwater Biology, 16, 615–620.

Lamberti, G. A., and A. D. Steinman. 1997. A comparison of primary production in stream ecosystems. Journal of the North American Benthological Society, 16(1), 95–104.

Leland, H. V. 1995. Distribution of phytobenthos in the Yakima River basin, Washington, in relation to geology, land use and other environmental factors. Canadian Journal of Fisheries and Aquatic Sciences, 52(5), 1108–1129.

Li, Q. P., P. J. S. Franks, M. R. Landry, R. Goericke, and A. G. Taylor. 2010, Modeling phytoplankton growth rates and chlorophyll to carbon ratios in California coastal and pelagic ecosystems, Journal of Geophysical Research. 115, G04003.

Liess, A, C. Faithful, B. Reichstein, O. Rowe, J. Guo, R. Pete, G. Thomsson, W. Uszko, and S. N. Francoeur. 2015. Terrestrial runoff may reduce microbenthic net community productivity by increasing turbidity: a Mediterranean coastal lagoon mesocosm experiment. Hydrobiologia, 753(1), 205-218.

Limnotek. 2016. Seton Lake aquatic productivity monitoring (BRGMON6): Progress in 2015-16. (pp. 1–194).

Marcarelli, A. M., C. J. Huckins, and S. L. Eggert. 2015. Sand aggradation alters biofilm standing crop and metabolism in a low-gradient Lake Superior tributary. Journal of Great Lakes Research, 41(4), 1052–1059. http://doi.org/10.1016/j.jglr.2015.09.004

McCauley E. 1984. The estimation of the abundance and biomass of zooplankton in samples. In J.A. Downing and F.H. Rigler (eds.). *A Manual on Methods for the Assessment of Secondary Productivity in Fresh Waters*. Oxford, U.K.: Blackwell Scientific Publications. 228-265.

Ministry of Forest, Lands and Natural Resource Operations. 2016. Section 93 Order – Terzaghi Target Flow Release and Annual Water Budget dated May 20, 2016. File: 76975-35/Bridge

Nürnberg, G. K. and B. D. LaZerte. 2001. Predicting lake water quality. In: C. Holdren, W. Jones and J. Taggart. Ed. Managing lakes and reservoirs. North American Lake Management Society, Madison, WI. Terrene Institute in cooperation with Office of Water Assessment Watershed Protection Division U.S.-EPA, p. 139-163.

Parsons, T.K., Y. Maita and C.M. Lalli. 1984. A Manual of Chemical and Biological Methods for Seawater Analysis. Pergamon Press, Oxford. 173 p.

Pawlowicz, R. 2008. Calculating the conductivity of natural waters. Limnology and Oceanography: Methods, **4**: 489–501.

Perrin, C.J., M.L. Bothwell and P.A. Slaney. 1987. Experimental enrichment of a coastal stream in British Columbia: effects of organic and inorganic additions on autotrophic periphyton production. Canadian Journal of Fisheries and Aquatic Science 44:1247-1256.

Perrin, C. J., & Richardson, J. S. 1997. N and P limitation of benthos abundance in the Nechako River, British Columbia. Can. J. Fish. Aquat. Sci., 54, 2574–2583.

Perrin, C.J. and R.H. Macdonald. 1999. A phosphorus budget and limnology in Carpenter Lake Reservoir, 1995-96. Report prepared by Limnotek Research and Development Inc., Vancouver, B. C., for R.P. Griffith & Associates, Sidney, B.C. 72 p.

Pieters, R. and G.A. Lawrence. 2011. Plunging inflow and the summer photic zone in reservoirs. Water Quality Res. J. of Canada 47(3-4): 268-275. doi: 10.2166/wqrjc.2012.143

Prescott, G.W. 1978. *How to Know the Freshwater Algae*. 3rd Edition. Wm. C. Brown Company. Dubuque, IA.

R Development Core Team. 2011. R: a language and environment for statistical computing. R Foundation for Statistical Computing, Vienna, Austria.

Rhee, G. Y. 1978. Effects of N:P atomic ratios and nitrate limitation on algal growth, cell composition, and nitrate uptake. Limnology and Oceanography 23:10-25.

Rhee, G. Y., and I.J. Gotham. 1980. Optimum N:P ratios and coexistence of planktonic algae. Journal of Phycology 16:486-489.

Rempel, L.L., J.S. Richardson, and M.C. Healey. 2000. Macroinvertebrate community structure along gradients of hydraulic and sedimentary conditions in a large gravel-bed river. Freshwater Biology 45: 57-73.

Riemann, B. P. Simonsen, and L. Stengaard. 1989. The carbon and chlorophyll content of phytoplankton from various nutrient regimes. Journal of Plankton Research. 11: 1037-1045.

Rosemond, A. D., P. J. Mulholland, and J. W. Elwood. 1993. Top-down and bottom-up control of stream periphyton: effects of nutrients and herbivores. Ecology, 74(4), 1264–1280.

Schwartz, S. S., and R. E. Ballinger. 1980. Variations in life history characteristics of Daphnia pulex fed different algal species. Oecologia, 44(2), 181–184. http://doi.org/10.1007/BF00572677

Shelson, A.L. and G.K. Meffe. 1995. Path analysis of collective properties and habitat relationships of fish assemblages in coastal plain streams. Can. J. Fish. Aquat. Sci. 52: 23-33.

Shortreed, K. S., K. F. Morton, K. Malange, and J. M. B Hume. 2001. Factors Limiting Juvenile Sockeye Production and Enhancement Potential for Selected BC Nursery Lakes. Canadian Science Advisory Secretariat. Research Document 2001/098. http://www.dfo-mpo.gc.ca/CSAS/Csas/DocREC/2001/RES2001_098e.pdf

Shuter, B.J. and K.K. Ing. 1997. Factors affecting the production of zooplankton in lakes. *Canadian Journal of Fisheries and Aquatic Science* 54: 359-377.

Steemann Nielsen, E. 1952. The use of radioactive carbon (^{14}C) for measuring organic production in the sea. J. Cons. Int. Explor. Mer. 18:117-140.

SYSTAT 13 Software, Inc. 2009. Chicago, IL.

Thorp, J.H. and A.P Covich. 1991. Ecology and classification of north American freshwater invertebrates. Academic Press.

Utermohl, H. 1958. Zur Vervollkommnung der quantitativen Phytoplankton methodik. Int. Verein. Limnol. Mitteilungen No. 9.

Wallace, J.B. and N.H. Anderson. 1996. Habitat, life history, and behavioural adaptations of aquatic insects. p12 – 28. In: R.W. Merritt and K.W. Cummins (Ed.). An Introduction to Aquatic Insects of North America. Kendall Hunt Publ. Dubuque Iowa. 862p.

Water Act Order. 2011. Province of British Columbia Water Act Order. Water Act Sections 87 and 88. License file numbers 0212289, 0115688, 0161431, 0210947, 0202694, 0265200, 0199585, 3005073, 3005075, 3005074.

Wetzel, R.G. 2001. *Limnology.* Academic Press. San Diego.

Wu, L., and D. A. Culver. 1992. Ontogenetic diet shift in Lake Erie age-0 yellow perch (Perca flavescens): A size related response to zooplankton density. Canadian Journal of Fisheries and Aquatic …, 49(9), 1932–1937.

Yentsch, C.S. and V.W. Menzel. 1963. A method for the determination of phytoplankton chlorophyll-a and phaeophytin by fluorescence. Deep-Sea Res. 10: 221-231.

Zuur, A. F., E. N. Ieno, and C. Elphick, C. 2010. A protocol for data exploration to avoid common statistical problems. Methods in Ecology and Evolution, 1, 3–14.

7 APPENDIX A

Tributary PO_4, TDP, TP, NO_3 and TDS

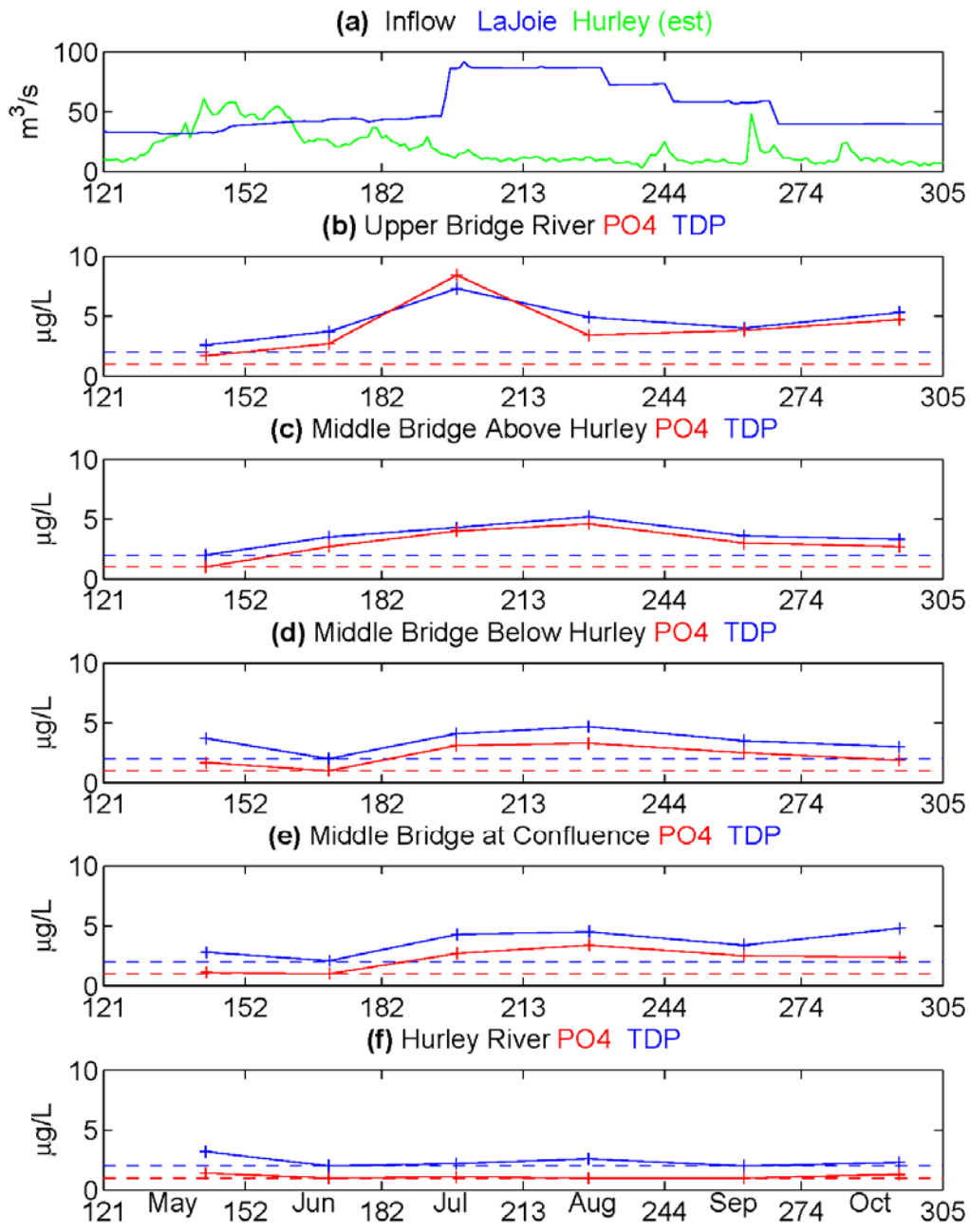

Figure AWQ1 (a) Outflow from LaJoie Dam, and inflow from the Hurley River (estimated as 25% of the local flow). (b-f) Phosphate (PO4) and total dissolved phosphorus (TDP), May to October, 2015.

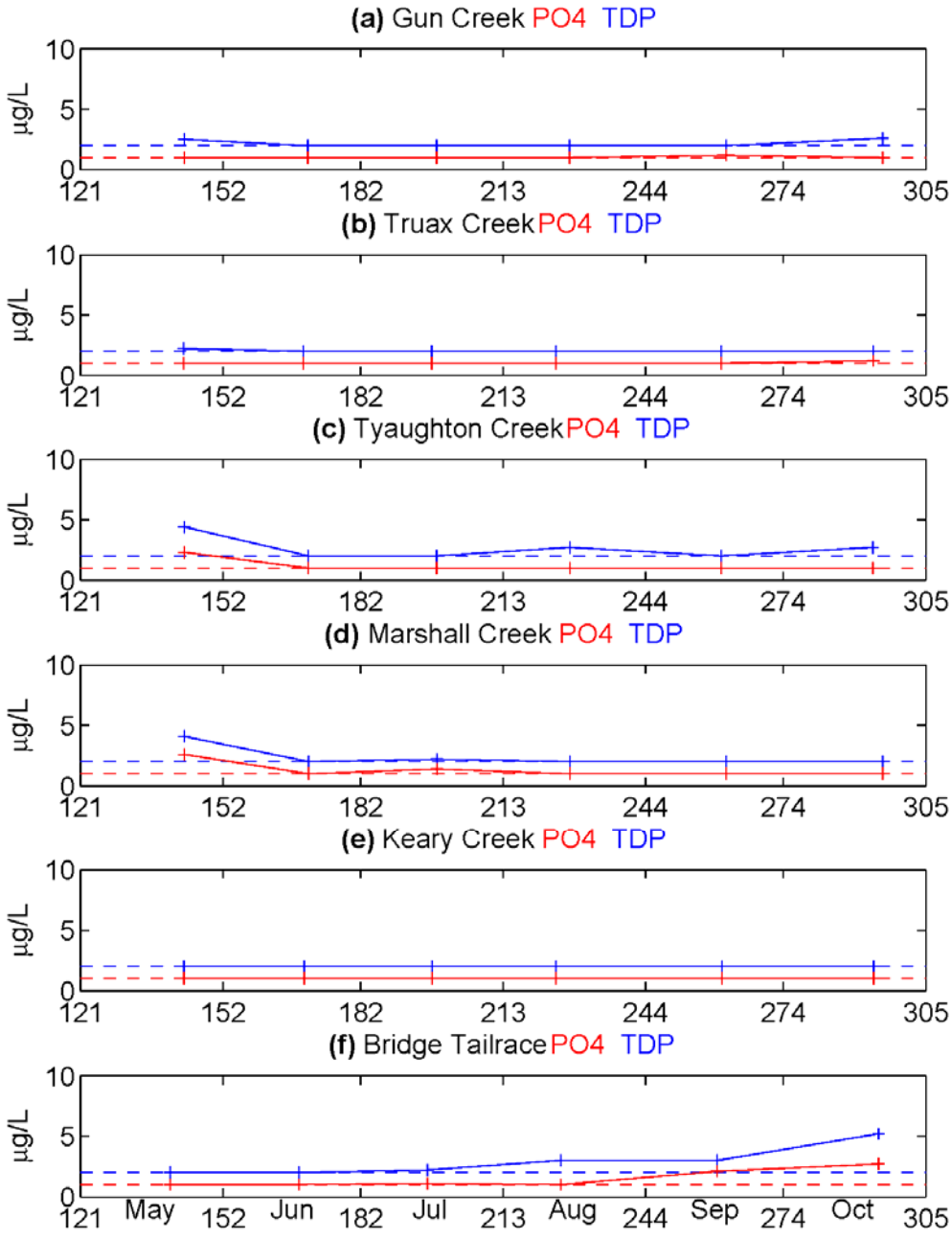

Figure AWQ2 (a-f) Phosphate (PO4) and total dissolved phosphorus (TDP), May to October, 2015.

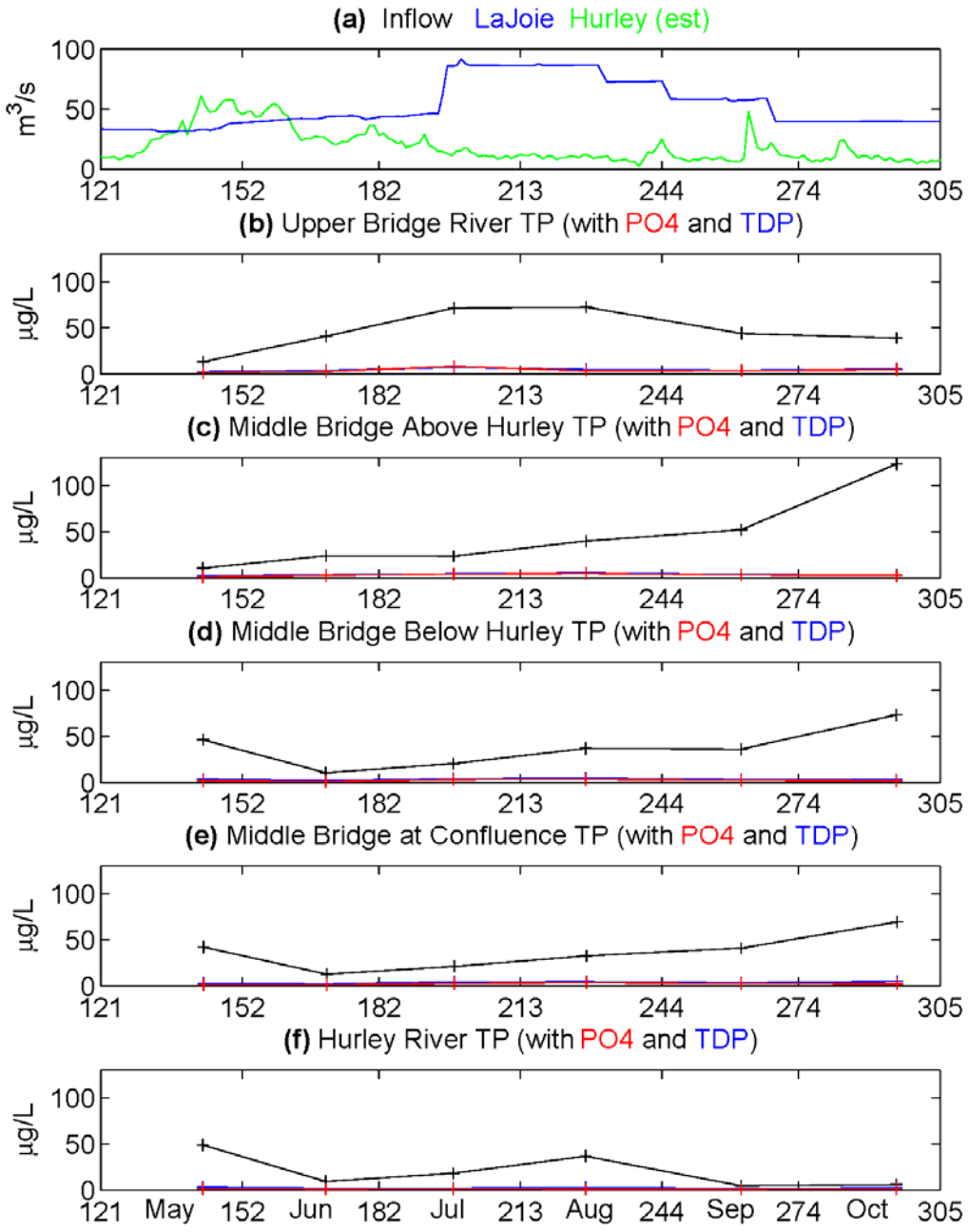

Figure AWQ3 (a) Outflow from LaJoie Dam, and inflow from the Hurley River (estimated as 25% of the local flow). (b-f) Total phosphorus (TP), May to October, 2015.

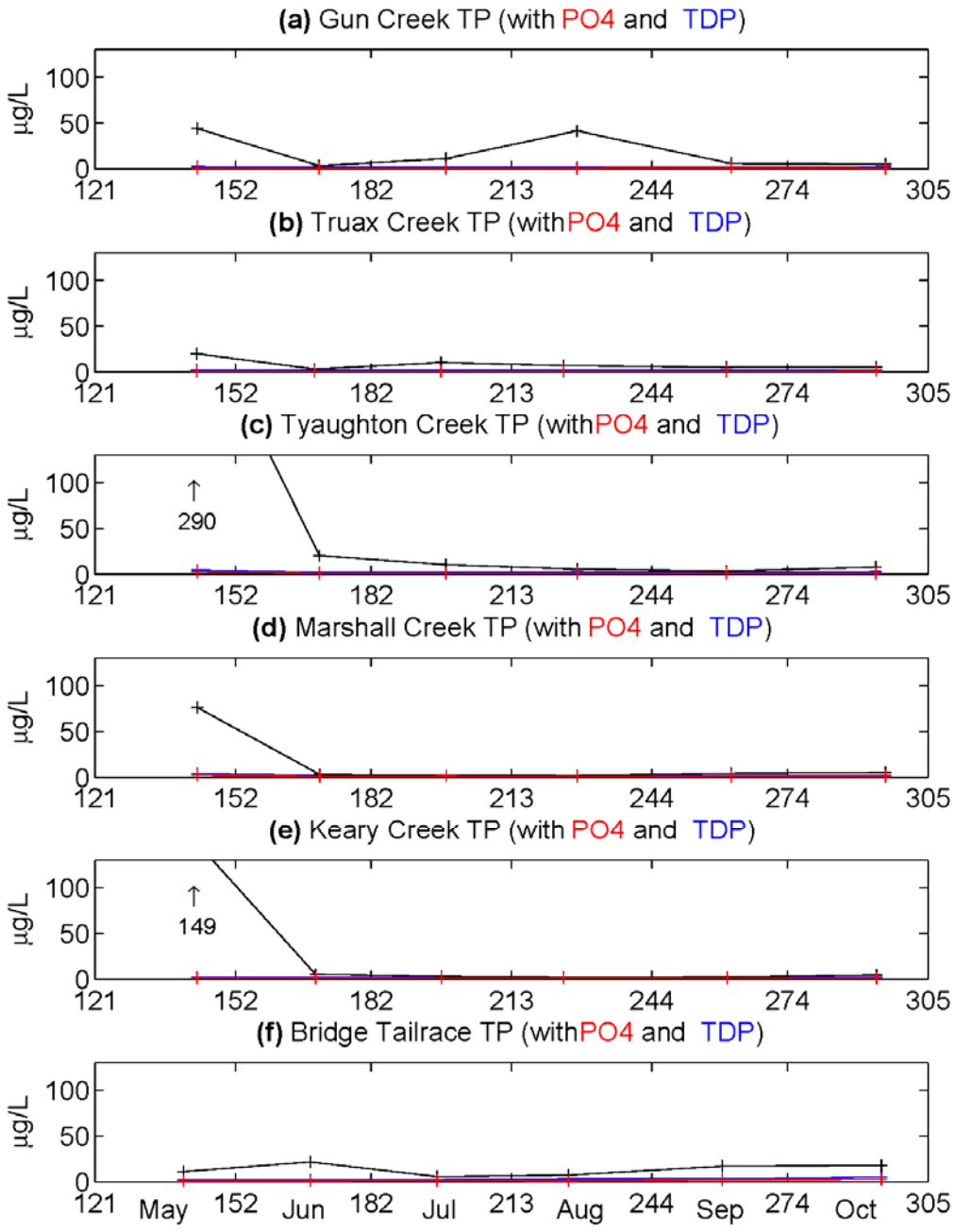

Figure AWQ4 (a-f) Total phosphorus (TP), May to October, 2015.

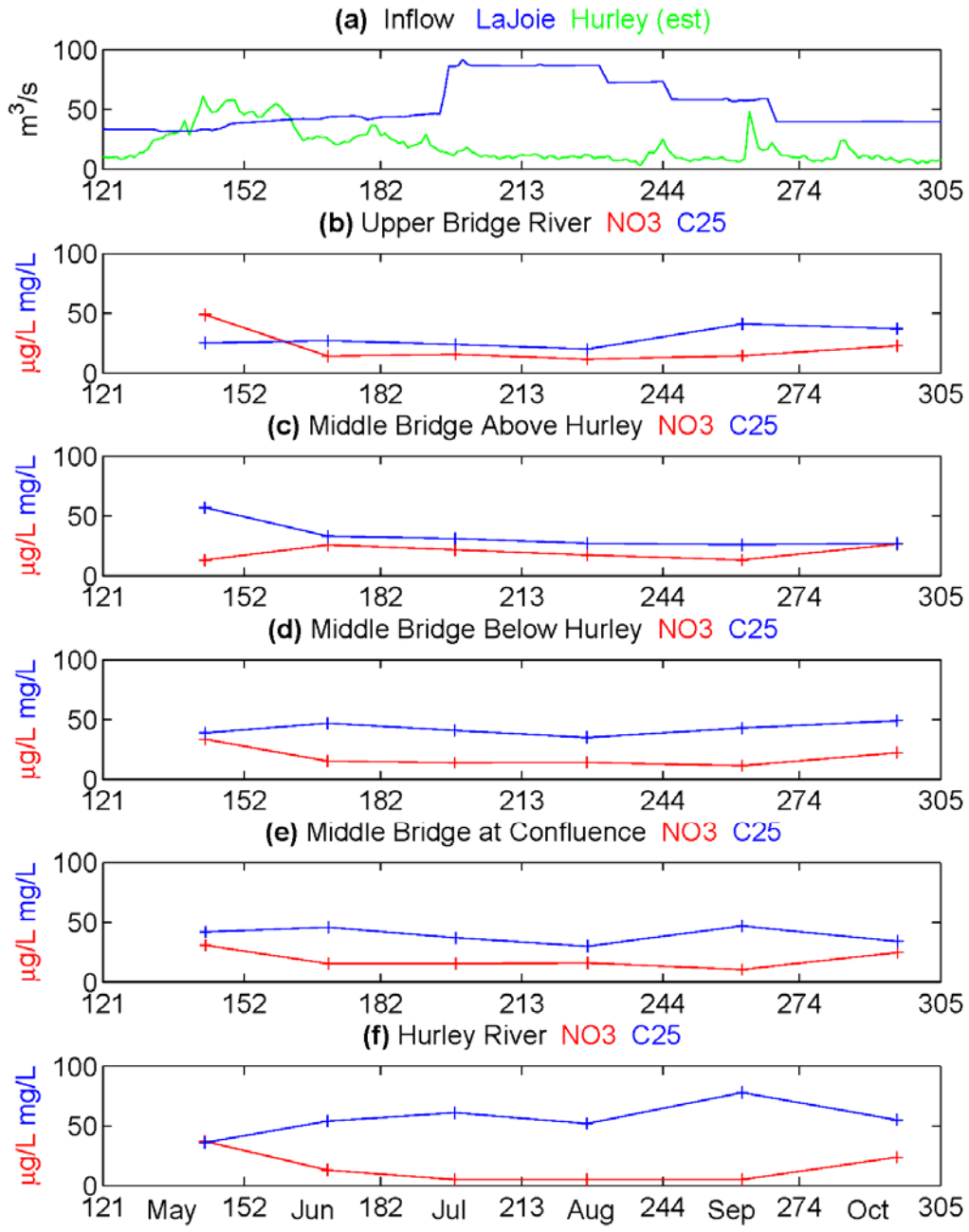

Figure AWQ5 (a) Outflow from LaJoie Dam, and inflow from the Hurley River (estimated as 25% of the local flow). (b-f) Nitrate (NO3) and total dissolved solids (TDS), May to October, 2015.

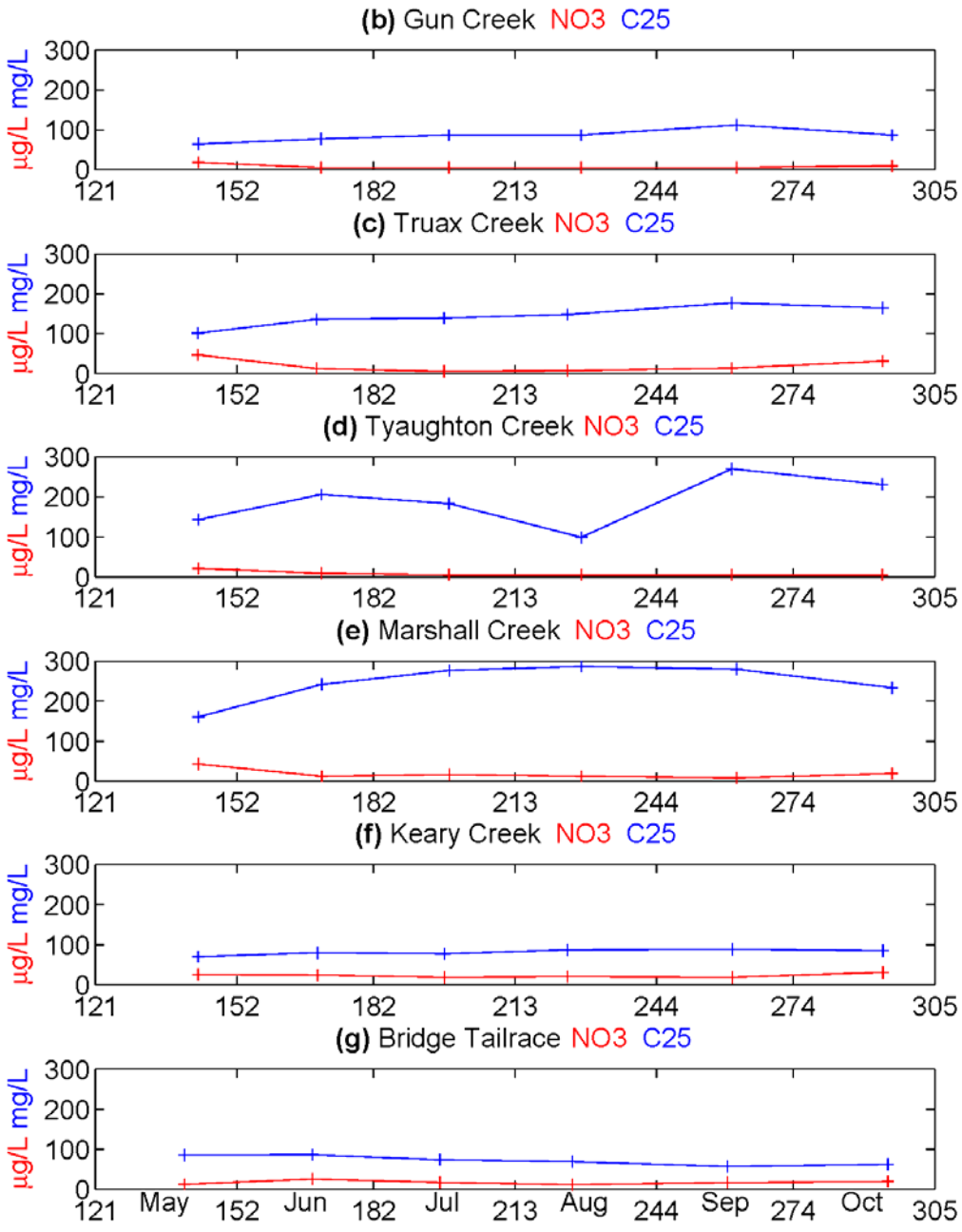

Figure AWQ6 (a-f) Nitrate (NO3) and total dissolved solids (TDS), May to October, 2015.